Aalto-yliopisto
Insinööritieteiden korkeakoulu

Tino Tuominen

Potential of Methanol in Dual Fuel Combustion

School of Engineering

Master's Thesis submitted in partial fulfillment of the requirements for the degree of Master of Science in Technology

Espoo, January 11th 2016

Supervisor: Professor Martti Larmi

Instructor: Teemu Sarjovaara, D. Sc. (Tech.)

Aalto University
School of Engineering

Aalto University, P.O. BOX 11000, 00076 AALTO
www.aalto.fi

Abstract of master's thesis

Author Tino Tuominen	
Title of thesis Potential of Methanol in Dual Fuel Combustion	
Degree programme Energy Technology	
Major/minor Transport Energy Technology	**Code** IA3031
Thesis supervisor Prof. Martti Larmi	
Thesis advisor(s) D.Sc. (Tech.) Teemu Sarjovaara	
Date 11.01.2016 **Number of pages** 75	**Language** English

Abstract

Depleting oil resources together with the climate change due to the use of fossil fuels are motivating to investigate alternative fuels and new combustion strategies used with them. At the moment, dual fuel combustion is one of the most promising new combustion strategies. Combining it to the use of renewable methanol as a primary fuel, it offers an interesting option for the conventional combustion engine.

This thesis focuses on investigating the theoretical potential of methanol in dual fuel combustion. The main objective of this study is to investigate the effects the use of methanol has on the in-cylinder conditions and on the cylinder charge at the end of compression stroke. Methanol operation is compared with three other fuels; methane, ethanol and indolene. In addition, using the compression temperature of methane as a reference case, the potential for increasing the compression ratio with methanol, ethanol and indolene is investigated in this thesis as well. Lastly, the potential improvements in engine performance are investigated with a simple combustion model.

The investigations in this study were conducted with GT-Power combustion engine simulation software. Simulations were performed systematically in five steps of which in the three first ones the effect of temperature and pressure, as well the effect of air-fuel ratio, on cylinder conditions were investigated. In the last two steps the potential for increasing the compression ratio was investigated together with the possible performance improvements. Due to the limitations in the simulation software, some simplifications had to be done. However, with the chosen approach the error made is known thus the simplifications are acceptable.

The results indicated huge potential in methanol operation. The high heat of evaporation of methanol decreased significantly the compression temperature compared to methane operation. Due to the significant cooling effect of methanol, the trapped air mass and, correspondingly, trapped fuel energy increased significantly improving the engine performance. In addition, compression ratio was able to be increased up to 24.1 with which the improvements in engine IMEP and indicated efficiency were remarkable. In summary, methanol shows great potential for increasing power output and decreasing simultaneously the specific emissions of NO_x due to lower cylinder temperature.

Keywords dual fuel, methanol, alternative fuels, GT-Power

Aalto-yliopisto
Insinööritieteiden korkeakoulu

Aalto-yliopisto, PL 11000, 00076 AALTO
www.aalto.fi

Diplomityön tiivistelmä

Tekijä Tino Tuominen	
Työn nimi Metanolin potentiaali dual fuel -palamisessa	
Koulutusohjelma Energiatekniikka	
Pää-/sivuaine Liikenteen energiatekniikka	**Koodi** IA3031
Työn valvoja Professori Martti Larmi	
Työn ohjaaja(t) TkT Teemu Sarjovaara	
Päivämäärä 11.01.2016 **Sivumäärä** 75	**Kieli** Englanti

Tiivistelmä

Rajallisten öljyvarantojen ja fossiilisten polttoaineiden ilmastoa lämmittävän vaikutuksen johdosta kiinnostus vaihtoehtoisia polttoaineita ja palamistekniikoita kohtaan kasvaa jatkuvasti. Dual fuel -tekniikka on tällä hetkellä yksi lupaavimmista vaihtoehtoisista palamistekniikoista. Yhdessä uusiutuvan metanolin kanssa se tarjoaa kiinnostavan vaihtoehdon perinteisille polttomoottoreille.

Tässä työssä keskitytään tutkimaan metanolin teoreettista potentiaalia dual fuel -palamisessa. Työn tärkein tavoite on tutkia, miten metanolin käyttö vaikuttaa sylinterin sisäisiin olosuhteisiin sekä sen täytökseen. Tutkimuksissa metanolia verrataan kolmeen muuhun polttoaineeseen; metaaniin, etanoliin ja indoleeniin. Tämän lisäksi tutkitaan voidaanko metanolia, etanolia ja indoleenia käyttämällä nostaa moottorin puristussuhdetta käyttäen metaanin puristuslämpötilaan vertailukohtana. Lopuksi tutkitaan mahdollisia parannuksia moottorin suorituskyvyssä käyttäen apuna yksinkertaista palamismallia.

Tutkimuksien suorittamiseen käytettiin polttomoottorien simulointiin tarkoitettua GT-Power-ohjelmistoa. Simuloinnit suoritettiin systemaattisesti viidessä vaiheessa, joista kolmessa ensimmäisessä tutkittiin imuilman lämpötilan, paineen sekä ilmakertoimen vaikutuksia sylinterin olosuhteisiin. Niitä seuraavissa kahdessa vaiheessa tutkittiin yhtäaikaisesti mahdollisuuksia korottaa puristussuhdetta sekä metanolin potentiaalia parantaa moottorin suorituskykyä. Simulointiohjelmiston yksinkertaisuuden vuoksi jouduttiin tutkimuksissa yksinkertaistamaan joitakin asioita, mutta tehtyjen virheiden luonne tiedossa voidaan yksinkertaistuksia pitää hyväksyttävinä.

Metanolin korkea höyrystysmislämpö laski merkittävästi puristuslämpötilaa metaaniin verrattuna. Samasta syystä sylinterin täytös kasvoi, jolloin polttoainetta kyettiin ruiskuttamaan enemmän saavuttaen näin parannuksia moottorin suorituskykyyn. Tämän lisäksi puristussuhde kyettiin nostamaan metanolia käyttämällä 24.1:een, jonka avulla saavutettiin merkittäviä parannuksia moottorin teholliseen keskipaineeseen ja indikoituun hyötysuhteeseen. Yleisesti ottaen metanoli osoitti suurta potentiaalia, sillä sen avulla moottorin suorituskykyä voidaan parantaa ja samanaikaisesti NO_x päästöjä vähentää alemman sylinterin lämpötilan johdosta.

Avainsanat dual fuel, metanoli, vaihtoehtoiset polttoaineet, GT-Power

Preface

This thesis was conducted in the laboratory of internal combustion engines at Aalto University with the financial aid from Henry Ford Foundation and Fortum Foundation. The thesis acts as a preliminary study for investigating the use of methanol in dual fuel combustion and research work is continued on the subject after this thesis.

I wish to thank the supervisor of this thesis, Professor Martti Larmi for overseeing the work and providing feedback. I also like to present my gratitude to the instructor D.Sc. (Tech.) Teemu Sarjovaara for his contribution to the working process of this thesis. His guidance has been indispensable. Then, I would like to thank Otto Blomstedt, Rasmus Pettinen, Olli Ranta, Tuomo Hulkkonen and Jari Hyytiä from the internal combustion engine laboratory for the interesting conversations both on and off topic. In overall, I would like to thank the whole staff in the laboratory of internal combustion engines for making the laboratory a pleasant place to work.

Most importantly, I wish to thank my family and all of my friends who have been there for me during the past years. Especially I am truly grateful to my parents Jari and Tarja who have supported me throughout my life and given me the opportunity to freely develop myself in every aspect of my life.

Espoo, January 11th 2016

Tino Tuominen

Table of Contents

Abstract

Tiivistelmä

Preface i

Table of Contents ii

Nomenclature iv

1 Introduction 1

1.1 Motivation 1

1.2 Objectives 1

2 Background 3

2.1 Methanol 3

2.1.1 Environmental benefits 3

2.1.2 Properties 4

2.1.3 Effects on combustion and emissions 4

2.2 Emission formation 7

3 Combustion processes 10

3.1 Dual fuel engines 10

3.1.1 Combustion characteristics 11

3.1.2 Ignition delay 13

3.1.3 Knock and pre-ignitions 14

3.2 SI engines 15

3.2.1 SI combustion 16

4 Parameter effects on combustion 18

4.1 Dual fuel combustion 18

4.1.1 Injection timing 18

4.1.2 EGR 20

4.1.3 Diesel substitution ratio 21

4.1.4 Compression ratio and inlet temperature 30

4.2 SI combustion 31

4.2.1 Ignition timing 31

4.2.2 Inlet temperature 32

4.2.3 Air-fuel ratio 32

4.2.4 EGR 34

5 Research methods.....36
5.1 Simulation software.....36
5.2 GT-Power model.....36
5.3 Simulation method.....37
5.4 Simulation steps.....37
5.5 Parameters.....38
5.6 Simulation uncertainties.....40
6 Results and analysis.....44
6.1 Equivalent fuel mass.....44
6.2 Equivalent fuel energy.....47
6.3 Equivalent lambda.....52
6.4 Variations in compression ratio.....56
6.4.1 Equivalent compression temperature (J).....56
6.4.2 Equivalent compression temperature (λ).....62
7 Conclusions.....68

Nomenclature

Abbreviations:

BMEP	Brake Mean Effective Pressure
BTDC	Before Top Dead Center
BTE	Brake Thermal Efficiency
CA50°	Point of 50% burnt fuel mass in crank angles
CAD	Crank Angle Degree
CFR	Cooperative Fuel Research
CI	Compression Ignition
COV	Coefficient of Variation
D	Diesel
D+M	Diesel-Methanol Dual Fuel
DDF	Diesel Dual Fuel
DF	Dual Fuel
DOC	Diesel Oxidation Catalyst
EGR	Exhaust Gas Recirculation
GHG	Greenhouse Gas
ΔH_{vap}	Heat of evaporation [kJ/kg]
HCCI	Homogenous Charge Compression Ignition
HRR	Heat Release Rate
H_u	Lower heating value [MJ/kg]
IMEP	Indicated Mean Effective Pressure

ISFC	Indicated Specific Fuel Consumption
LHV	Lower Heating Value
m	mass [kg]
$\dot{m}$	Mass flow [kg/s]
MBT	Maximum Brake Torque Timing
mfb	Mass Fraction Burnt
MON	Motor Octane Number
MSR	Methanol Substitution Ratio
n	Engine speed [1/s]
NG	Natural Gas
OEM	Original Equipment Manufacturer
P	Power [kW]
PM	Particulate Matter
PR_m	Premixed Ratio of Methanol
RCCI	Reactivity Controlled Compression Ignition
RE85	Fuel mixture of 15% of gasoline and 85% of ethanol
RON	Research Octane Number
rpm	Rounds per minute
SG	Spark Gas
SI	Spark Ignition
SOE	Start of Energizing
TDC	Top Dead Center

TWC	Three-Way-Catalyst
UHC	Unburned Hydrocarbons
vff	Vaporized Fluid Fraction
VGT	Variable Geometry Turbine
WOT	Wide Open Throttle

Chemical compounds:

C_2H_5OH	Ethanol
CH_3OH	Methanol
CH_4	Methane
CO	Carbon Monoxide
CO_2	Carbon Dioxide
H_20	Water
HC	Hydrocarbon
HO_2	Hydroperoxyl radical
N_2	Nitrogen
NO	Nitric Oxide
NO_2	Nitrogen Dioxide
NO_x	Nitrogen Oxides
O	Oxygen
PAH	Polyaromatic Hydrocarbons

Greek letters:

ε	Compression Ratio
γ	Isentropic Exponent
γ_g	Substitution Ratio
η	Brake Efficiency
η_i	Indicate Efficiency
λ	Air-fuel ratio
λ_{CH4}	Air-fuel ratio of methane
λ_{EtOH}	Air-fuel ratio of ethanol
λ_{Indo}	Air-fuel ratio of indolene
λ_{MeOH}	Air-fuel ratio of methanol

1 Introduction

1.1 Motivation

Depleting fossil oil resources are forcing the humankind to find alternative feedstocks for present fossil oil based products and fuels. Depending on the source, the conventional crude oil is forecasted to last for the next 40-50 years with known oil resources [1]. Although, unconventional oil resources are discovered more and more nowadays but, simultaneously, the costs are increasing since more effort is needed for utilizing these resources. In addition to the limited oil resources, there is a strong diesel/gasoline imbalance in Europe, meaning that there is an increasing mismatch between refinery production and demand for diesel fuel. In other words, nowadays the consumption of diesel in Europe is larger than European oil refineries can produce it. Together with the depleting oil resources, the diesel/gasoline imbalance increases the price of diesel fuel. Since especially heavy-duty engines are mostly operated with diesel fuel, the running costs will increase accordingly.

In addition to the depleting oil resources, environmental factors are at least as important reasons for finding an alternative fuel for diesel. Greenhouse gases (GHG) originating from combustion of fossil fuels are accelerating the climate change thus there is a real need in reducing the GHG emissions significantly. When speaking of GHG emissions in diesel engines, they practically consist solely of CO_2, thus any solution reducing CO_2 emissions is worth investigating. In order to lower CO_2 emissions, the use of renewable fuels together with new, more efficient, combustion strategies is needed. New combustion strategies are also needed to meet the increasingly tightening regulations for local emissions, in diesel engines mainly NO_x and PM.

Dual fuel combustion is one of the most promising new combustion strategies, and it is nowadays mainly used in the marine industry with natural gas as a primary fuel. Interest towards the use of dual fuel combustion in heavy duty engines in road traffic is increasing thus there is a need for further investigations. Using renewable methanol as primary fuel in dual fuel engine, it is a noteworthy option as a sustainable and ecological alternative fuel for heavy-duty engines. In order to use methanol with high efficiency and minimal exhaust emissions, it is necessary to investigate new combustion methods for methanol, while simultaneously increasing the understanding of the use of methanol in a dual fuel engine.

1.2 Objectives

This thesis focuses on investigating the theoretical potential of methanol in dual fuel combustion. The aim is to study the potential for improving the engine performance in heavy duty applications. Investigations are conducted with simulations and experimental studies are left out of the scope of this thesis. The main objective of this study is to investigate the effects the use of methanol has on the in-cylinder conditions and on the cylinder charge at the end of compression stroke. Factors such as compression temperature, compression pressure, trapped air mass and trapped fuel energy will be compared against three other fuels, ethanol, indolene and methane. With better understanding of the conditions before combustion, the main engine parameters, for example compression ratio, can be optimized for methanol, and the full potential of methanol can be utilized. Therefore, the potential for increasing the compression ratio, compared to methane operation, is investigated in this thesis with methanol, ethanol and indolene. In addition, simple combustion modelling is performed in order to get an idea of how the performance of methanol operation compares against the aforementioned fuels. Due to the limitations in the simulation software, the study concerns only the theoretical potential of methanol and more realistic approach is ruled out.

2 Background

2.1 Methanol

2.1.1 Environmental benefits

The dependency of oil can be reduced by using methanol which can be produced from several feedstocks, including renewable feedstocks. In addition, the latest technology allows methanol production also from chemically recycled CO_2. At the moment methanol is mostly produced from syn-gas, which in turn is produced from fossil hydrocarbon sources. Syn-gas is a mixture of CO_2, CO and hydrogen, and it is produced nowadays mostly from methane extracted from natural gas. Despite the fact that natural gas is a bit more environmentally friendly fuel than conventional fossil fuels, using it as a feedstock for methanol production does not reduce the dependency of fossil fuels. CO_2 reduction is also basically negligible so, in order to reduce CO_2 emissions and oil dependency, renewable feedstocks need to be used. Renewable bio-methanol can be produced using biomass as a feedstock. By biomass is referred to any type of plant or animal material. Bio-methanol is manufactured by gasifying biomass such as, for example, bio-waste from food industry. Another ecological option is to produce methanol from biogas with the same method as it is produced from natural gas. When using renewable feedstock, the net CO_2 emissions drop as CO_2 is absorbed by the feedstock in the growing stage.[1].

The most promising method for reducing GHG emissions is to recycle CO_2 from the flue gases of industrial and power/ heating facilities. The flue gases have a high concentration of CO_2 which can be then collected and used for methanol production. Collecting CO_2 also from vehicles could be possible, but the onboard CO_2 storage would be a big challenge, and therefore it is not a reasonable option at present time. The recycled CO_2 can be used in a process with methane to produce methanol. However, as methane is still a fossil fuel and it is non-renewable, replacing diesel with methanol produced from other fossil fuel is not a sustainable method. One solution could be to use hydrogen acquired from the electrolysis of water. However, the electrolysis of water requires a lot of energy which makes it less suitable option. Nevertheless, CO_2 recycling in large scale can be the solution for inhibiting the climate change as large portion of CO_2 emissions are emitted by industrial factories and power/heat generation facilities. When CO_2 could be recycled from the flue gases produced by these facilities, it would reduce CO_2 emissions dramatically. CO_2 can even be recycled from the atmosphere and used for methanol production. Using this atmospheric CO_2, the global warming could be stopped and CO_2 concentration could be even lowered in the atmosphere.[1]

2.1.2 Properties

Properties of methanol are greatly different compared to conventional transportation fuels. Comparison between methanol and the most common fuels are illustrated in table 1. More detailed comparison of the properties of methanol against diesel and methane is performed in the following chapter, and analyzed how the differences could affect the combustion and emissions.

Table 1. Comparion of methanol with more commonly used fuels[1]–[5]

	Methane	**Methanol**	**Ethanol**	**Gasoline**	**Diesel**
Chemical formula	CH4	CH3OH	C2H5OH	C4 to C12	C3 to C25
Composition [%]					
Carbon	75	38	52	86	86
Hydrogen	25	12	13	14	14
Oxygen	0	50	35	0	0
C/H ratio	3,00	3,17	4,00	6,14	6,14
Density [kg/m3]	0,72	790	790	720-775	820-845
Boiling temperature [°C]	-162	65	78	25-210	180-360
Research octane number	>127	109	109	90–100	--
Cetane number	-	3	11	20-25	min. 51
Autoignition temperature, °C	650	455	420	300	250
Flammability range in air (Volume %)					
Lower limit	5	7	3,5	0,6	0,6
Higher limit	15	36	15	8	7,5
Specific heat of evaporation [kJ/kg]	-	1 110	904	380 - 500	250
Lower heating value [MJ/kg]	50	19,70	26,80	41,2 - 41,9	42,9 - 43,1
Stoichiometric air/fuel ratio	17,2	6,7	9	14,8	14,5

2.1.3 Effects on combustion and emissions

Composition

Methanol is an oxygenated fuel and it contains roughly 50 % of oxygen of its mass. Diesel does not contain any oxygen, and it has been studied that mixing diesel with fuels containing oxygen, it lowers particulate matter emissions (PM) as there is locally more oxygen available for the combustion. On the other hand, NO_x emissions have been reported to increase because of the addition of oxygen. [6] However, these are mostly a problem in diesel combustion where PM and NO_x formation is the major problem. In SI combustion, if operated with stoichiometric mixture, PM emissions are rather low and NO_x emissions can be treated efficiently with TWC. Nevertheless, methanol could be a viable solution for reducing local emissions, especially PM emissions, produced in diesel engines.

Table 1 also illustrates the difference in C/H ratio of methanol and diesel. C/H ratio is the ratio between fuel carbon and hydrogen content and it is directly related to how much CO_2 emissions a certain fuel produces. As it can be seen, diesel fuel has a C/H ratio twice as big as methanol, thus burning methanol produces half the amount of CO_2. However, the energy content of methanol is half of the diesel's so it is needed to burn twice as much as diesel. Nevertheless, when calculated the carbon mass for energy equivalent amount of fuel, methanol contains less carbon thus less CO_2 emitted. As methane has lower C/H ratio combined with higher LHV compared to diesel, the CO_2 emissions are reduced. C/H ratio has also an effect on the adiabatic flame temperature as lower C/H ratio equals higher formation of water vapor. Water vapor has higher specific heat than other combustion products and therefore it lowers the adiabatic flame temperature, and the overall combustion temperature. Lower combustion temperature results in reduced NO_x formation.

Autoignition properties

In compression ignition engines, the fuel autoignites when autoignition conditions are met. The tendency for autoignition is described with cetane number, and it basically indicates how easily the fuel ignites under certain predetermined test conditions. Higher cetane number indicates shorter ignition delay, which leads to an improved combustion. Table 1 illustrates, that methanol has significantly worse autoignition properties than diesel fuel. However, cetane rating is a poor indicator of the autoignition properties of methanol, as its autoignition properties depends more strongly on the in-cylinder temperature than diesel-type of fuels, to which the cetane rating is based on [7]. As methanol is the simplest alcohol consisting of only one carbon atom, this simple chemical structure makes it chemically robust. Diesel fuel on the other hand is a mixture of different long straight chain hydrocarbons, which are more reactive than single carbon atom methanol molecules, thus making diesel easier to ignite. The difference in autoignition temperatures, illustrated in Table 1, indicates also higher reactivity of diesel fuel. The strong temperature dependency of methanol is demonstrated in the study of Mueller et al [7], where methanol autoignition tendency was improved with the presence of a glow plug. Without the glow plug, methanol did not ignite despite the fact that the in-cylinder temperature was above the autoignition temperature of methanol. Methane has really poor autoignition properties since the autoignition temperature is 650°C.

Lower heating value (LHV) and heat of evaporation

Methanol's LHV is roughly half of the diesel equivalent, which means that it is necessary to inject twice as much methanol in order to keep the engine output torque at the same level. Methanol has also approximately four times higher heat of evaporation which results that evaporating methanol requires roughly four times the energy as evaporating equivalent amount of diesel. This itself leads to a significant cooling effect of the cylinder charge but keeping in mind the difference in LHV, the cooling effect is therefore even more drastic. Cooler mixture has both positive and negative effects as it lowers the temperature at the end of compression. As NO_x emissions are strongly related to high temperatures, NO_x emissions can be expected to be significantly lower with the use of methanol [8]. Cooler charge cools also the engine components, which could improve the efficiency as the heat losses to coolant are reduced. On the other hand, as it was discussed in the section of autoignition, the autoignition of methanol is strongly dependent on the temperature, thus lower temperature worsens the ignitability of the mixture. Methane has the highest LHV, but as it is gaseous fuel there is no fuel evaporation and the compression temperature is higher. Additionally, since the temperature of the cylinder charge affects the density of air, cooler charge results denser air and volumetric efficiency increases due to that.

Stoichiometric air/fuel ratio

As methanol contains a large portion of oxygen itself, the need for oxygen in intake air is reduced. Therefore, the stoichiometric air/fuel ratio is 6.7 as it is 14.7 for diesel, thus burning equivalent amount of methanol requires less than half the air mass than burning diesel. However, LHV of methanol is a bit less than half of the LHV of diesel, so in order to burn energy equivalent amount of methanol, air needed for combustion is approximately the same than it is with diesel combustion. As methanol is injected into the intake port, the partial pressure of oxygen in the intake air is reduced which in turn can affect the ignition delay of the pilot fuel and the overall combustion process [9]. Therefore, the effect of port injection needs to be studied and whether there is some power loss due to the air displacement.

Flammability limits

Flammability limit describes the boundary conditions for the ignitable mixture of air and fuel. Compared to diesel, methanol and methane have significantly wider flammability limits, but as diesel combustion occurs with excess air/fuel ratio without homogenous mixture, comparison should be made with gasoline since it is used in SI engines. The flammability limits for gasoline are similar than with diesel, thus methanol and methane have similar advantage with flammability limits compared to gasoline. Wider flammability limits enable the use of leaner mixtures thus throttling can be reduced consequently and brake efficiency is improved due to lower pumping losses.

Octane rating

Octane rating, or number, describes how well the fuel resists self-ignition or knocking. Higher the octane number, better the resistance for self-ignition. In SI engines higher octane number means practically more efficient combustion and more power [8]. Methanol has higher octane number than gasoline, thus higher resistance for knocking and higher in-cylinder pressure is achievable. Methane has the highest octane rating which also provides higher resistance for knocking compared to gasoline. Therefore, higher compression ratio can be used for methanol and methane compared to gasoline powered engines. Octane number is measured with a procedure where the tested fuel is compared against a predetermined mixture of n-heptane and iso-octane. If the reference mixture contains 90% of iso-octane, the octane number is 90. The test fuel is combusted in CFR engine with variable compression ratio until knocking occurs, and the results are compared with those predetermined mixtures of n-heptane and iso-octane. There are two different methods used, research and motor method, which differ slightly from each other. The main differences are in engine speeds and mixture temperatures. In research method, engine speed of 600 rpm is used whereas in motor method the speed is 900 rpm. The intake mixture is preheated to a certain value in the motor method but in the research method only the intake air temperature is kept constant. [10], [11] Due to this, the octane number with motor method, MON, is always lower than with research method, RON.

Laminar flame speed

Turbulence is the main factor affecting the speed of the combustion, but the laminar flame speed is also a crucial property as it describes how fast the flame travels inside the propagating turbulent flame front. Especially at the beginning of the combustion, where turbulence is less prominent, laminar flame speed plays an important role. [12] Methanol is reported to have the highest flame speed, followed by ethanol, methane, gasoline and diesel having the slowest flame speed. [13]–[15] Higher flame speed results in improved combustion efficiency. It can also improve the lean operation characteristics as flame speed degrades with leaner mixture. For example, combustion duration could remain the same with lean burn combustion of methanol compared to stoichiometric combustion of gasoline. [8]

2.2 Emission formation

Unburned hydrocarbons

Unburned hydrocarbons (HC) are mainly a problem in combustion of premixed mixtures, and the contribution of diesel combustion on HC emissions is significantly lower. There are three main sources of HC emissions in SI engines, which are crevice losses, oil layer adsorption and flame quenching. When fuel is premixed with the intake air, parts of the mixture is forced into small gaps where the flame front cannot propagate. Largest contribution to crevice losses comes from piston ring pack and head gasket crevice. In expansion stroke, the HC escape from the crevices and as the conditions for oxidizing the unburned HC are unfavorable, they escape the cylinder within the exhaust gases. In adsorption mechanism, the HC is adsorbed into the oil layer on the cylinder walls at high pressure. At lower pressure during expansion stroke the adsorption reverses and HC returns to the combustion chamber. The third one, flame quenching, occurs due to colder temperature at the boundary layer close to cylinder walls. Temperature is too cold for the flame propagation and the HC in this thin boundary layer remains unburned. [16], [17]

Carbon monoxide

Carbon monoxide (CO) is formed as an intermediate step in the formation of carbon dioxide. Failure of oxidizing CO into CO_2 can depend on either lack of oxygen or too low temperatures. The extent of carbon monoxide formation is determined by the local air-fuel ratio, cylinder temperature and cylinder pressure. In the case of insufficient amount of air, the CO emissions have almost linear relationship to the air-fuel ratio. Operating in stoichiometric conditions, CO emissions will be significant due to the inhomogeneities of the mixture. There are locally rich regions, thus lack of oxygen leads to CO formation. Engine running with excess air, the CO emissions are low until the point when mixture is excessively lean and causes the flame to quench. [8]

Nitrogen oxides

Nitrogen oxides are a result of combustion in oxygen rich environment with presence of high temperature. Especially in diesel engines, the formation of nitrogen oxides is an issue due to the availability of excess amount of air. Nitrogen oxides from engines consist mainly of two types, NO and NO_2, and they are commonly referred to as NO_x. NO_x is formed through four mechanisms where atmospheric nitrogen or nitrogen from the fuel reacts with oxygen. These four mechanisms are thermal NO, prompt NO, fuel NO and NO generated via nitrous oxide[16]. From these mechanisms thermal NO is the most significant mechanism, as thermal NO is believed to be responsible of 90-95% of total NO_x emissions [18]. Therefore, thermal NO_x is the only mechanism reviewed here.

Thermal NO formation is described with extended Zeldovich mechanism, which consists of three reversible reactions

$$O + N_2 \xleftrightarrow{k_1} NO + N$$

$$N + O_2 \xleftrightarrow{k_2} NO + O$$

$$N + OH \xleftrightarrow{k_3} NO + H.$$

The first reaction has very high activation energy and it requires high temperatures for the first reaction to happen. As it can be seen, the first reaction provides nitrogen atoms for the next reaction, so it is the factor limiting the rate of NO_x formation. Thus, decreasing the combustion temperature is the most efficient way to reduce NO_x emissions. [16], [19] NO_x emissions are needed to control as they can cause respiratory diseases and, at ground level, NO_x emissions together with HC emissions forms ozone and photochemical smog. In addition, it destroys the ozone at high altitudes damaging the ozone layer.

Particulate matter

Particulate matter (PM) consists mainly of soot produced in fuel-rich conditions in the engine. Soot formation, together with NO_x, is the issue in diesel engines as there are always rich conditions due to nonpremixed flames. According to Warnatz et al [16] the soot is formed through the growth of polyaromatic hydrocarbons (PAH). The PAH are usually formed in rich conditions when small hydrocarbons are broken down from the fuel. In soot formation, particle-like structures are formed by conglomeration of the PAH molecules. After this, the particles grow by surface growth and by coagulation. The soot formation is dependent of the temperature as it is believed to occur in temperature range between 1000K and 2000K. [16] Figure 1 illustrates the steps in the soot formation. PM emissions can be reduced by providing longer mixing time, thus less fuel-rich mixture is present in the cylinder.

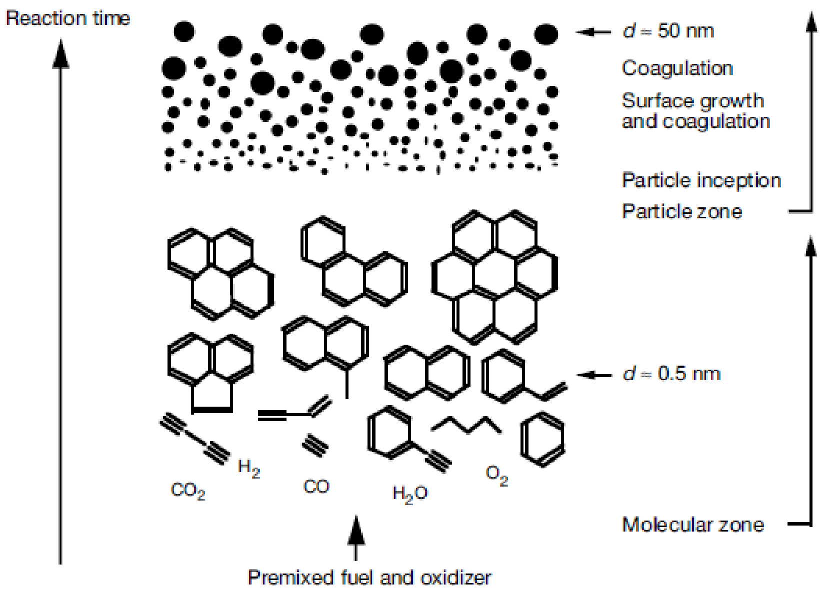

Figure 1. Scehmatic of soot formation. [16]

3 Combustion processes

3.1 Dual fuel engines

Dual fuel engines have awakened the interest of researches in hoping to find a solution for future development strategies of internal combustion engines. Diesel Dual fuel engines can obtain diesel-like efficiency and brake mean effective pressure (BMEP) with significantly lower NO_x and PM emissions. They can be designed to operate interchangeably with primary fuels other than diesel using diesel as a pilot fuel, or they can be operated solely with diesel fuel. [20] This flexible fueling strategy allows using renewable fuels easier, as conventional diesel fuel can be used in areas where there is no supply for renewable primary fuel.

In dual fuel combustion a fuel with low reactivity is ignited with a small amount of high reactivity fuel. It is a combination of combustion in spark-ignition engine and compression ignition engine. This is due to the fact that the primary fuel is premixed with air forming a homogenous mixture as in SI-engines. The homogenous mixture is then ignited with a small amount of diesel injected into the cylinder at the end of compression stroke. As diesel fuel, or so called pilot fuel, is ignited due to the heat of compression, dual fuel engine shares some characteristics also with conventional diesel engines. Thus, dual fuel combustion is a combination of mixture-controlled diffusion combustion known from CI engines, and turbulent flame propagation known from SI engines. Despite the fact that dual fuel engines have common features with both SI engines and CI engines, they have also some unique advantages and disadvantages of their own. [20]

One of the major advantages is the aforementioned fuel flexibility. This contributes the shift towards using more renewable fuels as the vehicle operator or owner does not have to be concerned about the fueling infrastructure of the renewable fuel. Additionally, dual fuel engines can reach often equal or better fuel economy under moderate or high load than with pure diesel operation. Secondly, as homogenous lean burn combustion is part of the overall combustion, the exhaust emissions typical to diesel engines could be lowered significantly. On the other hand, light load conditions are known to be a challenge in dual fuel engines, as HC and CO emissions can increase vastly due to the lean homogenous mixture. When homogenous mixture becomes increasingly leaner, it eventually causes poorer combustion and more fuel reacts only partially, thus HC and CO emissions are increasing. [20] At high load conditions, the challenges relate to premature combustion causing either engine knock or pre-ignitions.

Lean combustion of homogenous mixture is enabled by the use of diesel fuel as the source of ignition for the primary fuel. This is due to the larger amount of energy released by the burning diesel fuel than the ignition energy acquired from a common spark plug. As dual fuel engines operate with lean mixtures at light loads and high percentage of engine usage is at light load, issues with light load operation needs to be solved.

3.1.1 Combustion characteristics

G.A. Karim [9] states in this study "Combustion in Gas Fueled Compression Ignition Engines of the Dual Fuel Type" that the combustion process in a typical dual fuel engine depends both on the spray and ignition characteristics of the diesel pilot and on the type of gaseous fuel used, and its overall concentration in the cylinder charge. The combustion heat release characteristics are influenced by the complex physical and chemical interactions affecting between the combustion processes of the two fuel systems. According to Karim, the heat release of the combustion is considered to consist of three overlapping components, which are illustrated in Figure 2. [9] These overlapping components are labeled as I, II and III, and they stand for following phenomena:

I. Combustion of the diesel pilot
II. Combustion of methane in the premixed pilot-region
III. Preignition reaction activity and flame propagation through the premixed fuel-air mixture

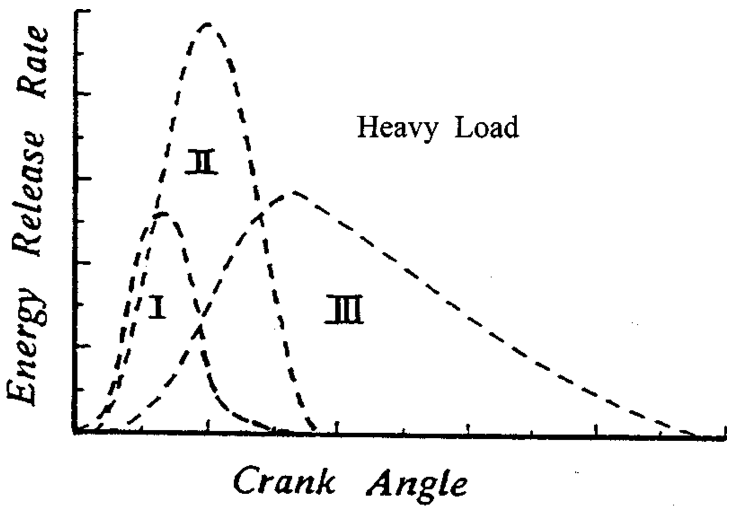

Figure 2. Schematic of energy release with heavy load. [9]

The contribution of each of these three parts to the total heat release depends on the load and a number of parameters. Especially the contribution of the third (III) part is strongly dependent of the load, as the concentration of the premixed fuel in the cylinder will vary in respect to the load. The premixed fuel-air charge is subjected increasingly to higher temperatures and pressures as piston approaches the top dead center (TDC). As temperature rises, the pre-ignition reaction activity in the cylinder can increase significantly and some partial oxidation of the premixed mixture can occur. These partial oxidation processes and products will affect the combustion following pilot fuel ignition. As the concentration of the premixed fuel in the charge is lower with light load, the contribution of pre-ignition reactions and the turbulent flame propagation of the premixed fuel-air mixture are consequently smaller. [9] The difference in heat release curves between light and heavy load are presented in Figure 2 and Figure 3, and as can be seen the contribution of the premixed fuel-air mixture (III) at light load is lower.

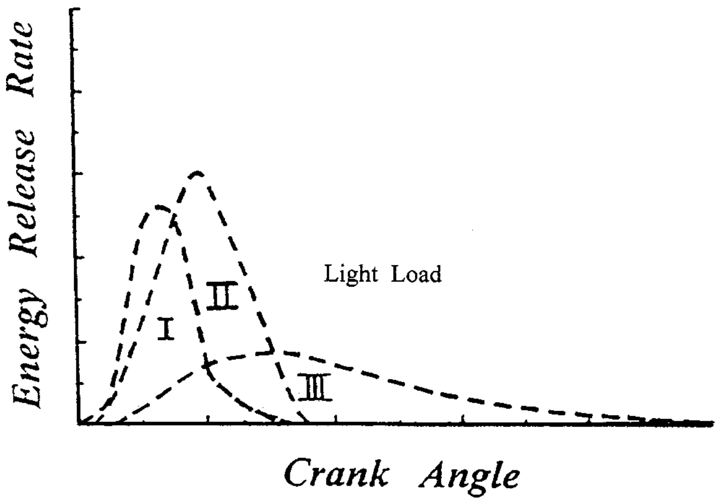

Figure 3. Schematic of energy release with light load. [9]

Figure 4 illustrates actual heat release rates of different load cases with constant pilot quantity. As it can be seen, the contribution of the third part increases as the load and, correspondingly, the concentration of the primary fuel increases.

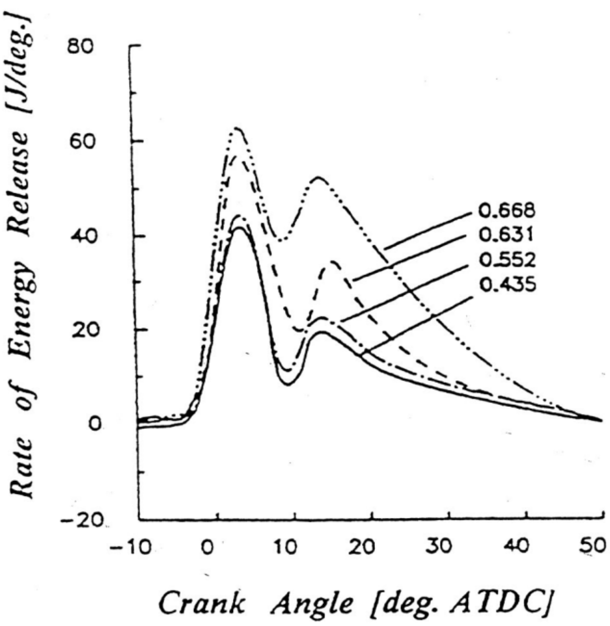

Figure 4. Effect of equivalence ratio on heat release rate with constant pilot fuel quantity. [9]

In addition to the three aforementioned components, Königsson [17] states in his thesis that there is a possible fourth contribution to the heat release, bulk ignition. Bulk ignition can occur at latter part of the combustion when large quantity of the remaining charge is ignited simultaneously. Figure 5 illustrates the hypothetical HRR curve according to Königsson. The numbering corresponds the labelling of figures 5 and 6, except number 4, which stand for the possible bulk ignition.

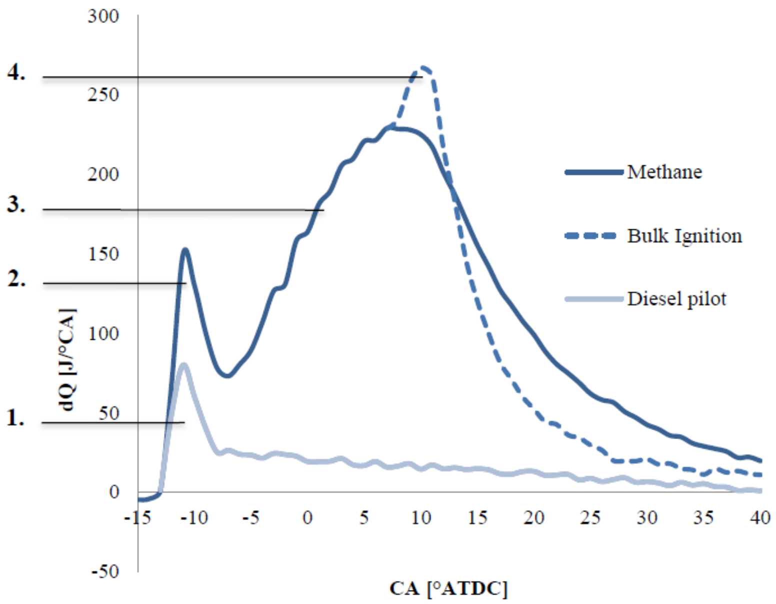

Figure 5. Hypothetical heat release curve of diesel dual fuel combustion.[17]

In summary, diesel dual fuel combustion consists normally of three major combustion processes, starting with the autoignition of diesel pilot fuel, followed by the combustion of primary fuel entrained and mixed with the pilot fuel spray, and finally ignition and turbulent flame propagation of the rest of the charge.

3.1.2 Ignition delay

When local air-fuel mixture is appropriate for ignition, the ignition in CI engine is dependent of the temperature and pressure affecting in the cylinder. Higher pressure indicates higher temperature resulting in shortened ignition delay. Karim states in his study that in dual fuel engines, the small quantity of pilot liquid fuel is injected into a mixture of gaseous fuel and air at mean temperature and pressure that may be different from the corresponding values for plain diesel operation. Hence, it would be expected that the processes of atomization, vaporization, and distribution of the small quantity of pilot fuel would be affected by any changes in the flow, thermal, and transport characteristics of the charge. [9] Factors such as pilot fuel quantity and quality, equivalence ratio and amount of residual gases in the cylinder have an effect on the processes related to diesel spray dispersion. When pilot fuel is injected to a homogenous mixture of fuel and air, the physical and transport properties of the mixture, namely lambda, are different compared to the cylinder charge in conventional diesel combustion. This results in longer ignition delay which is stated in several studies. [9], [21], [22] Duration of the ignition delay influences combustion quality as very short ignition delay results in poor dispersion of the ignition centers. On the other hand, too long ignition delay eventually leads to an increased number of misfiring cycles. Ignition delay influences the COV of IMEP, thus increased cycle-to cycle deviations require a higher margin towards knocking combustion and maximum cylinder pressure. Consequently the engine efficiency is reduced, thus optimal ignition delay is crucial to achieve. [23]

3.1.3 Knock and pre-ignitions

In dual fuel engines it is crucial that the premixed charge of primary fuel and air will not autoignite spontaneously at any point of the combustion process, as it affects the engine operation and in worst case scenario damage the engine. Depending on at what point the autoignition occurs determines whether there is onset of knock or pre-ignitions. Knock is defined as a phenomenon of excessively rapid rates of pressure rise in the cylinder, which is different for CI and SI engine. Diesel knock refers to the premixed part of the combustion where a significant amount of fuel is consumed at once and noise is generated. In SI engines knock refers to the autoignition of the unburned mixture ahead of the flame front causing very sharp pressure fluctuations able to damage the engine if allowed to progress uncontrolled. SI knock causes overheating of the walls as knock damages the boundary layer between the hot gases and cylinder wall. This, in turn, increases heat transfer losses leading to significant loss in efficiency. [9], [17] Due to the knocking phenomenon, the compression ratio of commercially available dual fuel engines operating with natural gas is limited to 11-13 compared to common value of 16 for diesel counterparts. [12], [23]

Königsson [17] has reported in his thesis concerning dual fuel operation with methane, that the heating of the cylinder walls caused by knocking can increase the tendency for pre-ignitions. A pre-ignition is a phenomenon of premature start of combustion of the premixed cylinder charge. This occurs before the injection of pilot fuel when there is locally high enough temperature for autoignition and ignitable mixture. A pre-ignition can lead to severe damages as pre-ignitions in the following cycles are likely to happen due to the bigger heat transfer to the cylinder walls of the first pre-ignition cycle. This is called runaway pre-ignitions as the control of the combustion is lost and it can damage the engine quickly. The reasons behind pre-ignitions can be divided to two categories: contribution of hot spots in the combustion chamber or pre-ignitions occurring at low speed in downsized, highly boosted, SI engines. For the latter category there are numerous parameters affecting the tendency for pre-ignitions and they are listed in the literature. [17] Pre-ignitions together with knock are issues at high load, and from those two the pre-ignitions are currently the limiting factor to the dual fuel efficiency and power density. [9], [17] The severity of the pre-ignitions compared to normal operation can be seen in Figure 6. In the figure is illustrated how the pressure curve of the pre-ignitions starts to incline before the pilot injection starts, hence indicating that the ignition started without the combustion of the pilot fuel.

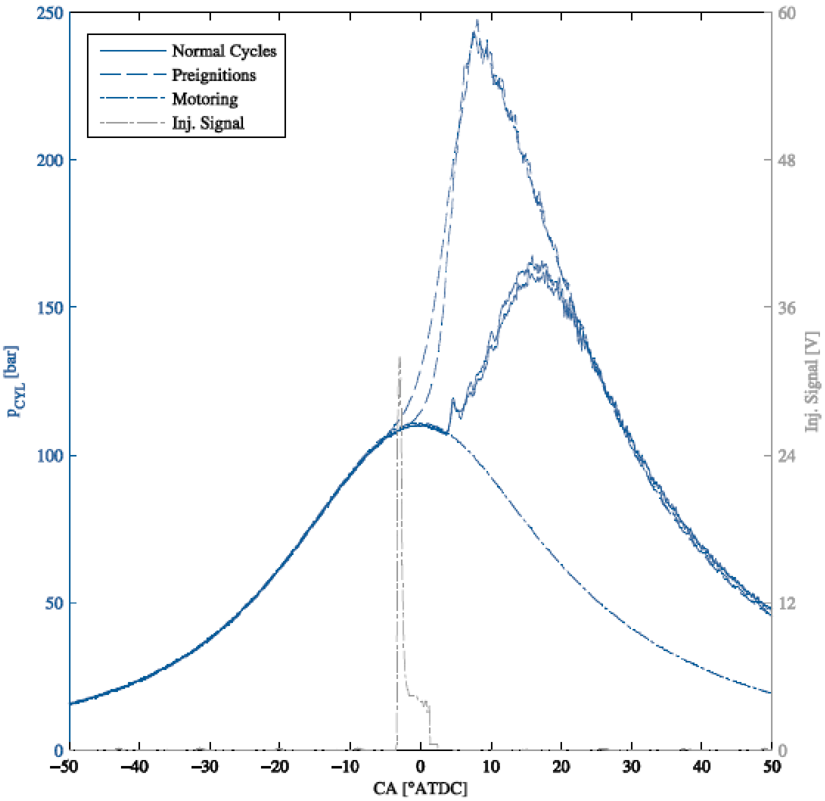

Figure 6. Cylinder pressure curves of normal combustion, pre-ignitions and motored operation. [17]

3.2 SI engines

Spark ignited engines are operating with Otto cycle, where the fuel is mixed with air prior to the ignition. Combustion is initiated with external ignition source, spark plug, where a spark is induced electronically. Due to this ignition type together with different properties of the fuels used in SI engines, the compression ratio is lower than in diesel engines. This in turn decrease the thermal efficiency of SI engine compared to diesel counterpart. SI engines are controlled quantitatively since the load is adjusted by controlling the air mass entering into the cylinder. Conventional SI engines operate with near stoichiometric, homogenous mixture of air and fuel. However, at low loads the air flow is needed to restrict in order to reach the stoichiometric mixture, and due to this the engine efficiency deteriorates as the air is needed to suck through the restriction. These pumping losses are the major reason for lower part load efficiency of SI engine compared to diesel one. [18]

The pumping losses can be reduced with lean burn strategies where the engine throttling is reduced. Some lean burn strategies have been developed both for heavy-duty and light duty applications. In light duty application is usually used so called stratified mixture formation where locally ignitable mixture is formed in the vicinity of the spark plug and rest of the cylinder charge is lean. This allows reducing the air throttling and improving the engine efficiency at part load. However, this can be usually applied only to lower torque and speed range in order to secure reliable combustion and output high engine torque. Depending on engine parameters, homogenous lean burn with conventional spark igtion is limited to lambda values in the range of 1 to 1.5 to prevent misfire and for optimum fuel consumption. [24], [25] In heavy duty applications, such as marine engines, the approach can be significantly different. As can be seen in Figure 7, which illustrates Wärtsilä SG engine operation for different air-fuel ratio and BMEP values, the desirable lambda value for the whole load range is around 2.2. In order to be able to reach such a high lambda values, a pre-chamber is used where a richer mixture is ignited and the exiting flames provide sufficient ignition energy for the overall homogenous lean mixture in the main combustion chamber. [26]

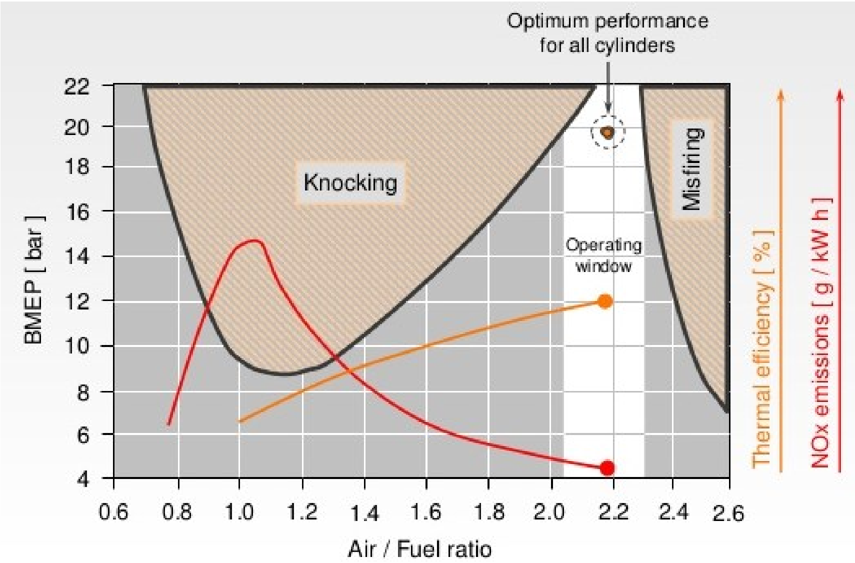

Figure 7. Operating chart for SG lean burn engine. [27]

3.2.1 SI combustion

In normal SI combustion the combustion of premixed charge proceeds from the spark plug as one turbulent flame front through the combustion chamber until it reaches the combustion chamber walls and the flame front extinguishes. An ignition delay is always present after the spark discharge as the chemical reaction require time to progress, and the energy from the discharge is too low to produce immediate combustion. Thus, the combustion starts properly after certain period of time and then proceeds rapidly. [25] In Figure 8 is presented a schematic of the heat release rate in SI engine, where it can be seen the shape of the heat release and, as well, the ignition delay.

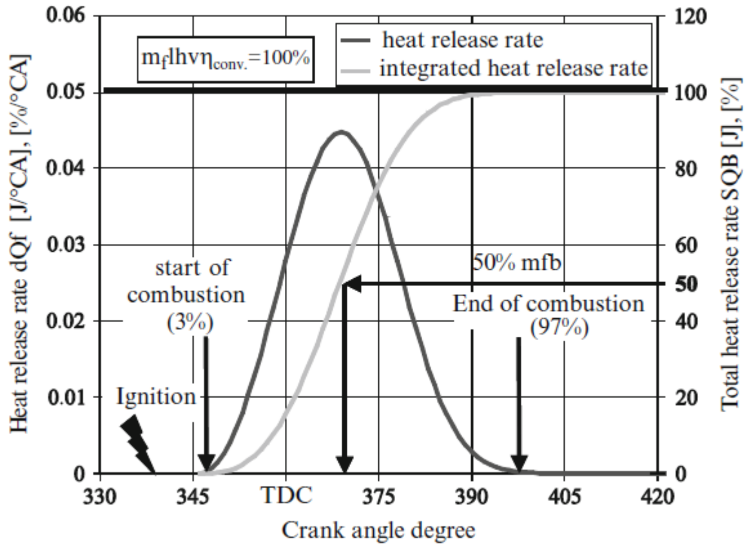

Figure 8. Presentation of heat release rate in SI combustion. [18]

In Figure 8 it is also illustrated the trend for mass fraction burned in relation to crank angles. Normally the combustion phasing is determined as a point in crank angles where 50% of the energy content of the fuel is released (CA50°). In the figure this is pointed out with label 50% mfb. The main parameter for adjusting the combustion phasing is ignition timing, or more commonly spark timing. The aim is to adjust the spark timing so that the efficiency is the highest possible. The maximum efficiency is achieved when operating as close as possible to knocking limit, at so called maximum brake torque timing, MBT. Several factors affect the spark timing such as, for example, engine speed and load and air-fuel ratio. As it was described in previous chapter concerning dual fuel combustion, knocking needs to be avoided in order to protect the engine. Figure 9 illustrates the typical pressure curve for normal combustion and for both combustion with slight and intense knock.

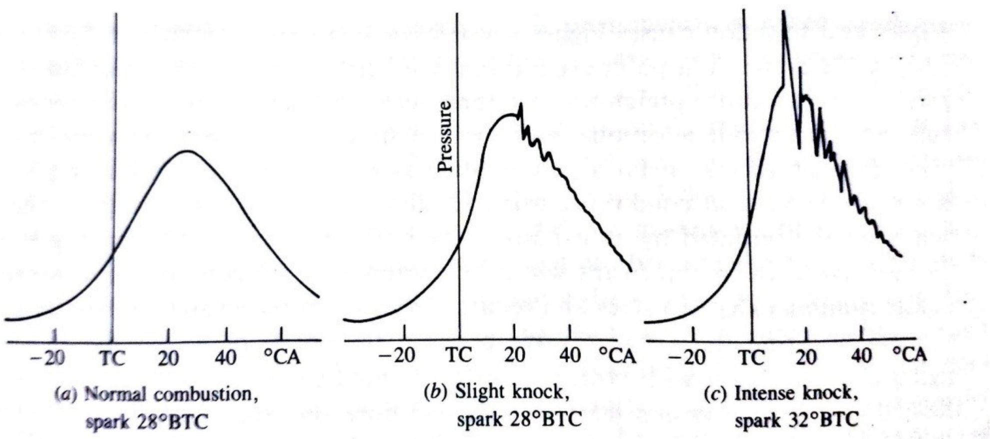

Figure 9. In-cylinder pressure traces for normal and knock combustion. [25]

4 Parameter effects on combustion

4.1 Dual fuel combustion

4.1.1 Injection timing

Combustion phasing plays a key role in the engine performance and emission formation as it affects directly to peak pressure and temperature of the combustion. The main parameters to have an effect on combustion phasing are injection timing and strategy. Especially at low loads combustion phasing has a significant influence on emissions and efficiency as dual fuel engines are unthrottled and operating with very lean homogenous mixtures. [9] Thus following discussion is focused on combustion phasing at low loads using single pilot injection with timing similar as in conventional diesel combustion.

At constant equivalence ratio, advancing the injection timing causes the combustion to shift to earlier stage of the compression stroke. Due to that the peak pressure and temperature are increasing as more of the fuel is burned before the top dead center (TDC). However, eventually the increasingly advanced injection will cause the combustion to retard. This is believed to happen due to more dispersed pilot spray in the cylinder, as too much advancement causes the spray to miss the piston bowl. Also the ignition delay is increased due to the lowering temperature level with increasingly advanced injection timing. Anyhow, more dispersed spray leads to a more homogenous heat release which in turn enables the use of advanced combustion modes such as HCCI and RCCI. [17], [28] These advanced modes, however, are out of the scope of this thesis and will not be discussed further. The aforementioned effects with methane DF combustion are illustrated in Figure 10, where the abbreviation SOE stands for start of energizing of the injector. As it can be seen, in this specific study advancing injection more than 25 CAD will retard the combustion.

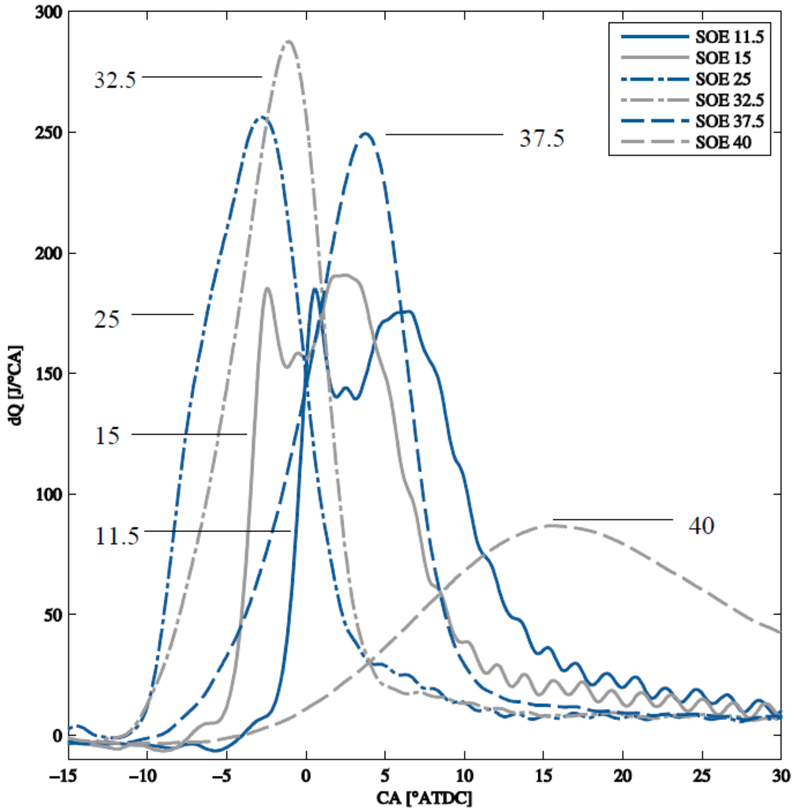

Figure 10. Effect of injection timing on heat release rate. [17]

As HC emissions are known to be a challenge in dual fuel engines at low load, they could be reduced significantly with injection timing. Several studies report that advanced injection timing reduces unburned HC emissions and increases combustion efficiency at lean mixtures. This behavior is believed to be a result of both longer ignition delay and earlier combustion phasing. Longer ignition delay could allow a better spray penetration and development, which in turn creates a larger mixture of pilot fuel, gaseous fuel and air. As combustion starts earlier due to the advanced injection, and larger amount of mixture is ignited simultaneously, combustion occurs faster and temperature is higher leading to lower HC emissions. The CO emissions behave similarly to HC emissions, but as NO_x emissions are formed increasingly with increasing temperatures, the NO_x formation increases with advanced injection. Nevertheless, as advancing the injection leads to a reduction in HC and CO emissions, it indicates that combustion efficiency is improved. Improvement in combustion efficiency could be a result of the longer period of high temperatures within the cylinder improving the oxidation of partially burned HC and CO.[17], [29] Figure 11 illustrates the relationship between the injection timing and different emissions for methane DF combustion.

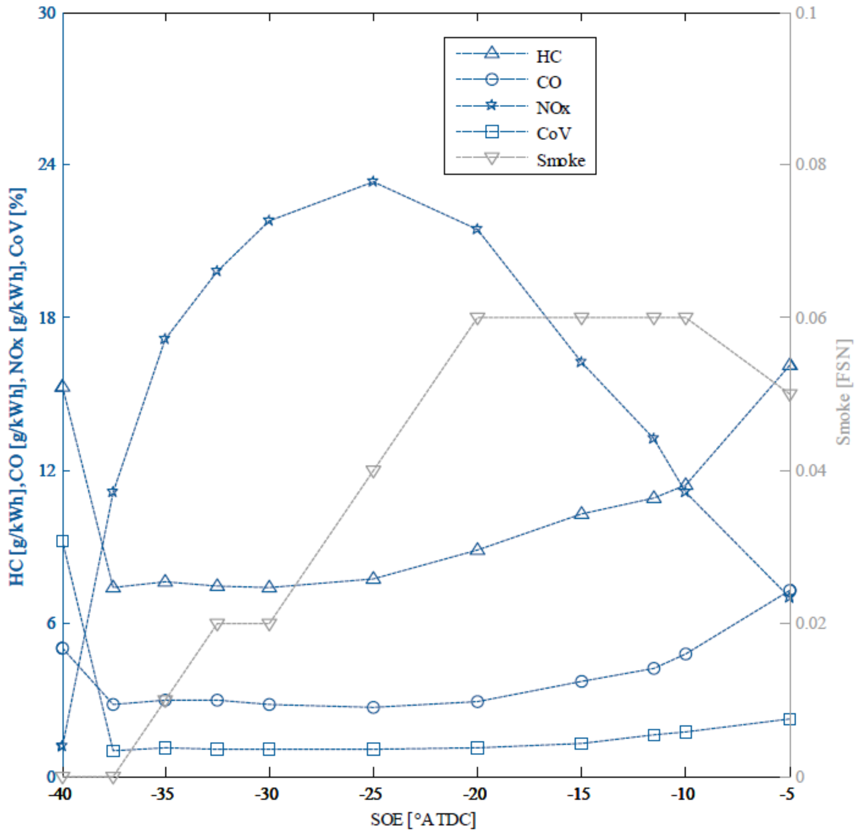

Figure 11. Emissions of HC, CO, NO_x, Smoke and CoV of IMEP in relation to injection timing. [17]

In the figure it can be also seen the behavior of HC and CO emissions when injection is excessively advanced. Königsson [17] states that as injection is advanced beyond 25° BTDC and the diesel spray becomes more and more dispersed, smoke and NO_x are reduced simultaneously without any penalty to HC or CO. At SOE of 40° BTDC, however, combustion stability deteriorates and emissions of HC and CO increases because of complete and partial misfire. [17] In addition to the direct effects on emissions, injection timing has also a crucial effect on engine knock, which was earlier described one of the challenges in dual fuel engines. Advancing injection too much, the tendency for knocking is increased and the engine output torque is reduced [29]. Injection timing has clearly a great influence on combustion behavior, which makes it one of the major parameters for controlling the combustion.

4.1.2 EGR

The presence of residual gases increase the ignition delay as the cylinder charge is diluted thus results in reduction of both the partial pressure of oxygen and the associated reaction activity. This leads to the corresponding changes in the effective temperature level during combustion. As the residual gases have higher specific heat, the compression temperature is also reduced, which increases the delay further. [9], [21] The residual gases can be trapped in the cylinder either via internal EGR or external EGR. At light load the influence of residual gases plays more important role as they can include partially reacted products which can have an important chemical and thermal effect on the ignition and combustion of the next cycle [22].

EGR has a strong influence on emissions as it can be used for phasing the combustion. More EGR means more dilution in the cylinder charge and combustion duration is increased. In addition, recirculated exhaust gases act as inert gases and they absorb some of the released heat of combustion as they are heated up. The combined effect of slower combustion and heat absorption leads to lower peak pressure and temperature, and NO_x emissions are reduced. PM emissions have tendency to increase in respect to increase in EGR, but with homogenous dual fuel operation PM emissions are otherwise very low, thus EGR does not have that big of an influence on overall PM emissions. EGR can be used to increase equivalence ratio of the in-cylinder mixture. As it is known, fuels have specific flammability limits and below certain equivalence ratio the flame cannot propagate properly. When EGR is increased it replaces corresponding amount of air in the cylinder and equivalence ratio is increased. However, using too much EGR will lead to over dilution of the charge and flame propagation suffer. Therefore excessive use of EGR leads to increase in HC and CO emissions and the correct balance between equivalence ratio and EGR rate is needed to study carefully.[30] As EGR lowers the compression temperature it reduces the risk of pre-ignitions as well [17].

4.1.3 Diesel substitution ratio

The diesel substitution ratio determines the combustion characteristics as it has a strong effect on the combustion phasing and emissions. It also determines whether the engine operates more similar to SI or CI operation as the bigger the substitution ratio, the smaller the premixed combustion part of the diesel pilot, and bigger portion of the total heat release comes from the turbulent flame propagation of the premixed cylinder charge. [17], [28] Simple illustration of the substitution ratio can be found in figure 15.

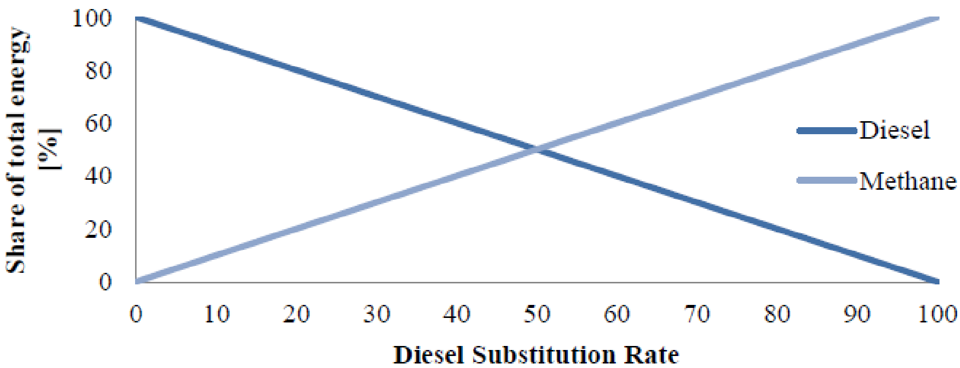

Figure 12. Diesel substitution ratio of NG/DDF engine in percentages. [17]

Ignition characteristics of the cylinder charge depend on the substitution ratio as bigger quantity of the high reactivity fuel forms bigger region of high reactivity charge. Serrano et al [30] have investigated NG dual fuel combustion and stated that an increase in the substitution ratio leads to a prolonged ignition delay due to the smaller portion of pilot injection, and due to the chemical interactions between diesel and gaseous fuel. In addition, local lambda is increasingly affected by increasing substitution ratio since the gaseous fuel replaces some of the air around the diesel spray. The quantity of diesel pilot enhances the first part of the combustion, determining the conditions for the following flame propagation of the primary fuel. It is shown for different gaseous fuel and gasoline dual fuel combustion, that the pilot quantity has a major effect on the ignition delay as the delay is reduced with increased amount of pilot. Larger quantity improves the pilot injection characteristics and forms locally richer mixture increasing the reactivity of the mixture, and resulting a reduction in the ignition delay. [31], [32] However, as it can be seen from Figure 13, increasingly larger pilots tend to have a smaller effect on the delay, whereas relatively small increases can lead great reduction in the delay (0.2 kg/h vs. 0.3 kg/h). [21] Due to that pursuing high diesel substitution ratio is possible, as even relatively really small pilot quantities can reduce the ignition delay significantly [9]. In Figure 13 the three most upper curves illustrates the point of ignition for dual fuel operation with different pilot quantities.

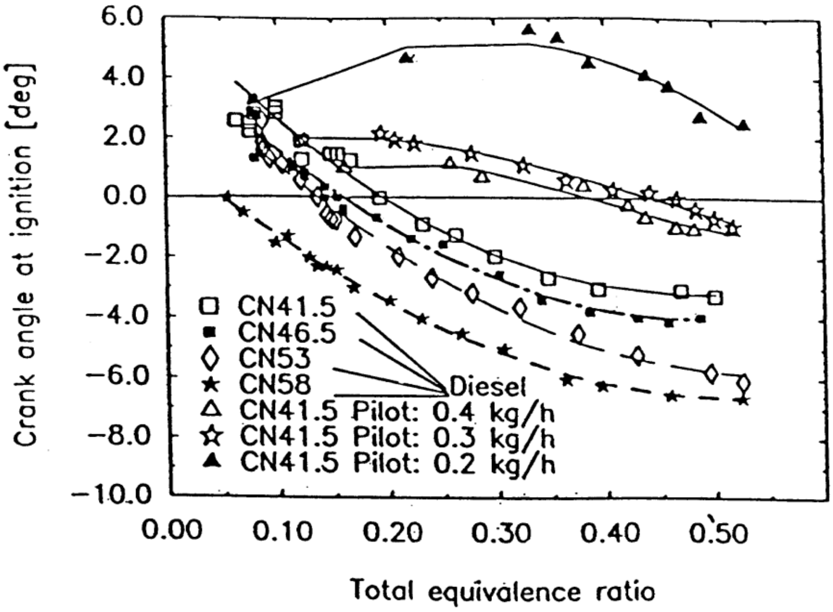

Figure 13. Variations of the point of ignition for different diesel qualities and dual fuel operation with different pilot fuel quantities. [21]

However, with constant pilot quantity, increasing the substitution ratio increases the equivalence ratio correspondingly, which in turn has certain effects on the ignition delay. Gunea [21] states in his study, that the gaseous fuel within the intake air produces variations in the properties of the charge. The variations in the specific heat ratio and the intake partial pressure of oxygen occur due to the displacement of air by the gaseous fuel. These affect the heat transfer within the cylinder charge, the temperature at TDC and the pre-ignition reaction activity and its associated energy release. Thereby, there are substantial effects on the pre-ignition processes of the pilot fuel and correspondingly on the length of the delay period. As the equivalence ratio increases, the ignition delay of the pilot diesel fuel initially increases both due to the reduction in partial pressure of oxygen and the reduction in the temperature of the charge at TDC. After certain maximum value of ignition delay, equivalence ratio is high enough and the pre-ignition reaction of the premixed charge increases resulting an increase in temperature, and a reduction in ignition delay [9], [22]. Figure 14 illustrates the effect of equivalence ratio on the ignition delay in dual fuel combustion with different gaseous fuels.

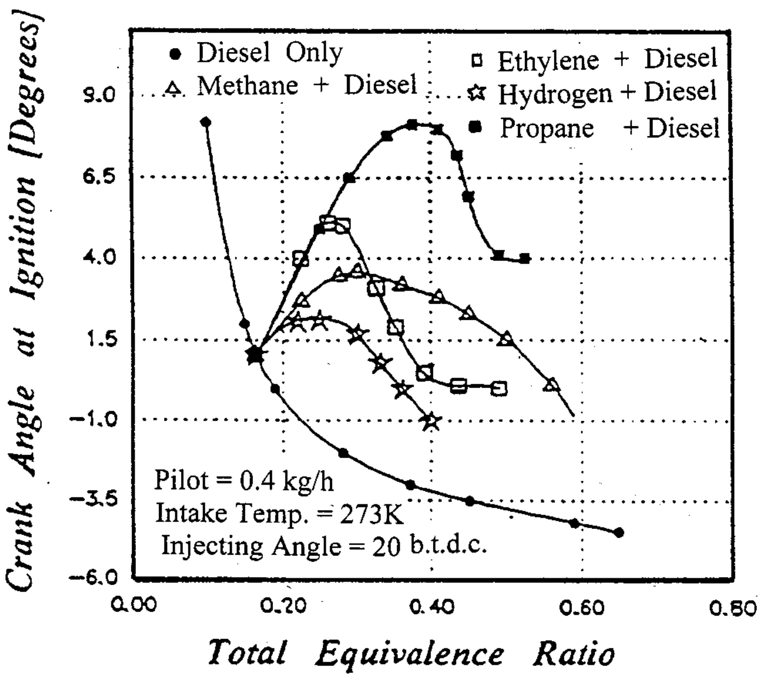

Figure 14. Ignition delay with constant pilot quantity for different fuels. [9]

As the ignition is strongly dependent on the substitution ratio, in terms to maximize the efficiency and minimize the indicated specific fuel consumption (ISFC), optimal values for the injection timing for different substitution ratios is necessary to study. [32], [33] Duffour et. al [32] have studied dual fuel combustion with gasoline, and in their research they observed, that the injection is needed to advance with increased substitution ratio in order to keep the combustion phasing approximately the same. This is also illustrated in Figure 15 where pressure and HRR curves for methanol dual fuel combustion are presented. As it can be seen from the start of the heat release, the ignition delay is increased as substitution ratio increases. Also the compression pressure is increasingly reduced with increasing substitution ratio due to the cooling effect of methanol evaporation. [34], [35]

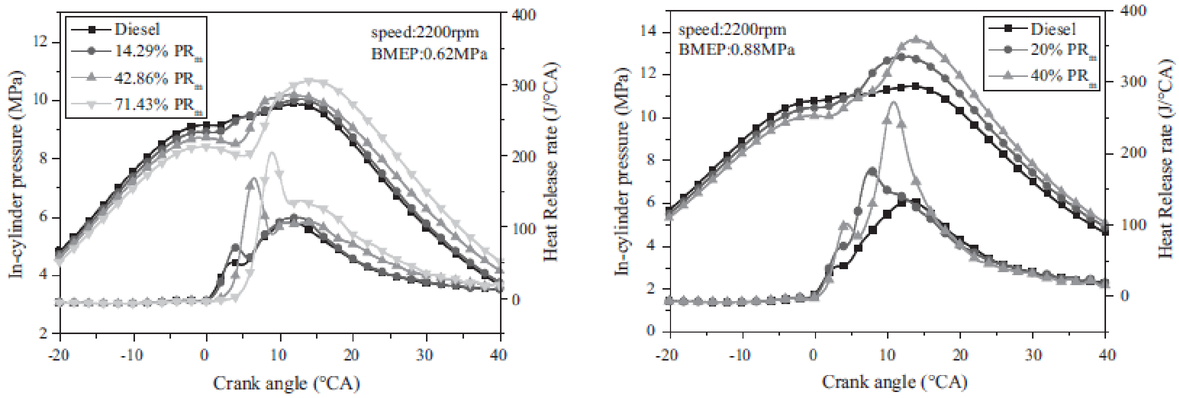

Figure 15. In-cylinder pressure and HRR at different loads for different substitution ratios. [34]

The substitution ratio affects also the combustion duration, as higher substitution ratio results in faster combustion of the premixed charge, and the overall combustion duration is reduced. This can be also seen in Figure 15 since the start of the combustion is later with higher substitution ratios, but the combustion is finished roughly the same time.

As substitution ratio is varied, it leads to corresponding variations to the pilot quantity and equivalence ratio. The flame propagation in dual fuel engine is affected strongly by the equivalence ratio as within very lean mixtures no consistent flame propagation will take place from the ignition centers and pilot fuel influenced burning regions [9]. This poor flame propagation with very lean mixtures is the reason for high HC emissions at light load. There exists a certain threshold value for the equivalence ratio, after which proper flame propagation occurs. This is called the flame spread limit. It determines the lowest concentration of the fuel mixed in the air which is able to provide the flame propagation. The flame spread limit is affected not only by the equivalence ratio but the pilot quantity as well. Pilot quantity affects the limit such a way, that as the quantity is increased, flame propagation is possible in leaner mixtures. [36], [37] This trend is illustrated in Figure 16.

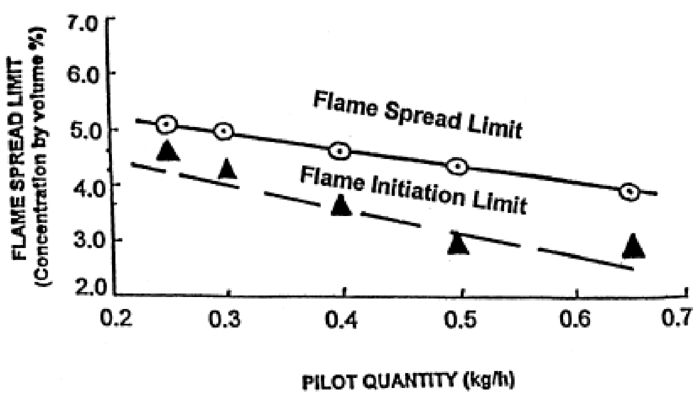

Figure 16. Flame spread limit of methane for different pilot quantities.[36]

Wang et al [38] have studied the operating range of a heavy duty dual fuel engine using methanol as a primary fuel. Results indicate that with different loads the methanol substitution ratio (MSR) was needed to be varied in order to retain stable combustion. According to the study, the MSR is limited at different loads by partial burn, misfire, combustion noise and knock. Partial burn occurs at low load when the MSR is increased too much and proper flame propagation does not occur. At low to medium loads the limiting factor is misfire. Increasing the MSR and simultaneously reducing the diesel pilot a limit is reached where the pilot quantity and in-cylinder temperature are too low for providing autoignition. Increasingly reduced pilot quantity eventually leads to misfire and reduction in engine efficiency. Misfire can also promote the following limiting factor, roar combustion, at medium to high load. Roar combustion, or combustion noise, is limiting the substitution ratio at higher loads as the HRR increases too much and pressure rise is too rapid. When misfire takes place, higher reactivity mixture is trapped partially in the cylinder for the next cycle, and it can promote premature ignition increasing the pressure rise rate correspondingly. As load is increased towards the maximum load, the limiting factor is knock or pre-ignition. [38] The substitution ratio at higher loads could be increased when using split injection. Sarjovaara et al [39] studied the use of RE85 in a dual fuel engine, and observed that splitting the pilot injection in two decreased the pressure rise rate. This could indicate that it could be a solution for using higher substitution ratio at high loads, where the excess pressure rise rate was a limiting factor. [39] Figure 17 presents the aforementioned combustion boundaries for different methanol substitution ratios. The same figure illustrates the brake thermal efficiency (BTE) contours, and it can be seen that at low loads the BTE is rather poor, but at medium to high loads BTE is improved. Similar trend of improving BTE at high loads with increasing methanol substitution ratio has been reported in several studies. [40]–[43]

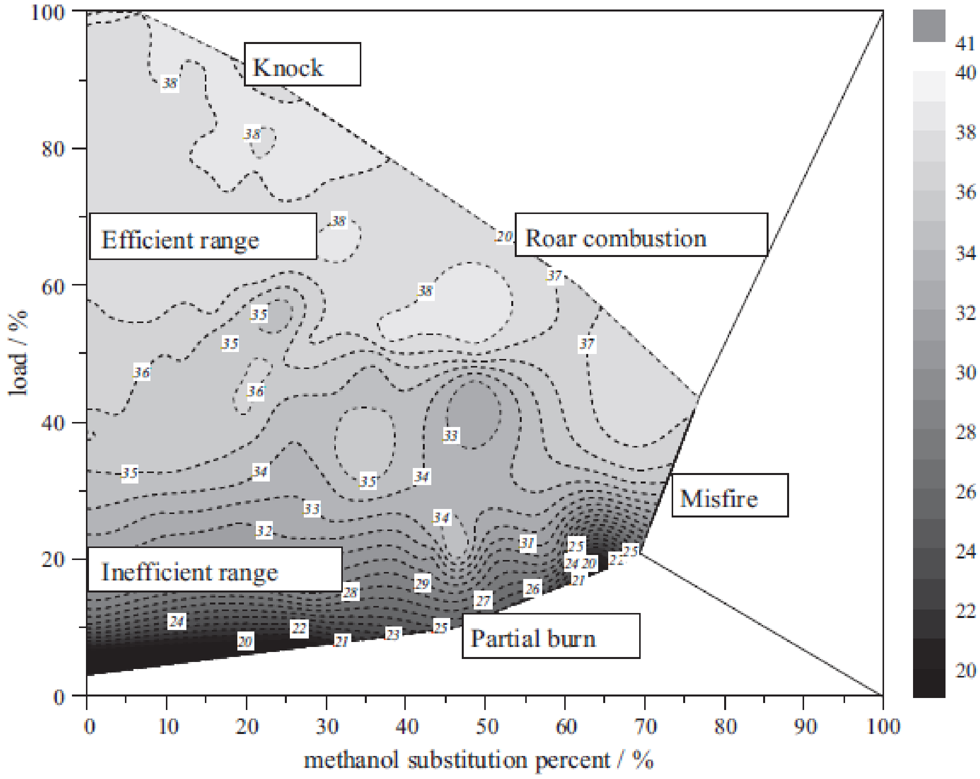

Figure 17. Operating range of methanol dual fuel engine. [38]

Rong et al. [28] have studied combustion of gasoline in optical dual fuel engine and observed that increasing the substitution ratio the ignition location gradually moves towards the cylinder center. This is due to the fact that with increased substitution ratio the pilot quantity is reduced, which in turn reduces the injection duration and spray penetration. Thereby the region of the highest reactivity mixture is located closer the center of the combustion chamber. [28] Figure 18 shows the combustion process for different substitution ratios, where γ represents the substitution ratio.

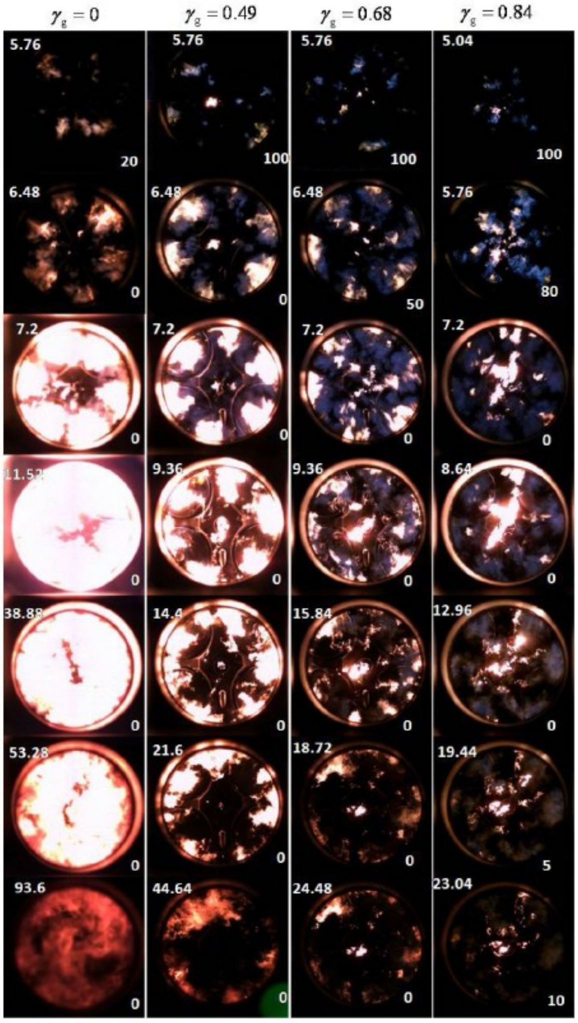

Figure 18. Optical visualization of the combustion process for different substitution ratios. [28]

The optical results show clearly the trend of the ignition location closing on the center of the combustion chamber with increasing substitution ratio. Ignition of the diesel pilot is shown as yellow spots at the beginning of the combustion and those spots moves closer to the center with increasing gasoline/diesel ratio. However, Dronniou et al [37] have conducted similar studies with methane, which has significantly higher octane rating, and observed that in the case of methane the ignition of premixed fuel initiates from the near-wall-region with both low and high substitution ratios.

Figure 18 also shows the effect of substitution ratio on emission formation, especially on soot formation. As can be seen, in pure diesel mode the combustion consists solely of yellow flames, which indicates large amount of soot emitted. On the contrary, with high substitution ratios the combustion consists mainly of blue flames from premixed gasoline combustion. This similar trend of smoke reduction is also observed in the study of Duffour et al [32] in which gasoline dual fuel engine was also investigated. Several studies report reduction in the particulate matter emissions with methanol dual fuel combustion as well. Reduction in PM emissions is reported to apply from low to high load. [34], [40], [41], [44] Using high substitution ratios the typical NO_x -soot tradeoff behavior known in conventional diesel engines can be discarded. Both NO_x and soot emissions approaches zero with increasing substitution ratio [34]. Figure 19 illustrates this behavior where A and B are different engine speeds, 1000rpm and 2200rpm respectively, and the numbers following A and B indicates the BMEP.

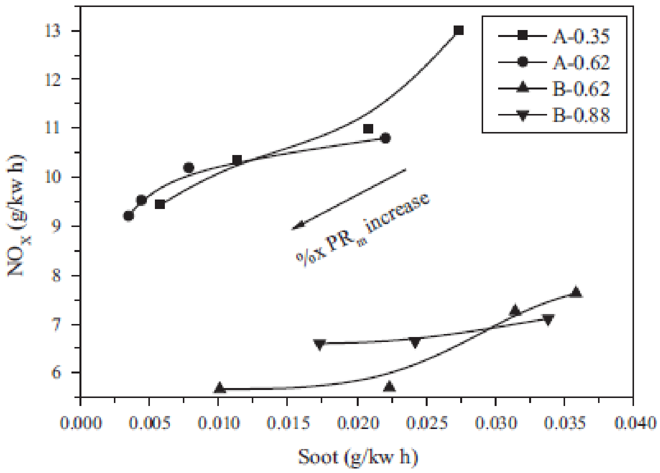

Figure 19. Relationship between NO_x and soot. [34]

Similar decreasing trend of NO_x emissions with increasing substitution ratio is reported also in other studies concerning methanol dual fuel combustion. [40], [42] However, as the total NO_x emissions decrease, there is a significant increase in NO_2 emissions. Increased NO_2 emissions can be explained by the formation mechanism of NO_2. It is formed mainly from the reaction of NO with HO_2 where the free radical HO_2 is a product from the methanol oxidation. Thus, methanol acts as a source for NO_2 formation, and increasing the substitution ratio the fraction of NO_2 of the total NO_x emissions increases. The overall reduction in NO_x emissions is a result of lower combustion temperature due to the methanol evaporation, and shorter period of high temperature present in the cylinder due to the faster combustion of premixed methanol-air charge. Also increased ignition delay contributes better mixing of the pilot fuel thus reducing locally rich regions resulting lower combustion temperature as well. [34], [40], [42] In dual fuel engines operated with methane, or natural gas, the NO_x formation trend can be significantly different. Königsson [45] has performed an emissions comparison between normal diesel operation, methane dual fuel operation with two different substitution ratio and SI combustion of methane. The comparison is illustrated in Figure 20.

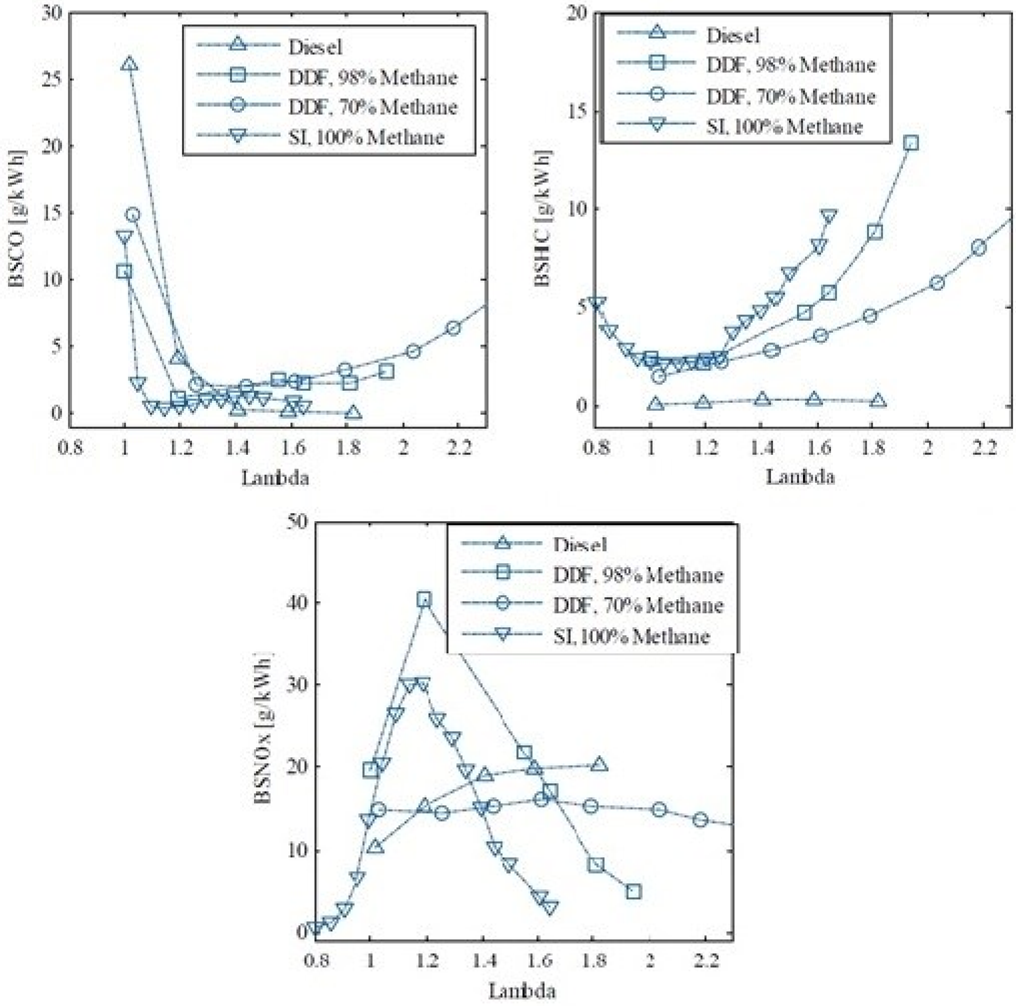

Figure 20. Emissions comparison between methane dual operation, SI and diesel operation. [45]

The Figure 20 clearly indicates the effect of substitution ratio on emissions formation. As can be seen, excess air coefficient λ together with substitution ratio plays an important role in the emission formation, especially in NO_x formation. NO_x emissions can be reduced significantly using high values of λ with high substitution ratio. However, with λ close to stoichiometric value, increasing the substitution ratio leads to very high NO_x formation.

In methane DF combustion the emissions of HC are increased together with increased substitution ratio. Due to increased substitution ratio richer cylinder charge is trapped in to the crevices. This behavior is enhanced at high λ as the charge becomes excessively lean for oxidizing the HC escaping the crevices in expansion stroke. [45] The trend is similar to methanol DF combustion as the total HC emissions together with CO emissions increase with increasing methanol ratio. [34], [40], [42], [43] In addition to richer premixed mixture trapped in the crevices with higher substitution ratios, with methanol the lower in-cylinder temperature results in bigger portion of incomplete combustion which in turn increases the HC and CO emissions. However, with methanol diesel oxidation catalyst is a viable solution for reducing the HC and CO emissions. Investigations have shown that with DOC the emissions of HC and CO can be decreased near to the same level than in corresponding diesel engine. [40], [42], [43] Although, the catalytic efficiency with high substitution ratio is relatively low at low engine speed and load due to low exhaust temperature. Therefore, the substitution ratio cannot be too high for these conditions. [34] In addition to the regulated emissions, methanol dual fuel engines produce increasing amounts of unregulated emissions of unburned methanol and formaldehyde as substitution is increased. Fortunately, both of the unregulated emissions can be treated efficiently with DOC. [34], [40], [41] The effect of substitution ratio on emissions clearly indicates that the nature of the combustion depends directly on the substitution ratio. Higher the substitution ratio, closer the combustion and emission formation is to SI operation.

4.1.4 Compression ratio and inlet temperature

Compression ratio is one of the major engine design parameter and it is the key factor determining the temperature and pressure at the end of the compression stroke. Higher compression ratio naturally results in higher compression temperature. Compression ratio has a direct effect on the thermal efficiency of an engine as with higher compression ratio the combustion gases can expand further, thus more work is done against the piston. [25] As it was earlier mentioned, the commercial engines available use compression ratio of 11-13. In pure diesel mode, however, the efficiency is reduced with such low compression ratios. Christen et al. carried out a simulation study with methane which indicated that variable valve timing combined with two-stage turbocharging can enable the use of higher compression ratio. In dual fuel mode strong Miller is used to prevent knock whereas in diesel mode full potential of diesel fuel can be obtained by increasing effective compression ratio. This is accomplished by reducing the Miller timing. [23]

Intake air temperature affects directly to the mean temperature of the charge during the pilot injection, which in turn affects the flame spread limit of the premixed charge. It is shown that increasing the inlet temperature, flame can propagate in leaner mixtures. [36] As the flame propagation is enhanced with higher inlet temperature, it reduces the emissions of HC and CO. On the other hand, higher temperature leads to higher emissions of NO_x. Additionally, high inlet temperature increases the tendency for knock and pre-ignitions at high load. In order to avoid knock and pre-ignitions without lowering the compression ratio, measures such as lowering the intake air and engine coolant temperatures and retarding the pilot injection can be performed. Therefore, higher inlet temperatures can be utilized primarily at light load to reduce the amount of throttling due to the smaller density of air in higher temperature. [45] However, with methanol the charge temperature decreases due to the fuel evaporation, thus the maximum cylinder temperature is decreased correspondingly. This is illustrated in the figure 19 where a comparison of diesel combustion and dual fuel combustion is performed. D stands for diesel and D+M for methanol dual fuel combustion. [46] As it can be seen, the drop in temperature is significant.

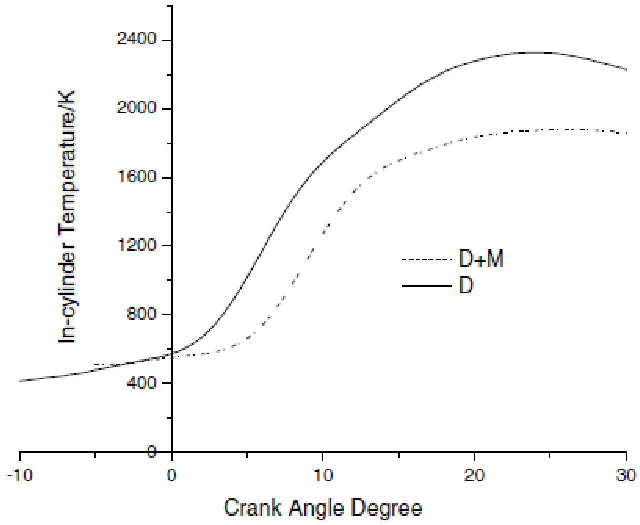

Figure 21. In-cylinder temperature for both diesel and dual fuel combustion at 80% load. [46]

4.2 SI combustion

4.2.1 Ignition timing

Spark timing determines the combustion phasing and knocking is avoided by adjusting the timing when necessary. Common knowledge, which is stated in every subject related textbook and article, is that when knock occurs it is suppressed by retarding the spark timing. Due to this the combustion shifts towards exhaust stroke and peak pressure reduces.[8], [18], [25], [47] For the same reason, the NO_x emissions are reduced as the peak temperature is reduced. Downside for this is that fuel consumption will deteriorate and increased exhaust gas temperature might cause some problems for example with the turbine of a turbocharger.[26] Although, higher temperature at the late phase of expansion stroke can help oxidizing the unburned HC flowing out of the crevices as piston moves downwards.

Xie et al.[48] carried out experimental study of the influence of engine load control strategy based on EGR and ignition timing on performance and emissions under the condition of stoichiometric mixture and WOT. It was noticed that advancing further the ignition timing it can extend the tolerated EGR limit. Therefore, for the load control method of using EGR and ignition timing with WOT, the proper ignition timing can enable higher level of EGR, extend the control range of load and also can be expected for it to secure good combustion process and performance.[48] The ignition timing is reported to have similar effect on combustion with lean mixtures than with EGR. Advancing the timing allows using leaner mixtures until the lean burn limit of the fuel is reached. In fact, the timing is needed to advance with lean mixtures in order to ensure stable combustion and maximum torque. [47]

4.2.2 Inlet temperature

Inlet temperature has the similar effects on the combustion than it is described in the previous chapter concerning parameter effects on dual fuel combustion. For SI operation, volumetric efficiency with different fuels was investigated in the study of Wyszynski et al.[49]. It was noticed that with methanol improvements in volumetric efficiency was achieved with increasing inlet temperature. This is due to the higher saturation pressure of the high temperature air. In other words, fuel evaporation is limited at lower temperature levels due to low saturation pressure of the fuel vapor. As more methanol is evaporating at higher temperatures, it results in enhanced cooling effect of the charge and, consequently, higher volumetric efficiency. On the contrary, with gasoline the volumetric efficiency was decreasing with increasing temperature as the saturation pressure was not reached at any tested temperature level. As gasoline was evaporated completely with the lowest temperatures, increasing the air temperature decreases the density of air and volumetric efficiency correspondingly. [49]

4.2.3 Air-fuel ratio

Air-fuel ratio has a significant effect on the engine knocking sensitive which is illustrated in the study of Zhen et al. [50] in which they were investigating knock limits of methanol combustion. They reported that the knock intensity peaks at lambda 1 and then decreases for both lean and rich mixture. Richer mixture enables greater knock suppression than lean mixtures, because of the cooling effect of evaporating fuel and possibly also due to the faster flame propagation of richer mixture. Faster flame propagation could ensure that the flame propagates through the unburnt region so fast that the autoignition conditions in the unburnt mixture is not reached. However, with rich mixtures the combustion efficiency deteriorates as there is not enough air to oxidize all the fuel. [50]. Studies with lean mixtures of methane have been also conducted and increasing knock suppression was reported with increasingly lean mixtures. The excess air absorbs part of the heat released during combustion resulting in lower temperature. In addition to this, combustion is slower with lean mixtures and in-cylinder peak pressure is decreased. [23], [47]

In addition to knock suppression, lean combustion can be used to reduce throttling losses and to improve engine efficiency. Methanol combustion was investigated in the study of J. Vancoillie et al. [51] in which it was reported that with lean combustion, lambda 1.14, the indicated efficiency is improved by 3% compared to throttled engine [51]. Einewall et al. [52] studied two different strategies for diluting the mixture of methane and air. The other strategy is simply to use lean burn strategy whereas the other is to use stoichiometric mixture diluted with EGR and using TWC for aftertreatment. With carefully designed high turbulence combustion chamber, they were able to operate the engine at lambda 1.6 and the brake efficiency with lean combustion was very close to 40%. The efficiency with lean combustion was slightly higher than with the EGR strategy but, on the other hand, the EGR strategy with TWC reduced 99,9% of NO_x emissions and 90-97% of HC emissions compared to the lean burn strategy. [52]

Combusting increasingly leaner mixtures require higher ignition energy and conventional spark plug ignition can provide reliable combustion until certain point. Using a pre-chamber with a spark plug and pilot injection, leaner mixtures can be combusted. The overall mixture in the main combustion chamber remains lean whereas in the pre-chamber the mixture is close to stoichiometric. This lean burn technology is tested with methane by several authors. Getzlaff et al. [53] studied pre-chamber spark plug with pilot injection and compared it to a case without pilot injection. Lambda value for pilot injection was able to reach approximately 1.7 whereas without pilot injection the lambda was limited to around 1.3. Compared to stoichiometric combustion at part load, the fuel consumption of the lean combustion with pilot injection was reduced by 10% and NO_x emissions by 98%. [53] Different approach for achieving substantially lean mixture were investigated by Davy et al. [54] since in their study partially stratified charge was used in methane combustion to enable lean mixture. Near spark plug was formed a rich mixture whereas rest of the mixture was lean. They were able to use lambda values up to 1.74 with stable combustion and, similar to the other studies, NO_x emissions were decreasing with the use of this strategy. [54] Figure 22 illustrates the emissions formation trends of conventional SI engine for different equivalence ratio.

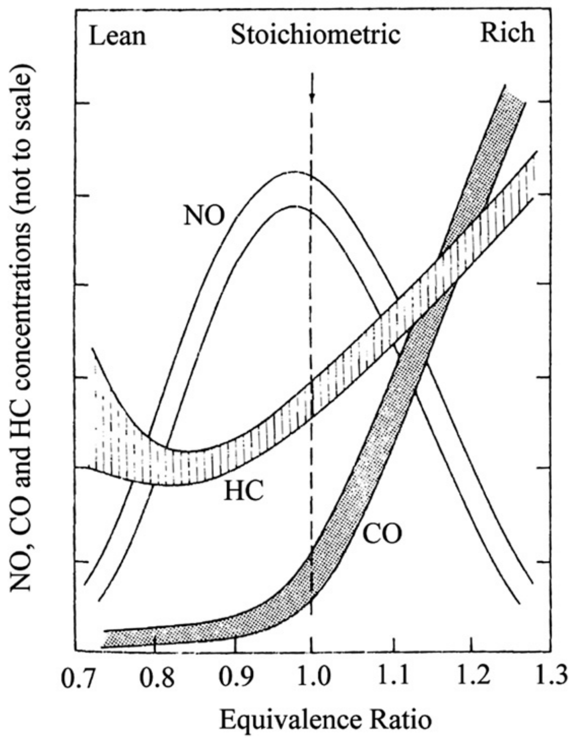

Figure 22. Emission formation trends for different equivalence ratio. [25]

The air-fuel ratio has also effect on the volumetric efficiency depending on the fuel used. The maximum volumetric efficiency increases with less volatile fuels when lambda increases. As it was mentioned in previous chapter, saturation pressure limits the amount of fuel which can be evaporated with certain air-fuel ratio. Methanol having low molar air-fuel ratio, more methanol is injected for the same lambda value compared to gasoline, thus the air reaches saturation point faster. When the in-cylinder lambda increases, the relative amount of methanol decreases thus more of it evaporates and cools down the mixture resulting improved volumetric efficiency. For volatile fuels such as gasoline, the efficiency decreases as all the fuel is evaporated even with rich conditions, and no further cooling effect will be present for larger air mass as lambda increases. In other words, with increasing lambda the air mass relative to the fuel mass increases resulting that the same fuel mass has to cool down larger amount of air. Due to this the temperature of the air entering the cylinder increases and the volumetric efficiency decreases. [49]

4.2.4 EGR

For given ignition timing, the combustion duration is prolonged and COV of IMEP is increased with increasing EGR rate. Increased EGR will decrease the temperature and flame propagation speed, but also the sensitivity for misfire and partial burning cycles increases. [49] This unwanted behavior is illustrated in the study of Korakianitis et al. [12] in which stoichiometric combustion with natural gas was studied. It was reported that increasing EGR can lead to increased UHC emissions as the mixture becomes overly diluted. [12] Amount of EGR is restricted by the presence of unstable combustion since the cyclic variations will increase with higher dilution levels. Cyclic variations reduce the mean efficiency of the engine and can make the engine unfit for driving purposes. Diluting the mixture will reduce the turbulent burning velocity inside the cylinder, rendering the combustion less isochoric. This will decrease indicated efficiency. [51] Figure 23 illustrates the limiting factors of mixture dilution in relation to BMEP. At low loads EGR is restricted by poor engine stability and at high loads too low EGR rate increases knock tendency.

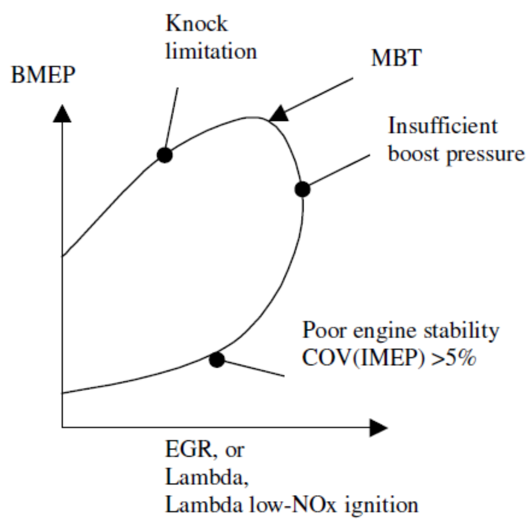

Figure 23. Limitations of lean burn or EGR diluted combustion. [52]

Similar to lean combustion, increasing EGR rate suppresses knock accordingly due to the lower temperature and prolonged combustion duration. However, effect of EGR on temperature is greater due to higher specific heat of CO_2 and H_2O molecules in the exhaust gases compared to pure air. Effect of EGR on knocking in methanol combustion was investigated in the study of Zhen et al. [50]. In the study multi-dimensional simulation was used to investigate the knock tendency in a high compression ratio spark-ignition methanol engine. Compression ratio of 17.5 was used in the investigation and it was reported that together with EGR and appropriate spark timing knock could be suppressed significantly. Thus, EGR is an important strategy in the development of the high compression ratio SI methanol engine. In turbocharged engines, cooled EGR at stoichiometric conditions allows higher indicated mean effective pressure than an undiluted mixture. [50]

Experimental methanol engine with high compression ratio was used in the study of Brusstar et al. [55] in which they investigated methanol combustion with excessive EGR and relatively high boost pressure in order to operate the engine without throttling. Stoichiometric mixtures were possible to combust with compression ratio of 19.5 due to the use of EGR up to 50% while simultaneously using a VGT turbocharger to ensure needed air mass for stoichiometric combustion from low to high load. With this load control strategy better efficiency than corresponding diesel engine was achieved at wider operating range with a peak efficiency of nearly 43% compared to 40% of the diesel one. Poorer efficiency of the diesel engine was considered to be result of the parasitic losses of the high-pressure diesel fuel system and the differences in combustion and heat transfer processes. The cooling effect of methanol reduces the compression work and the slower rate of heat release of methanol combustion reduces heat losses. The emissions with the use of excess EGR were extremely low with conventional aftertreatment system. TWC was possible to implement to engine due to stoichiometric mixture. [55] Vancoillie et al. [51] achieved also efficiency up to 42% when studying methanol combustion with similar strategy and engine than Brusstar et al. [55]. In the study of Vancoillie et al. [51] the EGR load control was compared to throttle control and part load efficiency was improved up to 20%.

5 Research methods

5.1 Simulation software

The investigations were done solely by simulations for which GT-Power, combustion engine simulation software from Gamma Technologies was used. According to the software developer's webpage, GT-Power is the industry standard engine performance simulation tool which is used by all major engine manufacturers and vehicle OEMs. It is used to predict engine performance quantities such as, for example, power, torque, airflow, volumetric efficiency, fuel consumption and pumping losses. In addition to basic performance predictions, GT-Power includes physical models for extending the predictions, for example cylinder and tailpipe-out emissions. It is 1-D simulation software which means that it calculates the processes only as a function of time, not as function of place. GT-Power is useful tool for determining effects of various design changes and operating conditions of the engine operation. Despite the fact that it simplifies some characteristics of the combustion process, GT-Power can still provide sufficiently accurate results. Especially if the model is calibrated and validated with data from a real engine.

5.2 GT-Power model

A single-cylinder engine model was used which was taken apart from a six-cylinder engine model based on AGCO Power's 84-series six-cylinder engine. The six-cylinder model was calibrated for the real engine operation thus using one cylinder from it with related piping was considered to be viable solution. In Figure 24 is presented the simulation model, where can be seen the main building components. As it can be seen, port injection strategy is used with a single injector. Originally, two injectors were used so that each intake port had its own injector. But as the author was in contact with the support team of the software developer regarding the uncertainties of the simulations, they suggested moving the injector further away from the valves. Nevertheless, this did not seem to have any noticeable effect on the simulation results.

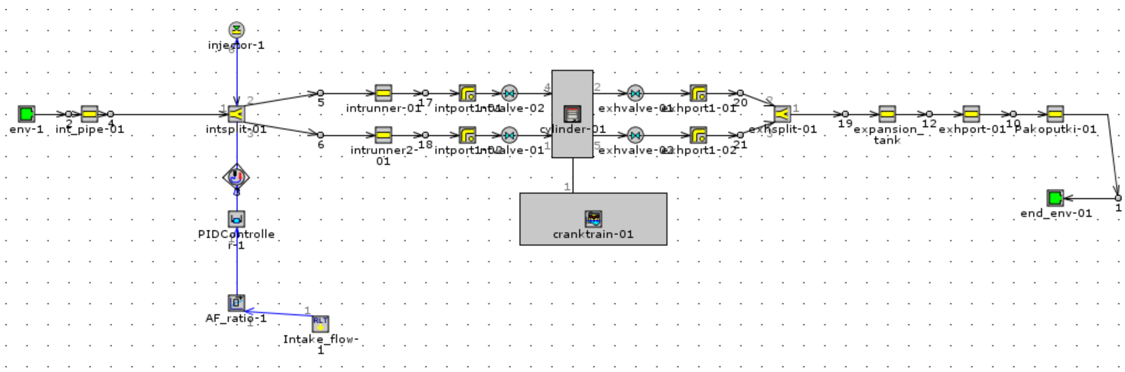

Figure 24. Simulation model

5.3 Simulation method

Four fuels, methanol, ethanol, indolene and methane were used in the simulations. Indolene is used as a surrogate for gasoline since it is a research gasoline which is used as gasoline in the simulation software. Most of the simulations were conducted without combustion, as the conditions after compression stroke were the point of interest. The conditions at TDC have a direct effect on the combustion process since the compression stroke is followed by the combustion of fuel-air mixture. However, in the two last simulation steps, simple combustion model was used to get an idea of the possible efficiency and performance improvements. The conditions at TDC depend strongly on the fuel evaporation occurring both in the intake manifold and in the cylinder during intake stroke. Therefore, modelling the fuel evaporation is in crucial part in the simulation accuracy. However, as it is explained more in details later in the chapter concerning simulation uncertainties, there were some problems in evaporating the fuel realistically. Due to this, the fuel is expected to evaporate purely by the heat extracted from the intake air. Hereby, the full theoretical potential of methanol can be reached since the fuel evaporation on the cylinder and intake manifold walls is discarded, and the cooling effect is maximal.

5.4 Simulation steps

Investigations of the conditions at the end of compression stroke were conducted systematically in five steps:

1. Simulations with equivalent fuel quantity were performed for each of the fuels. With the same fuel mass for each fuel, the difference in the heats of evaporation should be clearly seen, especially in the in-cylinder temperature. Since the LHVs are dissimilar for the fuels, achieving similar performance in a real engine would demand adjusting the injection quantity correspondingly.

2. Due to the differences in LHVs, the next step was to study how the conditions change when energy equivalent amount of fuel is injected. Hereby the cooling effect of methanol is enhanced since, for example, methanol is needed to inject over twice the amount of methane in order to reach the same energy content. Thus, the evaporating methanol should have significant cooling effect on the cylinder charge as the heat of evaporation is the highest of the investigated fuels.

3. Since the air-fuel ratio varies greatly between different fuels with energy equivalent fuel quantity and each of the fuels has different air-fuel ratio, conditions were needed to study with the same air-fuel ratio as well. Same lambda values were used for all fuels which illustrated the full potential of methanol operation.

4. After the three first steps, the possibility of increasing the compression ratio for the liquid fuels was investigated using methane as reference fuel. In the literature, the compression ratio used in commercially available NG DF engines is in the range of 11-13. In this thesis compression ratio of 11 was chosen for the methane operation in these last two simulation steps. With this compression ratio, the compression temperature of methane operation was studied with energy equivalent fuel injection. The fuel quantity was the same than in the cases with equivalent fuel energy. Then the compression temperature of methane operation was compared to the compression temperatures with the other fuels. Based on these results the compression ratios for methanol, ethanol and indolene were adjusted in order to reach the same compression temperature than in methane operation. This approach, increasing the compression ratio based on the temperature level occurring with energy equivalent fuel quantity, would be the easiest starting point for experimental studies as the fuel quantity would be easy to adjust for each fuel. In addition, a simple combustion model is also added to the simulations here in order to achieve an understanding what kind of pressure and temperature levels are present during the combustion. This gives a preliminary knowledge what kind of pressure level and air-fuel ratio is possible to test in a real engine. In addition, very rough estimate of possible performance improvements is also acquired.

5. In order to investigate the full potential of methanol in dual fuel combustion, the compression ratio should be adjusted based on the compression temperatures acquired with equivalent lambda values. In order to reach the same lambda value, methanol can be injected over 2.5 times the amount of methane in the same air mass. As methanol evaporation lowers the compression temperature, the compression ratio could be increased even more than what is accomplished by using the energy equivalent fuel quantity. In this last step, the compression ratio was adjusted separately for each lambda value since the compression temperature varies in relation to lambda. In other words, lower lambda enables higher compression ratio and vice versa.

5.5 Parameters

The main simulation parameters to be varied during the simulations were intake pressure, intake temperature, fuel quantity and air-fuel ratio. Compression ratio of 17.1 was used in the first three steps, which is the same ratio as it is in the AGCO 84-series engine. In table 2 is presented all the parameters and how they are varied within each step.

Table 2. Simulation parameters

	Speed [rpm]	Intake T [°C]	Intake p, abs [bar]	Fuel mass [mg]	Air-fuel ratio (λ)
Equivalent fuel mass			Δ0.5 bar		
Methane	2000	20	0.2 - 3.2	100	-
Gasoline	2000	20	0.2 - 3.2	100	-
Ethanol	2000	20	0.2 - 3.2	100	-
Methanol	2000	20	0.2 - 3.2	100	-
Equivalent fuel energy		Δ10°C	Δ0.5 bar		
Methane	2000	20 - 50	0.2 - 3.2	105.3	-
Gasoline	2000	20 - 50	0.2 - 3.2	119.8	-
Ethanol	2000	20 - 50	0.2 - 3.2	189.8	-
Methanol	2000	20 - 50	0.2 - 3.2	249.3	-
Equivalent lambda			Δ1 bar		Δ1
Methane	2000	50	2 - 4	-	1 - 3
Gasoline	2000	50	2 - 4	-	1 - 3
Ethanol	2000	50	2 - 4	-	1 - 3
Methanol	2000	50	2 - 4	-	1 - 3
Equivalent compression T (J)			Δ0.5 bar		Δ1
Methane	2000	50	1.5 - 3	-	1 - 3
Gasoline	2000	50	1.5 - 3	-	1 - 3
Ethanol	2000	50	1.5 - 3	-	1 - 3
Methanol	2000	50	1.5 - 3	-	1 - 3
Equivalent compression T (λ)			Δ1 bar		Δ0.5
Methane	2000	50	2 - 3	-	1.5 - 2.5
Gasoline	2000	50	2 - 3	-	1.5 - 2.5
Ethanol	2000	50	2 - 3	-	1.5 - 2.5
Methanol	2000	50	2 - 3	-	1.5 - 2.5

For the first two steps, the intake pressure sweep started from 0.2 bars to simulate the vacuum in the engine during intake air throttling. In the cases with equivalent fuel mass, only one temperature level (20°C) was used as the purpose was to just illustrate the differences in the heat of evaporation between the fuels. The temperature dependency was investigated in the next step with the cases of equivalent fuel energy. Intake temperature of 50°C was used for all the following steps since it is considered to be normal intake temperature level of a diesel engine. The needed fuel quantity for each fuel with the cases of equivalent fuel energy was calculated by using, again, the AGCO 84-series as a reference engine. As the single-cylinder model is based on a six-cylinder engine, the power output of the reference engine was used for calculating the needed cylinder power of the single cylinder. The needed injection quantity can be calculated from the cylinder power with following equations

$$\dot{m} = \frac{P}{H_u \cdot \eta} \quad (1)$$

$$m = \frac{\dot{m}}{\frac{n}{2}} \quad (2)$$

where P is the output power of one cylinder, H_u the lower heating value, η the engine efficiency and n is the engine speed in revolutions per second. The power output of the six-cylinder reference engine was 200 kW and efficiency of 38% was used in the calculations.

The descriptions for the last two steps in the table are separated with abbreviations J and λ. They stand for Joule and lambda, respectively, referring to the two different methods for adjusting the compression ratio for the last steps. Joule refers to the method in which the compression ratios for the different liquid fuel operations were adjusted with energy equivalent fuel mass as a reference case, and lambda refers to the method where lambda equivalent fuel mass was used as a reference case. Since the operating window for lean-burn combustion is around lambda value of 2, Figure 7, the last simulations focus on lambda values from 1.5 to 2.5.

5.6 Simulation uncertainties

During the simulations it was noticed that the most significant source of uncertainty is the fuel evaporation modelling. With methane this was not an issue as it is already in gaseous form. However, with methane a slight error could be made as the temperature drop due to pressure differences between the fuel supply and the intake manifold was not taken into account. Nevertheless, the error was estimated to be less than one percent if the injection pressure would be 8 bars, which is acceptable in this context. The fuel evaporation in the intake manifold can be modelled in two ways in the software. The simpler option is to use 'Vaporized fluid fraction' –attribute inside the injector object which defines the portion of the fuel what is evaporated immediately after the fuel injection. In this solution, the energy required to evaporate the fuel is taken solely from the intake air. The issue here is that the user defines the fraction of the fuel which is evaporated and it can be something completely different than what would happen in reality. In addition, the effects of hot intake valves and the walls of the intake manifold are completely neglected, which, in reality, are usually in major role in the fuel evaporation. Due to this, it was noticed that when using similar fraction for methanol, ethanol and indolene, the temperature in the intake manifold decreased way below zero degrees with methanol operation. This can be expected when bearing in mind the differences in the heats of evaporation. However, it is not realistic behaviour, so different approach was tested as well.

Intake ports can be modelled with a modelling object that calculates the fuel evaporation at the intake port walls. With this model all of the fuel is injected as liquid on to the walls of the intake port and the energy for fuel evaporation is absorbed from the walls. For the model, user have to specify the distillation curve of the fuel, and as methanol and ethanol are single component fuels having a single boiling point, the model did not seem to work properly. When comparing methanol injection to indolene injection with equivalent fuel mass, the model evaporated methanol completely whereas fraction of the indolene was remaining in liquid fuel. This could be realistic due to higher boiling point of indolene. However, increasing methanol injection until a certain point, the phenomenon reversed and most of the methanol remained in liquid form. This was considered to be quite strange behaviour. When observing the mass of the methanol vapour in the case of complete methanol evaporation, the vapour mass was significantly greater than with the boundary case where most of the methanol was remaining in liquid fuel. Naturally, with increasing fuel mass the fuel film on the walls thickens and, due to the heat absorbed by the liquid fuel mass on the wall, more energy is needed for evaporating the same amount of fuel than with smaller injection quantities. However, it could be expected that this decreasing nature would occur linearly so that as the fuel mass increases, the vapour mass decreases slightly due to the specific heat of liquid methanol present on the walls. On the contrary, here the change in vapour mass was sudden and therefore the model was considered to function illogical.

Due to the illogical behaviour of the supposedly more realistic port fuel evaporation model, the simpler approach was used in the thesis since then at least it is know what kind of an error is done. In order to solve the problem with excessively cold temperature in the intake manifold, the vaporized fluid fraction attribute was corrected so that the temperature in the manifold is same for methanol, ethanol and indolene. For indolene, a value of 0.3 was given in the manual of the software, thus it was used as a reference value. Vaporized fluid fractions for methanol and ethanol were calculated to match the same amount of energy absorbed from the air by 0.3 fraction of indolene. For the first step of the simulations only the different heat of evaporation needed to be taken into consideration as the fuel mass was same for each fuel. With energy equivalent fuel quantity, the different injection quantities had to be considered also. Corrected fractions were calculated with the following equations

$$vff_1 = \frac{\Delta H_{vap_i}}{\Delta H_{vap_{ind}}} * 0.3 \tag{3}$$

$$vff_2 = \frac{H_{u_i}}{H_{u_{ind}}} * \frac{\Delta H_{vap_i}}{\Delta H_{vap_{ind}}} * 0.3 \tag{4}$$

where *vff* stands for vaporized fluid fraction, ΔH_{vap_i} stands for heat of evaporation of methanol/ethanol, $\Delta H_{vap_{ind}}$ is the heat of evaporation of indolene, H_{u_i} is the lower heating value of methanol/ethanol and $H_{u_{ind}}$ is the lower heating value of indolene. 0.3 refers to the vaporized fluid fraction which is used with indolene operation. Equation 3 is used for the cases with equivalent injection mass and equation 4 is used for the rest of the simulations. Although, equation 4 gives correct vaporized fluid fraction only for the cases with energy equivalent operation, the error is considered to be rather mild with the rest of the simulations as the fuel is anyhow vaporized completely in the air. In the chapter discussing about results, the behaviour of the temperature in the intake manifold with different vaporized fluid fractions is illustrated.

Fuel evaporation in the cylinder is also very simplified in the software. If the user does not define the in-cylinder evaporation specifically, the fuel is not evaporated until the start of the combustion. This was not suitable for this thesis as the purpose was to investigate the conditions at TDC before the combustion. However, the way the evaporation is defined in the software causes significant error margin as, again, the user itself has to define the evaporation rate of the fuel. In the evaporation object of the model the evaporation is defined so that the user inputs a point in crank angles when 50% of liquid fuel entering the cylinder is evaporated. In addition, the user has to define also the fraction of the fuel which is evaporated at the cylinder walls. These two attributes affects significantly the conditions at TDC as the crank angle attribute practically defines how much of the fuel is evaporated before the intake valve closure. This in turn has a direct effect on the volumetric efficiency as the temperature reduction due to evaporating fuel increases the air density. The more the fuel evaporates before intake valve closure, denser the air becomes and betters the volumetric efficiency. Then again, the evaporation at the walls decreases the amount of energy absorbed from the air reducing the cooling effect and decreasing the volumetric efficiency. As the cooling effect is affected by the evaporation at the walls, the temperature and pressure level in the cylinder is also affected accordingly. Hereby, the user can easily affect the end results by changing these values which in turn naturally affects the accuracy of the simulations. As there is no literature available on what inputs should be used for the tested fuels, it was decided to use same input values for each fuel. The evaporation at the walls was neglected in order to determine the maximum effect of the fuel evaporation, and the point of 50% of fuel evaporated was determined so that all the fuel was evaporated during the intake and compression stroke. Again, this approach was chosen because this way it is known the nature of the error.

Another source of error regarding the fuel evaporation is the saturation pressure which is limiting the maximum amount of fuel vapour in the air. As it was described in the chapter 4.2, with methanol injection the saturation pressure is reached in normal engine conditions, thus part of the fuel remains in liquid form. However, the software does not take into account the saturation pressure of the air. User can define the fuel to be evaporated completely no matter how much fuel is injected, and therefore it can easily exceed the saturation pressure. This can be, however, solved in reality for example by increasing the intake air temperature and therefore it is not considered to be that significant error.

Combustion modelling is carried out with a simple model which brings some simplification to the results as well. In the model the user defines the Wiebe function, heat release curve, for the combustion. With each fuel and case, the same Wiebe function was used and this is not the case in reality. The heat release of combustion depends on several factors including air-fuel ratio and intake pressure. The approach of keeping it constant, despite the varying air-fuel ratio and intake pressures, results in inaccuracies. Also, as it is known, different fuels have different chemical reactivity which naturally affects the rate of heat release. The combustion phasing is adjusted for all the fuels using the same values inside the Wiebe function object than it is used for methane. For methane, the phasing is adjusted so that the pressure at TDC during combustion is approximately equal to the compression pressure. This was done due to the fact that with some other approaches the combustion started way before TDC and maximum pressures were extremely high. With the selected approach, the combustion is starting more or less at TDC which will cause inaccuracies but is still more realistic than overly advanced combustion. As the error is in the same range for all of the fuels, and the aim is merely just to illustrate the possible improvements in indicated efficiency and IMEP, the aforementioned errors are acceptable.

6 Results and analysis

6.1 Equivalent fuel mass

Firstly, it was necessary to tune the vaporized fluid fraction for methanol and ethanol operation in relation to indolene operation. The corrected fractions were calculated with equation 3 giving the values of 0.089 and 0.114 for methanol and ethanol operation, respectively. In the simulations for verifying that the calculations provide satisfying estimation of the vaporized fraction, intake air temperature of 20°C was used. Verification was done by comparing the minimum temperature at inlet port outlet between these three fuels and the comparison can be seen in Figure 25. In the figure the temperature is plotted against the intake pressure, and it can be seen that the calculated fractions correspond well to the temperature level present with indolene operation. In addition, the error produced by using the same vaporized fraction than with indolene is illustrated in the figure with dotted lines. As the injection quantity is the same throughout the intake pressure sweep, lambda is greater at lower intake pressures and the error is correspondingly greater at lower intake pressures. In the figure, lambda range from 0.2 bars to 3.2 bars is also presented to illustrate the excessively rich and lean conditions at both extremities of the pressure sweep.

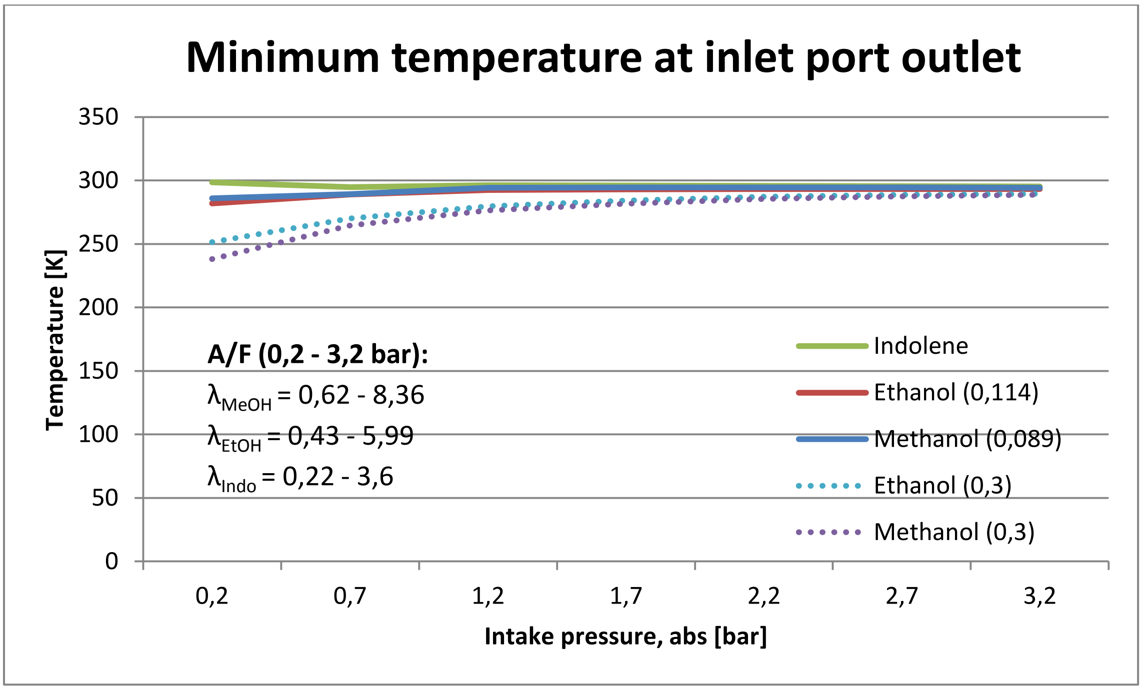

Figure 25. Comparision of minimum inlet temperature for different fluid fractions.

The compression temperature with equivalent fuel mass together with the lambda range is shown in Figure 26. As expected, the temperature in methane operation is the highest followed by indolene operation. The alcohol fuels provide the lowest compression temperatures but, unexpectedly, they have practically the same compression temperature with all the intake pressure levels but 0.2 bars. Based on pure fuel properties, methanol should have lower compression temperature due to higher heat of evaporation. However, this behavior could be explained when looking at the compression pressure and trapped air mass with each fuel. It was noticed that the cooling effect of methanol increases slightly the trapped air mass compared to ethanol. This in turn increases the compression pressure and as it is known, higher pressure results in higher temperature. In addition, as the fuel quantity is rather low and the air-fuel ratio is high, it could be that the additional cooling effect of methanol is therefore bypassed by the increased specific heat of the air.

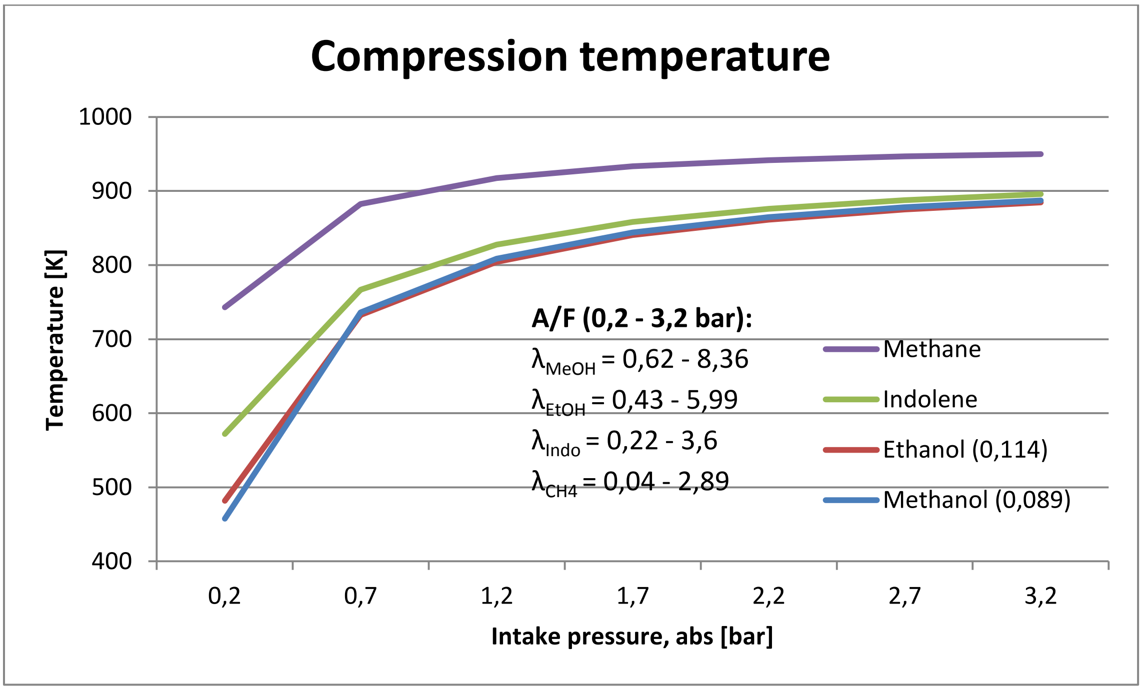

Figure 26. Compression temperatures of the fuels in relation to intake pressure.

The compression pressure and trapped air mass can be seen in Figure 27 and Figure 28. As can be seen, both of them increase linearly in relation to intake pressure. The highest pressure is present in methane operation followed by methanol, ethanol and indolene having the lowest compression pressure. The same order applies for the trapped air mass. The potential of alcohol fuels are seen in the improvements in trapped air mass, as larger air mass enables larger fuel mass and higher power.

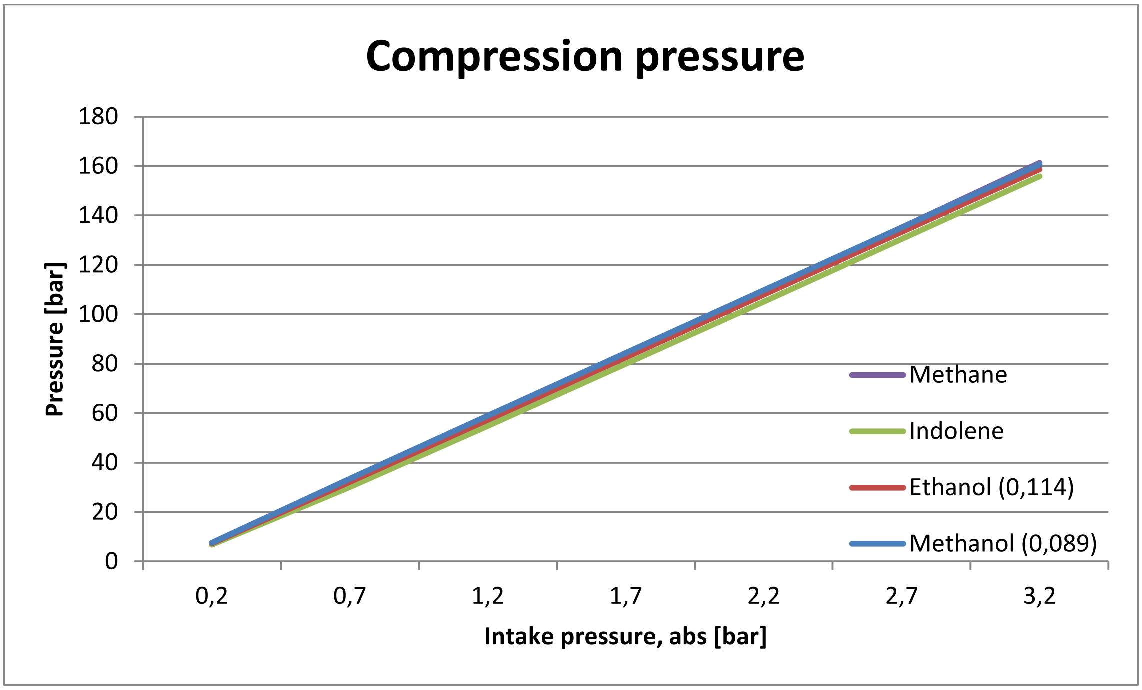

Figure 27. Compression pressures of the fuels in relation to intake pressure.

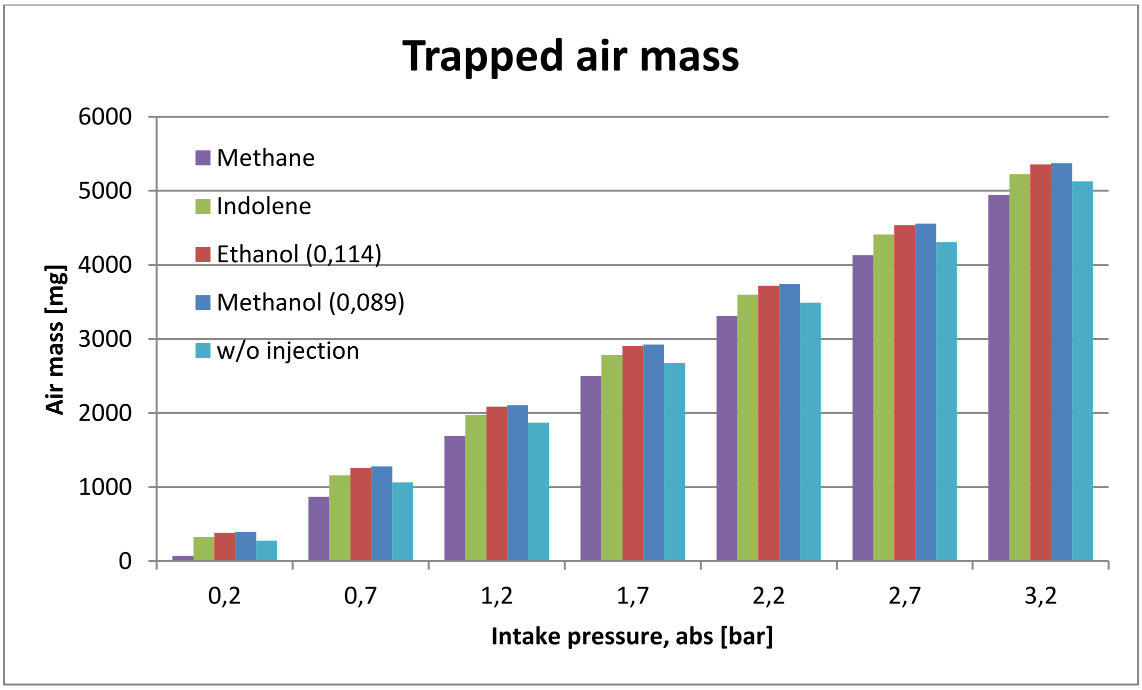

Figure 28. Comparison of trapped air masses with equivalent fuel quantity.

6.2 Equivalent fuel energy

Similar to the cases of equivalent fuel mass, the corrected vaporized fluid fractions for methanol and ethanol were calculated first. As it was explained in the chapter 5.6, with equivalent fuel energy the fuel quantity varies between the fuels so it was needed to take into account. Therefore, the vaporized fluid fractions were calculated using the equation 4. In Figure 29, both the minimum inlet port outlet temperature and the vaporized fluid fractions for methanol, 0.0429, and ethanol, 0.0717, can be seen. These calculated values for vaporized fluid fractions were used in the rest of the simulations reported in the following chapters. In addition, similar to figures in previous chapter, the lambda range is also presented Figure 29.

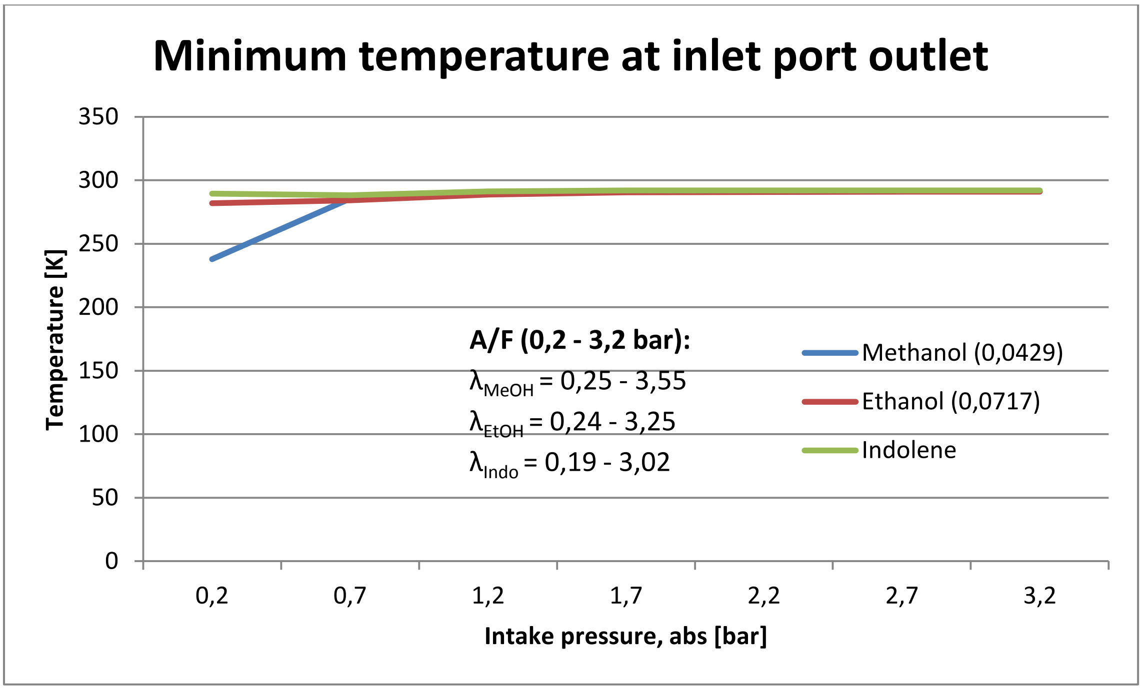

Figure 29. Illustration of the matching temperature levels with corrected fluid fractions.

The conditions at TDC were investigated for each fuel separately by varying the intake temperature together with the intake pressure. Firstly, it was noticed that the lambda value was decreasing way below the stoichiometric value with intake pressures less than 1.2 bars. This decreasing nature is due to the fact that since the fuel quantity is kept constant for all the pressure levels, with decreasing pressure the amount of air is decreased correspondingly and the air-fuel ratio becomes richer. In dual fuel engines, the premixed mixture is close to stoichiometric or lean mixture, hence simulation points leading to excessively low lambda values can be discarded. The relation between intake pressure and lambda values is illustrated in Figure 30. The excessively rich conditions can be observed with intake pressures lower than 1.2 bars. In addition, it can be seen that, at all pressure levels, the lambda values for methanol are significantly greater than methane's corresponding ones. This indicates that for the same intake pressure more methanol could be injected into the cylinder. In other words, more energy could be trapped in the cylinder increasing the cylinder power.

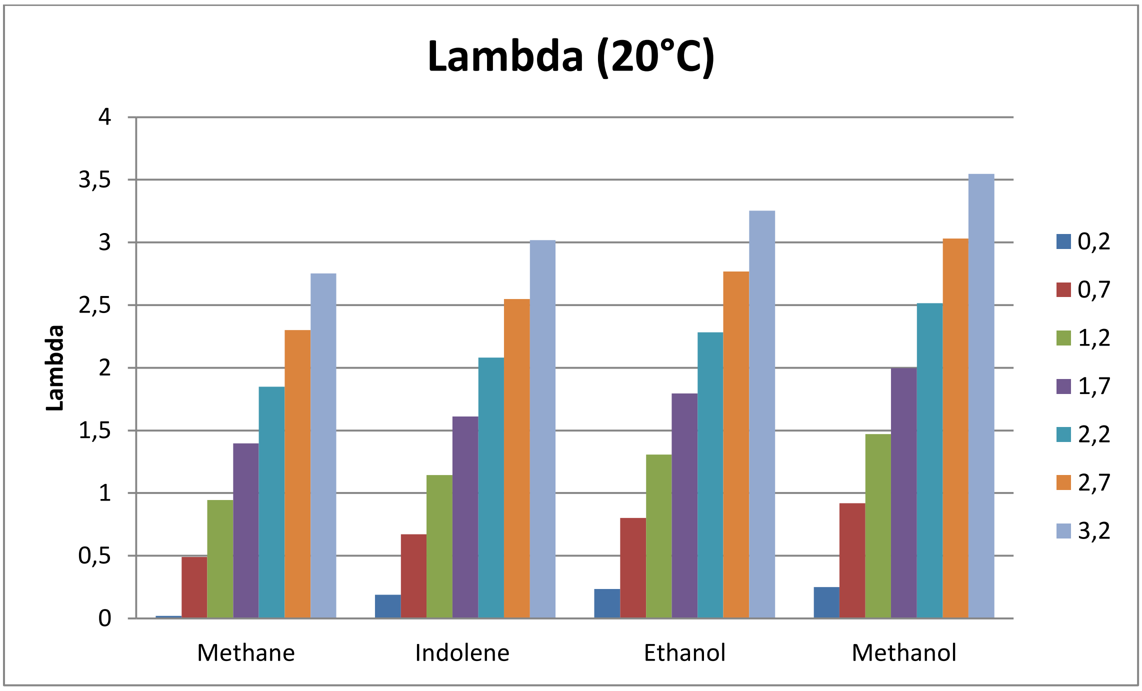

Figure 30. The effect of intake pressure on lambda value at 20°C intake temperature.

Figure 31 presents the compression temperature of methanol against intake pressure with different intake air temperatures. Additionally, the figure includes the compression temperature of methane with 50°C intake air temperature as a comparison and as an illustration that the trend for other fuels is more or less the same. As it can be seen, the compression temperature is decreasing with decreasing intake pressure. This is due to the richer mixture at lower intake pressure since there is less air to be cooled than with higher intake pressure levels. The compression temperature follows linearly the change in intake temperature since the increments between the curves are equal size at each intake pressure point. Since the trend in intake temperature was identical with other fuels tested, the results with other fuels are not illustrated here in separate figures. The linear dependency of the intake air temperature is also shown in Figure 32, where a comparison of compression temperature with different fuels against intake air temperature is presented.

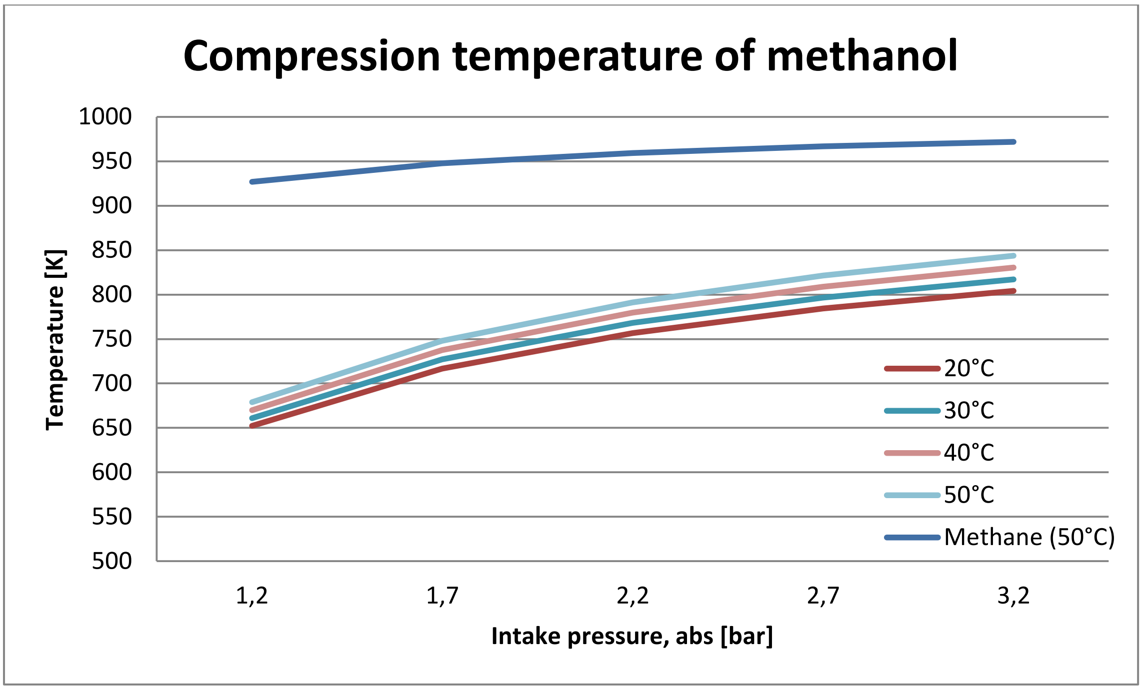

Figure 31. Compression temperature of methanol for different intake temperatures and pressures.

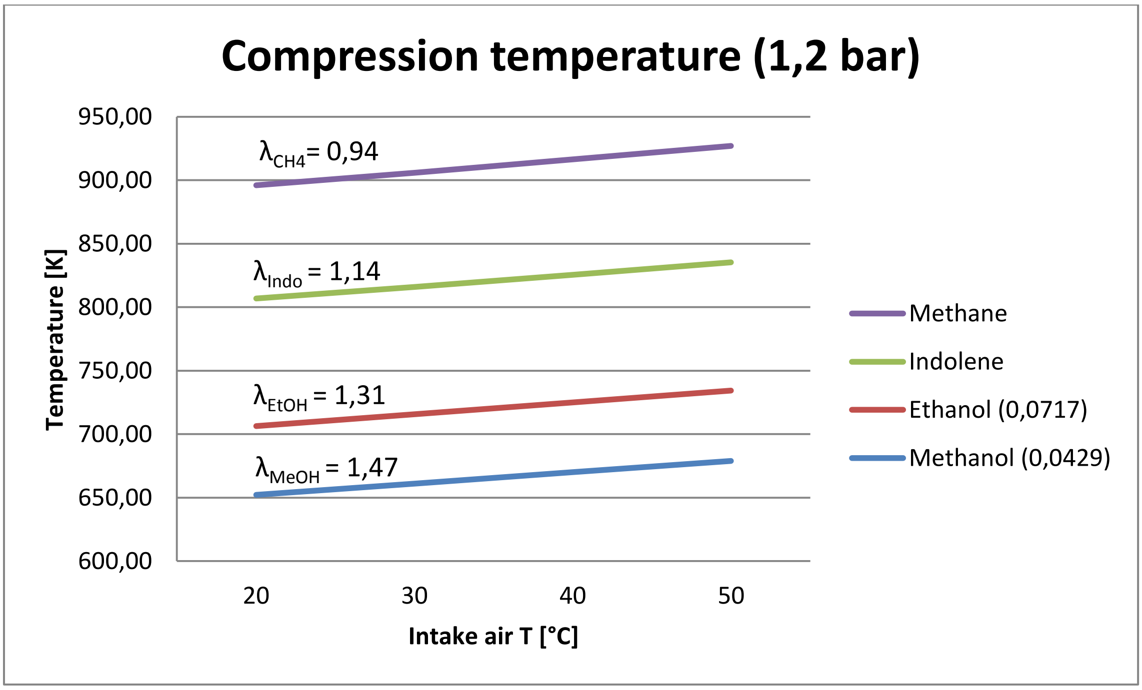

Figure 32. Compression temperatures of the tested fuels in relation to intake air temperature.

Figure 32 together with Figure 33 illustrates the differences in the compression temperatures between the fuels. It was shown that methanol has the lowest temperature throughout the whole range of intake pressure and temperature points. On the contrary, methane operation has the highest temperature level. This was expected since it is the only fuel injected as gas having therefore the lowest cooling effect on the inducted air. Among the liquid fuels, the order of the temperature levels was as anticipated since the order follows directly the order of the heats of evaporation of the fuels. The significantly lower compression temperatures with alcohol fuels were result of higher heat of evaporation combined with low LHV. Lower LHV results in greater injection quantity in order to reach the same energy content. Figure 33 illustrates the compression temperature in relation to intake pressure with intake air temperature of 50°C. It can be observed that compression temperature has a stronger dependency on intake pressure with alcohols than with methane or indolene. With methanol and ethanol, the steeper rise of the temperature after 1.2 bars is considered to be a result of significantly increased air mass at higher pressures, and thereby the cooling effect is reduced. As methane is already in gas phase, the effect of intake pressure on temperature is not that drastic since the intake air is not cooled via the heat absorbed by evaporation. In the same figure is also presented the lambda values for each fuel at each pressure level.

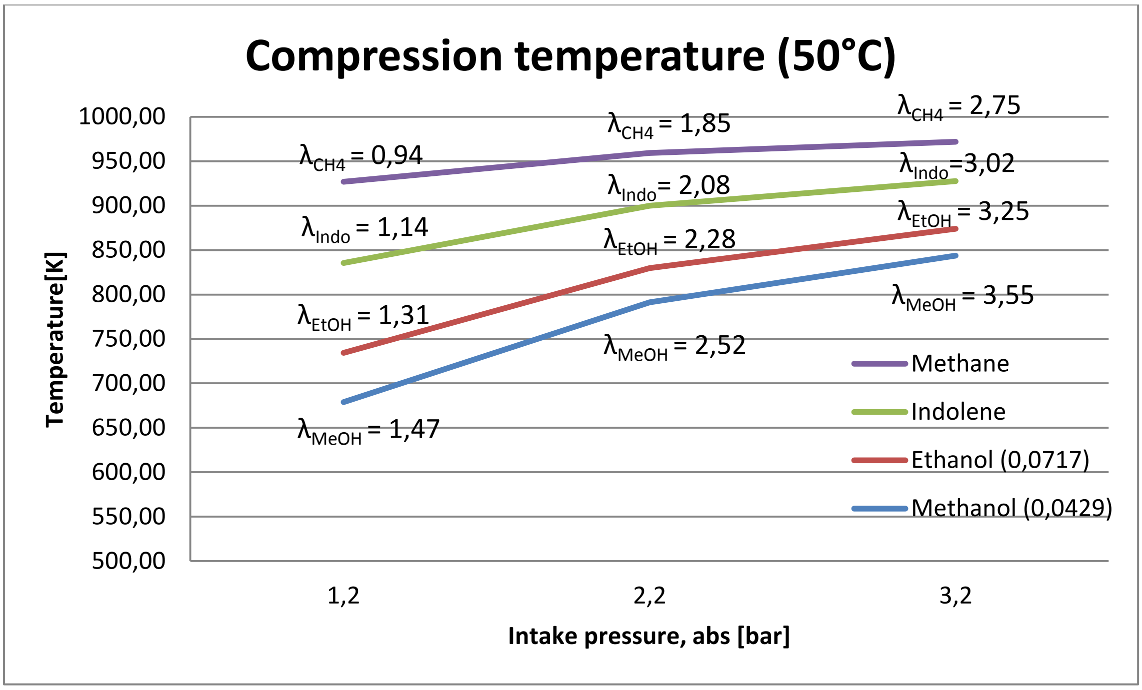

Figure 33. The effect of intake pressure on compression temperature at intake air temperature of 50°C.

Similar to the compression temperature, the compression pressure followed the intake air temperature linearly. This can be seen in Figure 34 where compression pressure is plotted against intake air temperature at 1.2 bar intake pressure. As both compression temperature and pressure have linear dependency on the intake air temperature, the effect of the intake air temperature can be predicted easily. Therefore, it was justified to eliminate it as a variable in further simulations and use only single value for the intake air temperature. In the Figure 34 can be seen the differences in compression pressures between the investigated fuels. The absolute differences were quite small but comparing the order of the fuels to the order of the compression temperatures, it can be seen that it is completely different. Methane has still the highest value, but then, despite the lower compression temperature, it is followed by methanol, ethanol and indolene in the respective order. This is considered to be result of higher total mass entering the cylinder with methanol and ethanol. The denser air due to charge cooling increases the trapped air mass and, in addition, the total in-cylinder charge mass is increased further due to larger fuel quantity with methanol and ethanol.

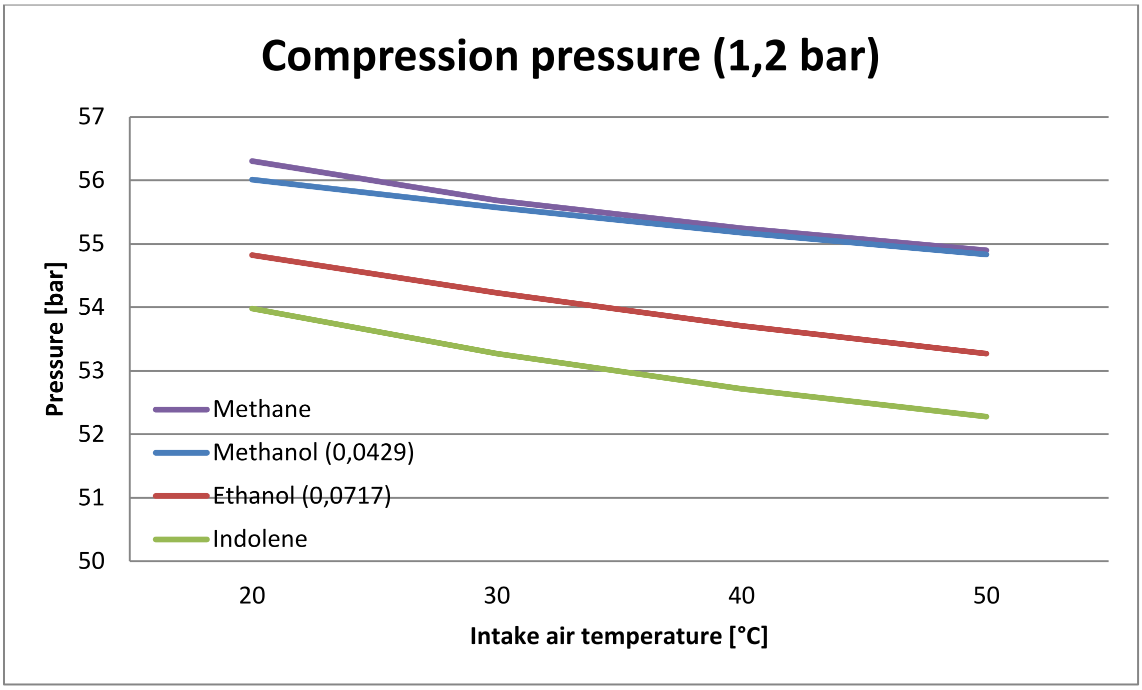

Figure 34. The effect of intake air temperature on compression temperature with 1.2 bar intake pressure

The effect of intake pressure on compression pressure is illustrated in Figure 35. The compression pressure acts as expected as it increases linearly with increased intake pressure due to the increased air mass trapped in the cylinder.

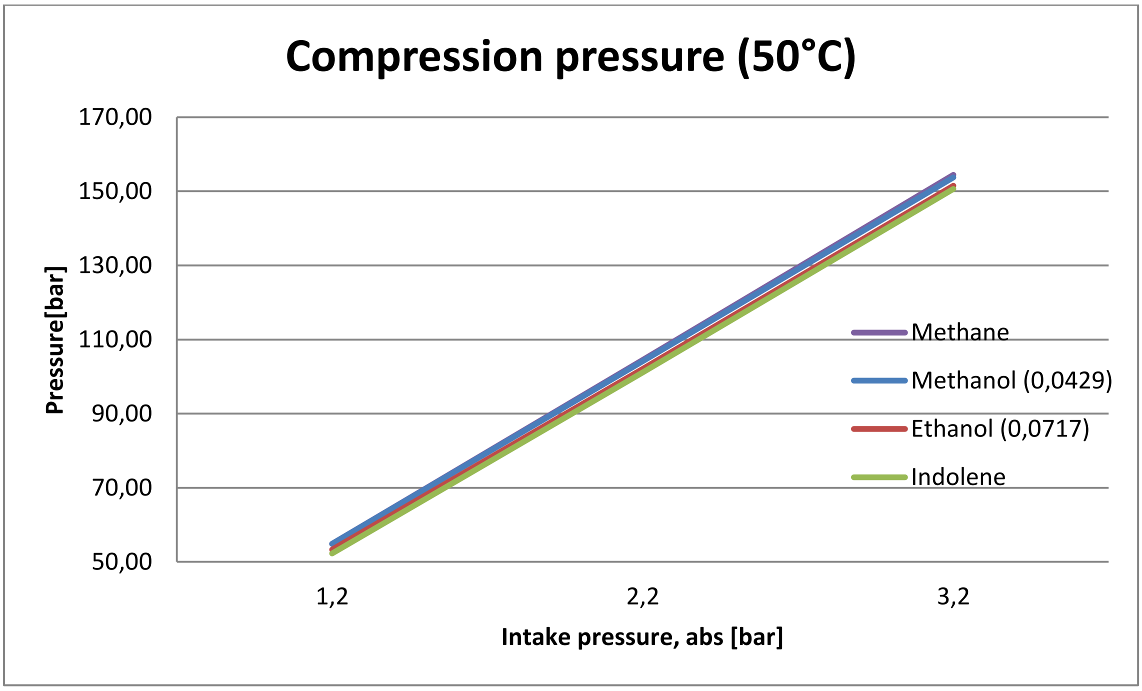

Figure 35. Compression pressure against intake pressure for different fuels.

Variations in trapped air mass can be seen in Figure 36, which confirms the assumption, that methanol has the biggest trapped air mass. In the figure, the effect of lower compression temperature at 1.2 bars can be also observed as the relative difference in air masses between methanol and methane is significantly larger compared to the difference at 3.2 bars. Notable is also that without fuel injection the air mass is actually lower compared to all the fuels except methane. However, as the evaporation at the intake manifold and cylinder walls is neglected, the results seen here is only a theoretical potential. Nevertheless, as methane is injected as gas in reality, the results provide a good picture of the replacement of fresh air by methane vapor. This is one of the downsides of methane operation.

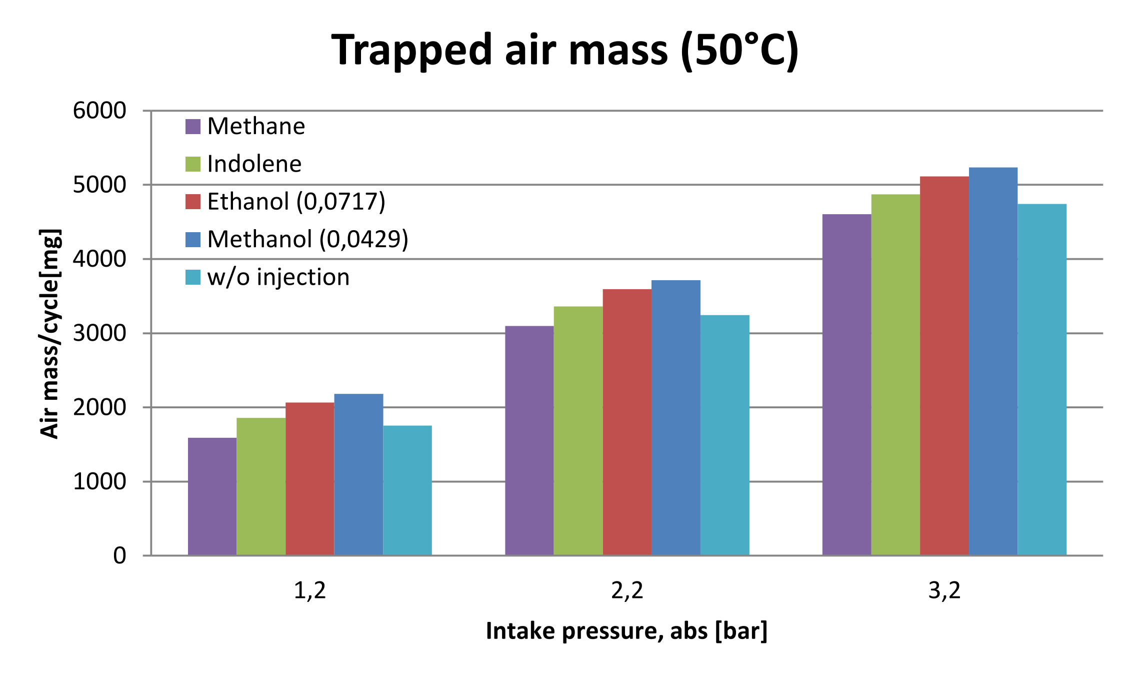

Figure 36. Comparison of trapped air mass with intake air temperature of 50°C

6.3 Equivalent lambda

In order to investigate the full potential of methanol, the same lambda value for each fuel is needed to be used. The simulations were conducted with intake pressure sweep from 2 to 4 bars but as the results were linearly dependent on the intake pressure, only results with 3 bar (abs) pressure level are presented here. Clear differences were observed between the results of energy equivalent and lambda equivalent fuel quantity. In Figure 37, the compression temperatures for the four tested fuels are plotted against lambda. Expectedly, with increasing lambda the compression temperature increases due to reduced fuel quantity. The same kind of behavior of the temperature can be seen here than it was illustrated in Figure 33. The cause for this behavior is the same as the air-fuel ratio is increasing in both figures when moving to the right on the x-axis. However, comparing the case with 3.2 bar intake pressure in Figure 33 to the results in Figure 37, the potential decrease in compression temperature with lambda control is evident. As the intake pressure was 3 bars for the results presented in Figure 37, the compression temperature with methanol operation can decrease up to 270K at lambda 1 when compared to the case with 3.2 bar intake pressure in Figure 33. Despite the fact, that there was a 0.2 bar difference between the cases, the reduction in temperature is still remarkable. Most importantly, when comparing the fuels against each other in Figure 37, significant differences in the compression temperatures can be seen. Comparing methanol to methane, the reduction in compression temperature is 150 – 350K depending on the lambda value. This indicates that NO_x emissions could be reduced significantly with methanol operation. Alternatively, since there is such a great reduction in compression temperatures, the compression ratio for other fuels than methane could be thus raised to reach the same compression temperature. This is discussed further in the following chapters.

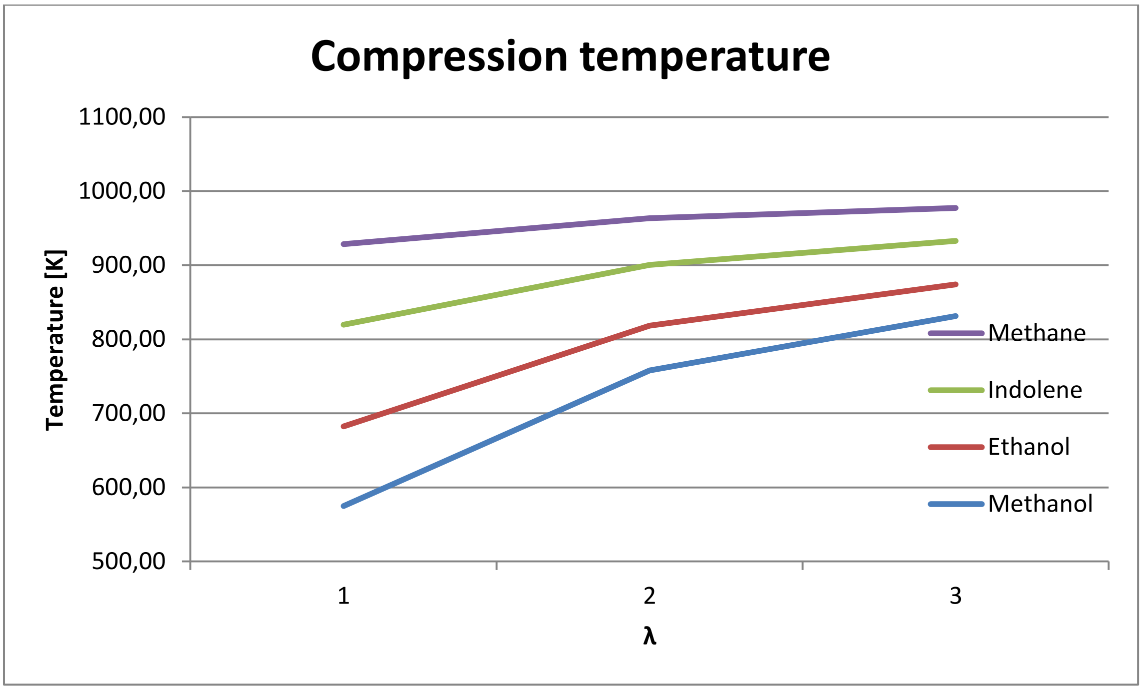

Figure 37. Compression temperature for different fuels in relation to lambda values.

In Figure 38, the compression pressure for different lambda values is presented. The relationship between compression pressure and lambda was the same as it was between compression temperature and lambda. Increasing the lambda increases the pressure since less fuel is evaporated. Similar to the results in chapter 6.2, methane has the highest compression pressure and indolene the lowest. At lambda value of 1, methanol, ethanol and indolene had almost the same compression pressure but with increasing lambda the compression pressure with methanol operation increased more in relation to ethanol and indolene. Apparently, at lambda 1 the extensive cooling effect of methanol bypassed the effect of increased total charge mass in the cylinder, and the compression pressure is lowered significantly.

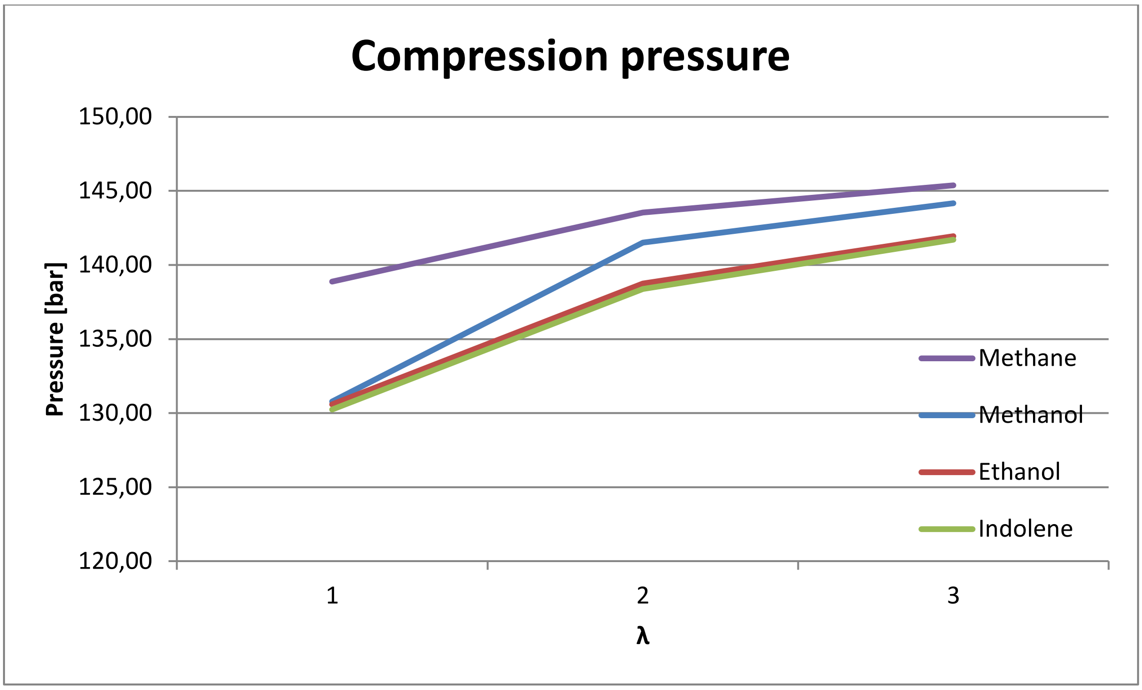

Figure 38. The effect of lambda on the compression pressure for different fuels.

The increasing nature of trapped air mass with decreasing lambda can be seen in Figure 39. As the fuel mass increases with decreasing lambda, the intake air becomes increasingly denser resulting larger trapped air mass. However, with methane the behavior was the opposite since the air mass was increasing together with increasing lambda. This is due to the decreasing methane vapor with increasing lambda values. In other words, less air is replaced by the methane vapor. The differences between the fuels are significant which indicates great potential of power improvement for methanol operation compared to the other fuels.

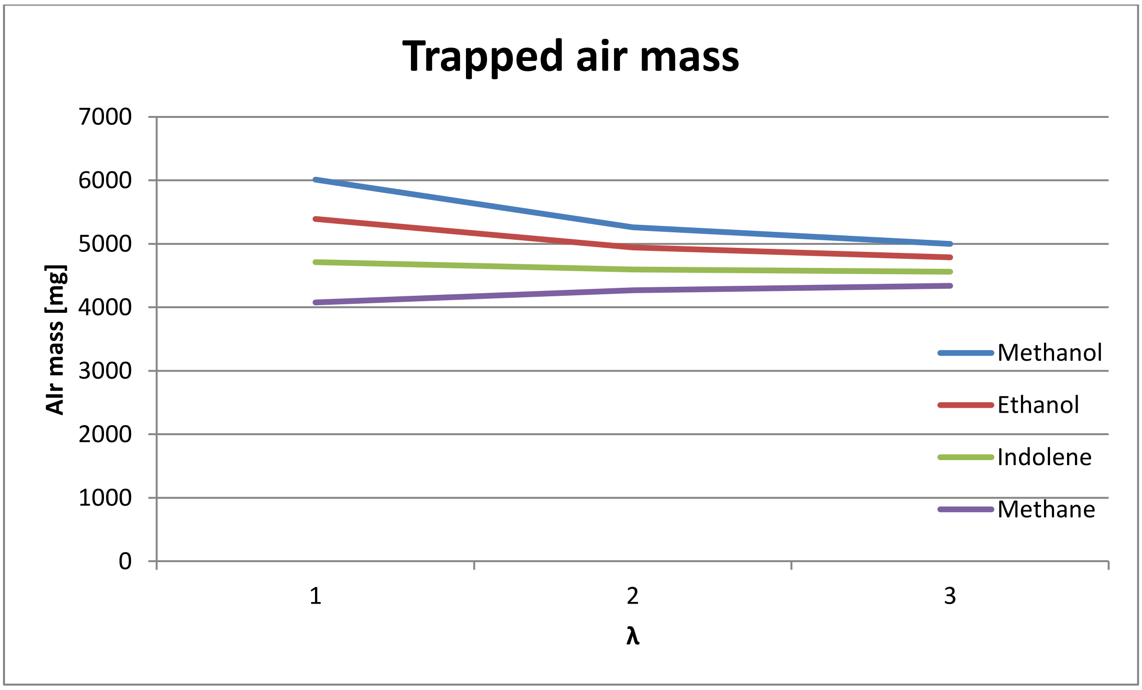

Figure 39. Trapped air mass in relation to varying lambda.

The potential improvement in power output can be seen in Figure 40 which illustrates a comparison of the trapped fuel energy between the investigated fuels. Naturally, trapped fuel mass increases with decreasing lambda as the mixture becomes richer. Since the fuels have different LHV, the fuel mass itself does not describe the actual fuel energy entering the cylinder. Therefore, the fuel energy entering the cylinder is calculated based on the LHV and the fuel mass. As there are significant differences in the trapped air masses between the fuels, and with lambda control the air mass affects directly to the trapped fuel mass, there are significant differences in trapped fuel energy, correspondingly. The differences in trapped energy followed the same trend as it is illustrated in the Figure 39. In addition to the influence of trapped air mass on trapped fuel energy, the trapped fuel energy is also affected by the combination of stoichiometric air-fuel ratio and LHV of the fuel. Looking into the fuel properties used in GT-Power, methane has 2.66 times higher stoichiometric air-fuel ratio than methanol. Thus, for the same lambda, methanol is able to be injected 2.66 times the amount of methane into the same air mass. When calculating the energy input based on the fuel properties used in the software, 11 % more energy is possible to reach using methanol with lambda value of 1. This indicates that there is a significant potential of increasing the engine output even with equivalent air mass. When taking into consideration the difference in trapped air mass, methanol provides 67 % more energy into the cylinder with lambda value of 1. Hereby, methanol shows remarkable potential for increasing the engine output power compared to methane.

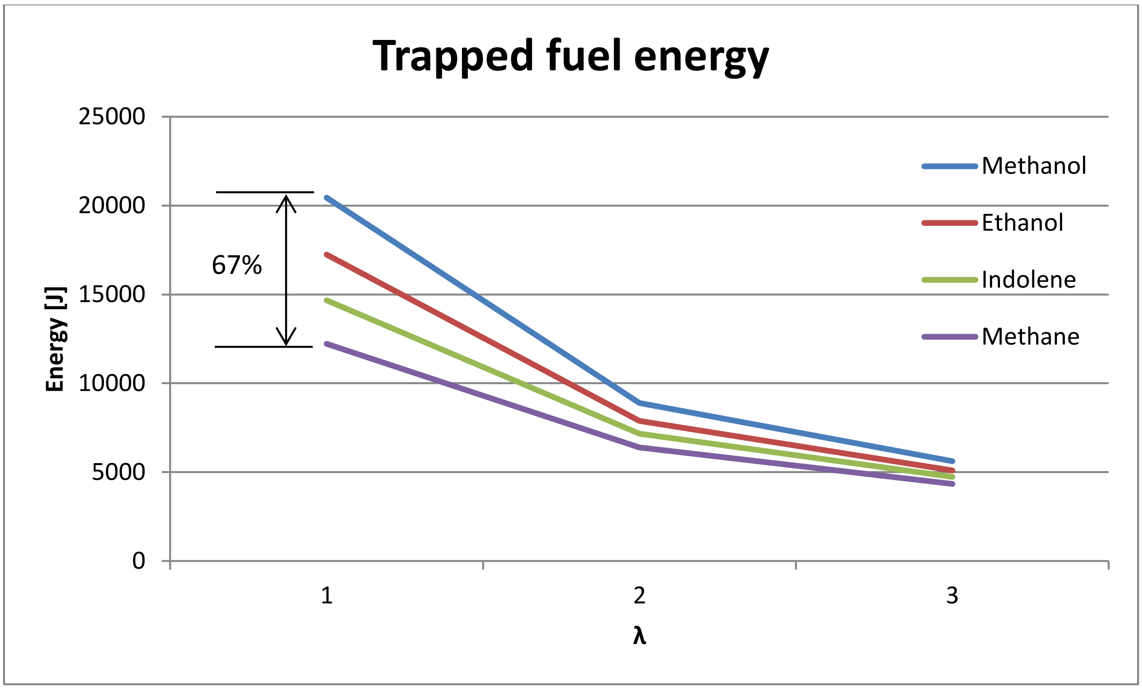

Figure 40. The effect of lambda on trapped fuel energy.

6.4 Variations in compression ratio

6.4.1 Equivalent compression temperature (J)

Compression temperature is in major role in the autoignition of combustion in diesel and dual fuel engines. It is strongly determined by compression ratio thus varying the compression ratio the temperature can be either increased or decreased. Since natural gas consists mainly of methane and is already used in commercial applications, methane was used as a reference case in the following simulations. The compression ratios for the other fuels were adjusted so that the compression temperature equals the compression temperature with methane operation using compression ratio of 11. In this chapter the compression ratios were adjusted by using the same fuel masses as it is used in the cases with energy equivalent fuel quantity. The resulting compression ratios were 18, 15.9 and 12.8 for methanol, ethanol and indolene, respectively. Similar to the previous simulation results, the effect of intake pressure was linear thus here is presented only the results with 3 bar (abs.) intake pressure. Moreover, 3 bar intake pressure is considered to be a realistic value for real engine operation in heavy duty applications. In Figure 41, compression pressures together with individual compression ratios for each fuel are shown with respect to lambda.

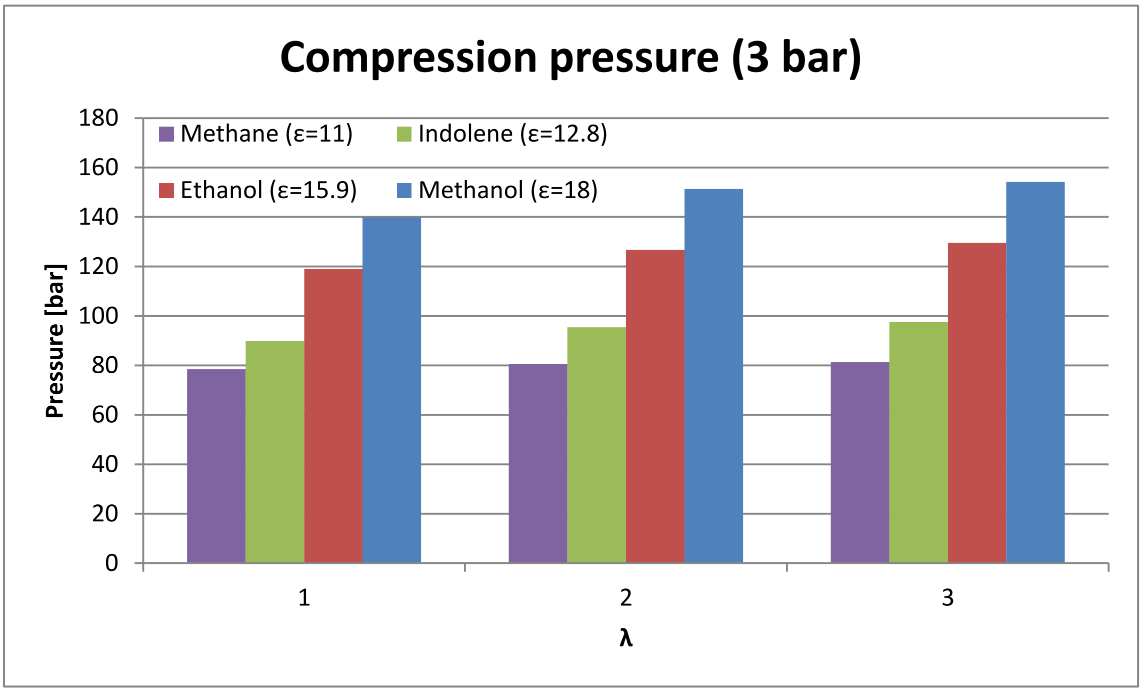

Figure 41. Compression pressures for different fuels with respect to lambda.

The relationship between lambda and compression pressure followed similar trend than described in the chapter 6.4 since the pressure increases together with increasing lambda. Naturally, the compression pressure is higher with higher compression ratio, thus methanol has the highest pressure and methane the lowest. Looking at the absolute values of the compression pressure of methanol, it can be noticed that with all lambda values the pressure is in the acceptable range. The typical maximum cylinder pressure in commercial engines is around 200 bars which is clearly not exceeded here. However, since the combustion increases the maximum cylinder pressure in typical engines, the comparison with the typical maximum of 200 bars should be done with maximum combustion pressure. First, the cylinder pressure curves for the four fuels are presented in Figure 42 at 3 bar intake pressure and with lambda value of 2. Since the combustion phasing was adjusted so that the pressure at TDC is approximately equal to the compression pressure, comparing Figure 42 to Figure 41 it can be seen here that the pressures at TDC correspond quite well the compression pressures for each of the fuels.

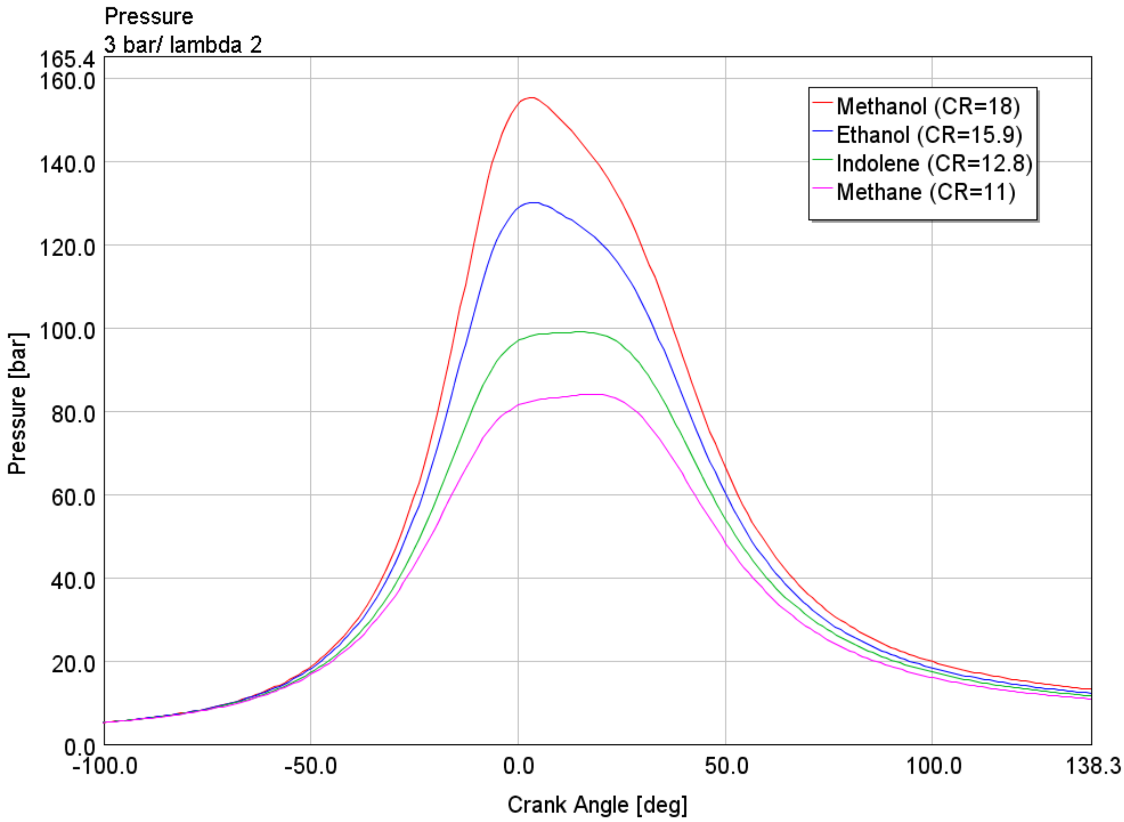

Figure 42. Cylinder pressure curves with lambda 2 and intake pressure of 3 bars.

Maximum combustion pressures for different lambda values are presented in Figure 43. Again, when comparing Figure 41 to Figure 43, it can be seen that the maximum pressure for lambda values of 2 and 3 do not increase significantly from the corresponding compression pressures, which is not normally the case in typical engines. This is considered to be acceptable because the same error was made with all the fuels thus the differences between the fuels are well illustrated. With lambda value of 1 the maximum pressure increased significantly for all of the fuels compared to compression pressure. Despite this significant increase, the highest pressure barely exceeds over 200 bars for methanol operation. Therefore, based on these observations compression ratio of 18 could be used with methanol in dual fuel engines for all lambda values. Since dual fuel engines are operated with lean mixtures, the maximum pressure reached in real application should be less than the maximum pressure reported here with lambda value of 1. This is confirmed in the literature as well since compression ratios even up to 19.5

has been used in experimental tests with methanol. In addition, maximum pressure can be easily affected with better combustion phasing in reality thus the peak value in methanol operation with lambda value of 1 could be lowered.

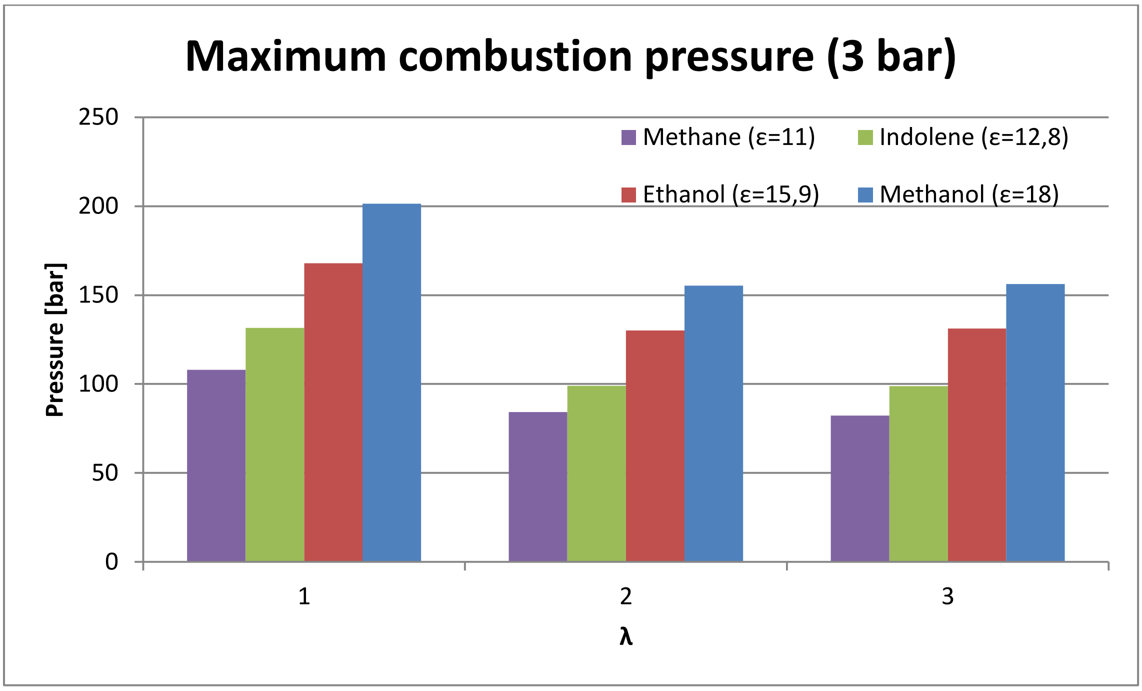

Figure 43. Maximum combustion pressures for different lambda values.

For the performance comparison, IMEP and indicated efficiency (η_i) were selected since they illustrate the potential for improvements in two significant performance indicators in engines, torque and efficiency. As it is known, the output torque of an engine is directly proportional to the mean pressure affecting in the cylinder and this pressure information is provided with IMEP. IMEP for different lambda values are presented in Figure 44, where it can be seen that behavior in relation to lambda is the same as it is with the maximum combustion pressure.

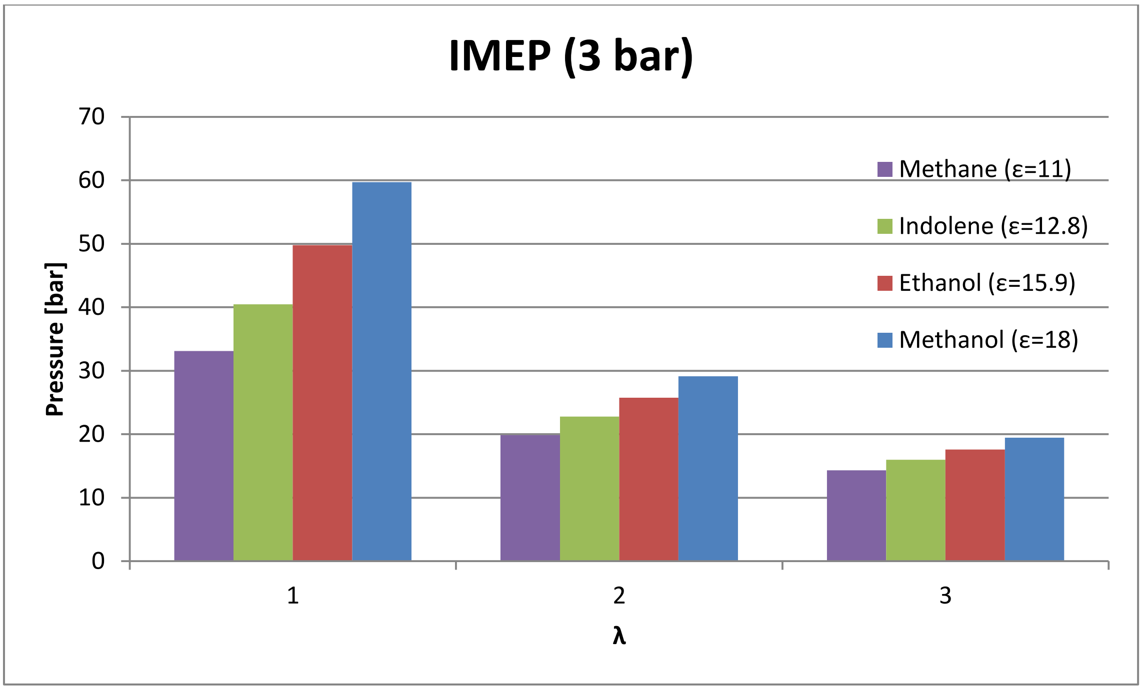

Figure 44. IMEP with respect to lambda.

As can be seen in the Figure 44, the best performance was achieved with methanol for all used lambda values. Methanol is followed by ethanol, then indolene and methane operation provides the poorest performance figures. This correlates directly the results reported in previous chapters since the trapped air mass and fuel energy follows the same order. Naturally, the difference between methane and the other fuels decreases as lambda increases since the differences in the trapped air mass and fuel energy decrease correspondingly. For lambda value of 1, the IMEP of methanol is very high compared to commercially available engines where IMEP over 30 is not present normally. However, in this thesis IMEP between 30 to 40 bars are still considered to be achievable as they could be reached with research engines. Since lambda value around 2 is the most interesting one for lean combustion operation, it can be seen that the IMEP for methanol operation at lambda 2 is just below 30 which is in the acceptable range. Nevertheless, methanol operation with lambda 1 could be still possible since the maximum combustion pressure was still in acceptable range. These results indicate significant potential for increasing the engine performance with methanol operation. When comparing methanol to methane, the increase in IMEP is in the range of 40 – 80 percent depending on the lambda.

The results for indicated efficiencies are shown in Figure 45. Similar to already reported trends, the efficiency increases with increasing lambda. This behavior corresponds to the behavior of lean-burn engines in reality, as it is explained earlier in this thesis. For methanol operation, indicated efficiencies of 46, 51 and 54 % were achieved with lambda values of 1, 2 and 3, respectively. These are very high values since in modern diesel engines the indicated efficiency is around 40 % and over 50 % efficiencies are met only in large slow-speed-engines. Also, in reality, lambda value of 3 is most likely too lean to provide proper combustion, thus partial burn and misfire would occur. Since the simulation model burns all the fuel present in the cylinder, no matter what the air-fuel ratio is, the efficiency and other performance values maintain unrealistically high values at extremely high lambda values.

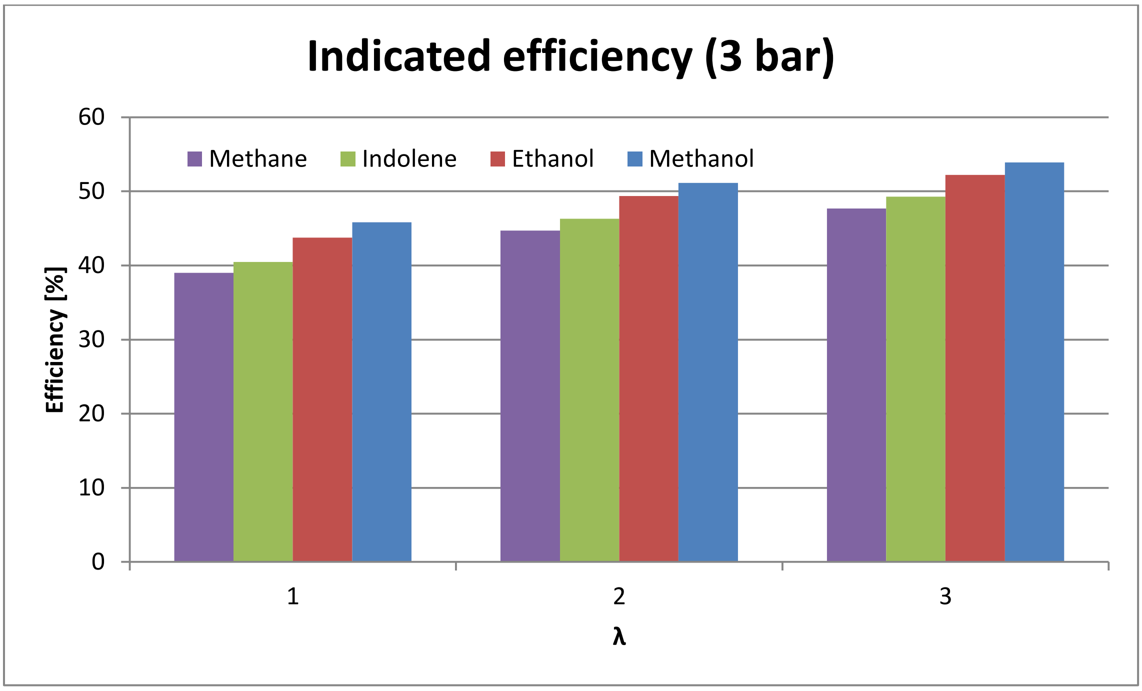

Figure 45. Indicated efficiency for different lambdas.

Comparing the indicated efficiencies between the tested fuels, it can be seen that the differences are rather large between the fuels, especially between methane and methanol. The difference between methanol and methane is 13 – 17 % depending on the lambda value. At the most interesting value, lambda of 2, the efficiency is improved by over 14 %. Better the efficiency, better the fuel economy. As methanol is proven to provide cooler compression and combustion temperature, the indicated efficiency is increased compared to methane due to reduced heat transfer losses. Then again, indicated efficiency is strongly dependent on the variations in compression ratio. The dependency of the indicated efficiency on compression ratio can be illustrated with the equation for theoretical indicated efficiency. Following equation presents how to calculate the theoretical efficiency of an engine:

$$\eta_{i,th} = 1 - \frac{1}{\varepsilon^{\gamma-1}} \qquad (4).$$

In the equation, ε equals compression ratio and γ is the isentropic exponent. As it can be seen, one of the two variables in the equation is compression ratio. In Figure 46 is shown a comparison between the indicated efficiency acquired with simulations and indicated efficiency calculated by using the equation 4. The simulations were conducted with methanol using lambda value of 2 and intake pressure of 3 bars.

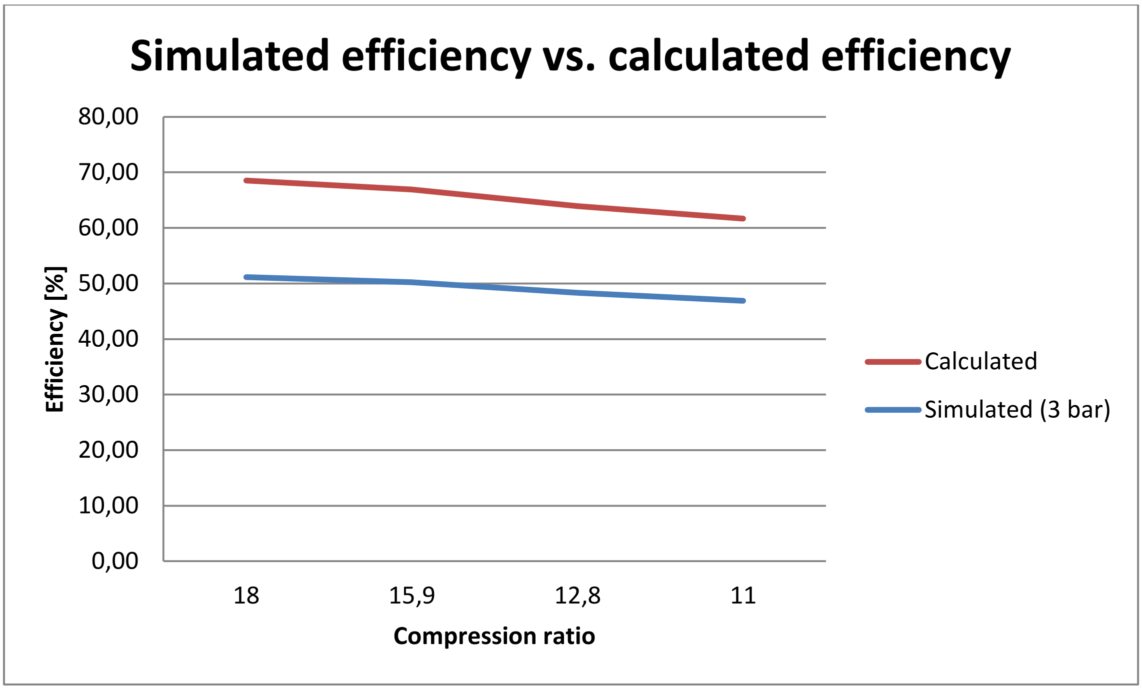

Figure 46. llustration of the differences between simulated and theoretically calculated indicated efficiency.

The simulated efficiency follows the same kind of trend as the calculated efficiency, thus the results correspond the theoretical approach well. The absolute values for simulated efficiency are naturally lower since the indicated efficiency is affected also by heat transfer and pumping losses. They are not taken into consideration in the simple equation for calculating the theoretical efficiency.

The compression ratios used in this chapter were adjusted using the equivalent fuel energy case of methane as a reference case. Since the lambda value for energy equivalent cases where not specified, even greater compression ratio could be used in order to reach the same compression temperature level than with methane operation. This is illustrated in Figure 47, where it can be seen that the compression temperature with methanol, ethanol and indolene is significantly lower with lower lambda values. Therefore, compression ratio can be increased even more when adjusting the ratio using equivalent lambda as a reference case.

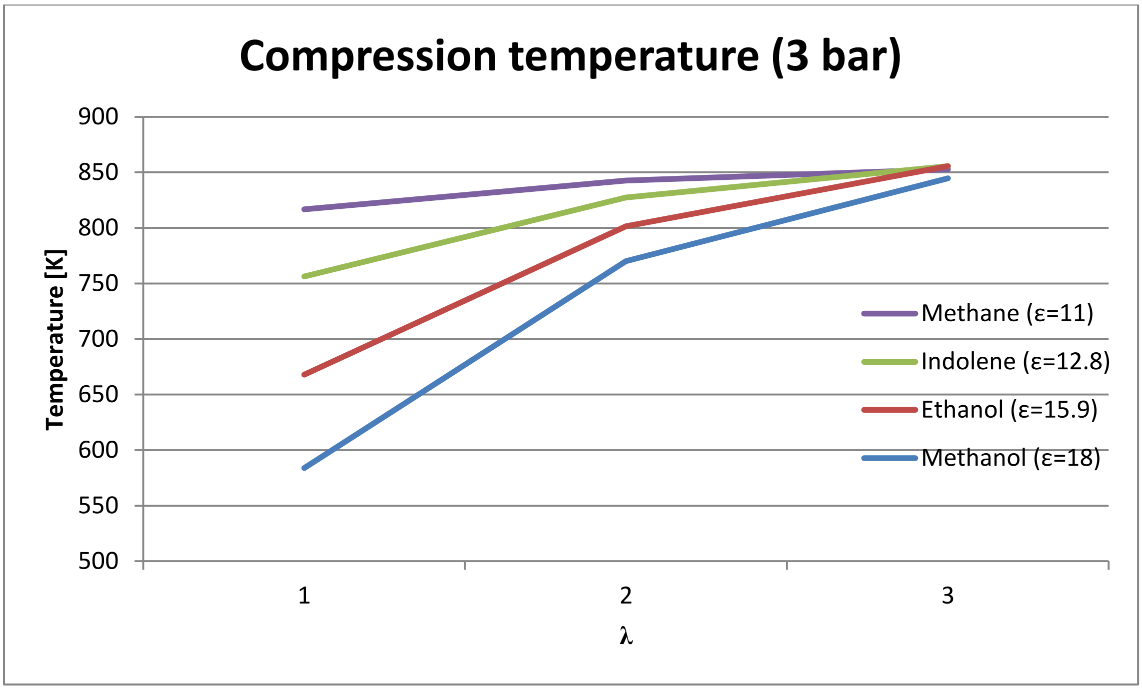

Figure 47. Compression temperatures with respect to lambda values.

6.4.2 Equivalent compression temperature (λ)

Since there was still potential to increase the compression ratio, in this chapter the compression ratio is adjusted in relation to lambda values. Similar to previous chapter, the compression temperature of methane operation with compression ratio of 11 was used as reference case. However, now the compression ratios for methanol, ethanol and indolene were adjusted separately for each lambda value since decreasing lambda value increases the cooling effect. The compression ratios were adjusted with intake pressure of 2 and 3 bars. However, the compression ratios for ethanol and indolene did not change at all with the two different intake pressures, and for methanol the change was negligible. Thus the same compression ratios were used for both 2 bar and 3 bar intake pressures. In Figure 48, the compression ratios used in the simulations are illustrated in respect to lambda values. The reference compression temperatures used for adjusting the compression ratios were 836, 845 and 851 K with intake pressure of 2 bars, and 833, 842 and 848 K with intake pressure of 3 bars. As can be seen in the figure, in order to reach the same temperatures than with methane operation, the compression ratios were extremely high, especially for methanol operation. Since the cooling effect of the cylinder charge is reduced with increasing lambda, the compression ratio decreases together with increasing lambda.

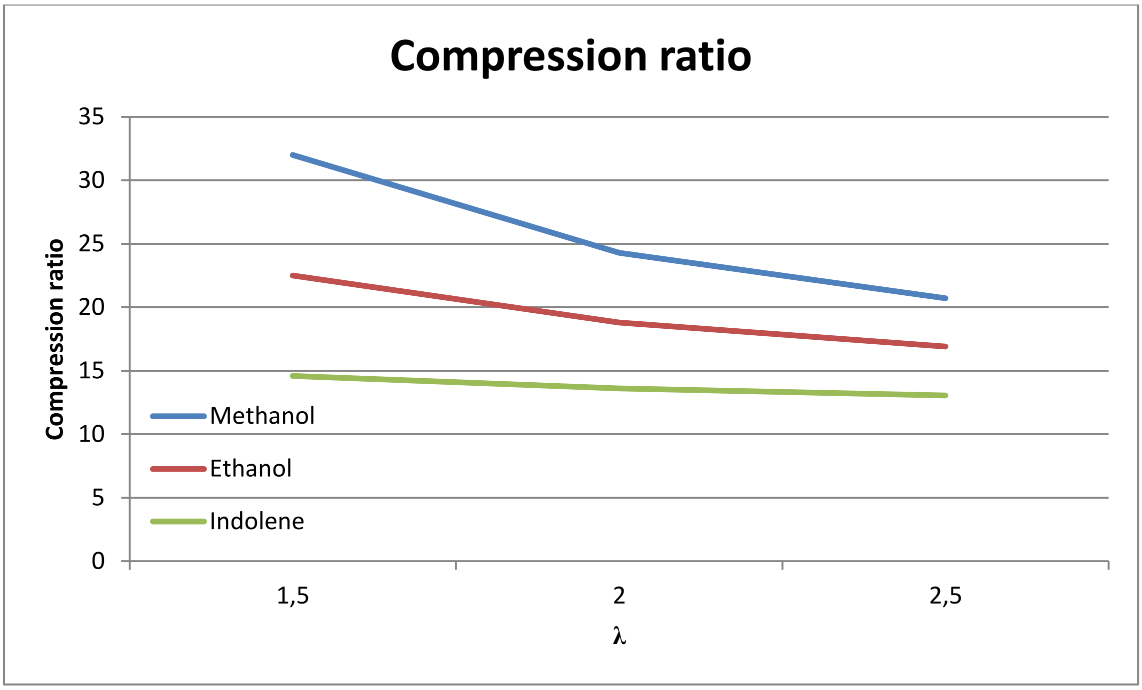

Figure 48. Compression ratios for equivalent compression temperatures with respect to lambda.

Simulations were conducted with both 2 bar and 3 bar intake pressure but since the compression ratio were the same for both pressure levels, and all of results acquired with 2 bar pressure level were in the acceptable range, results with 3 bar intake pressure are reported here as they are the most interesting ones. In addition, as it is reported earlier in this thesis, the results follow linearly the intake pressure and therefore the relative differences between the fuels were practically the same whether 2 bar or 3 bar intake pressure were used. For methane operation, the same results are used in this chapter as it was used in the previous chapter since the compression ratio remains the same. In Figure 49, the compression pressures for the tested fuels are presented with respect to lambda. In addition, compression ratios used for each fuel and lambda value are also illustrated here. The same manner is applied for the rest of the figures in this chapter.

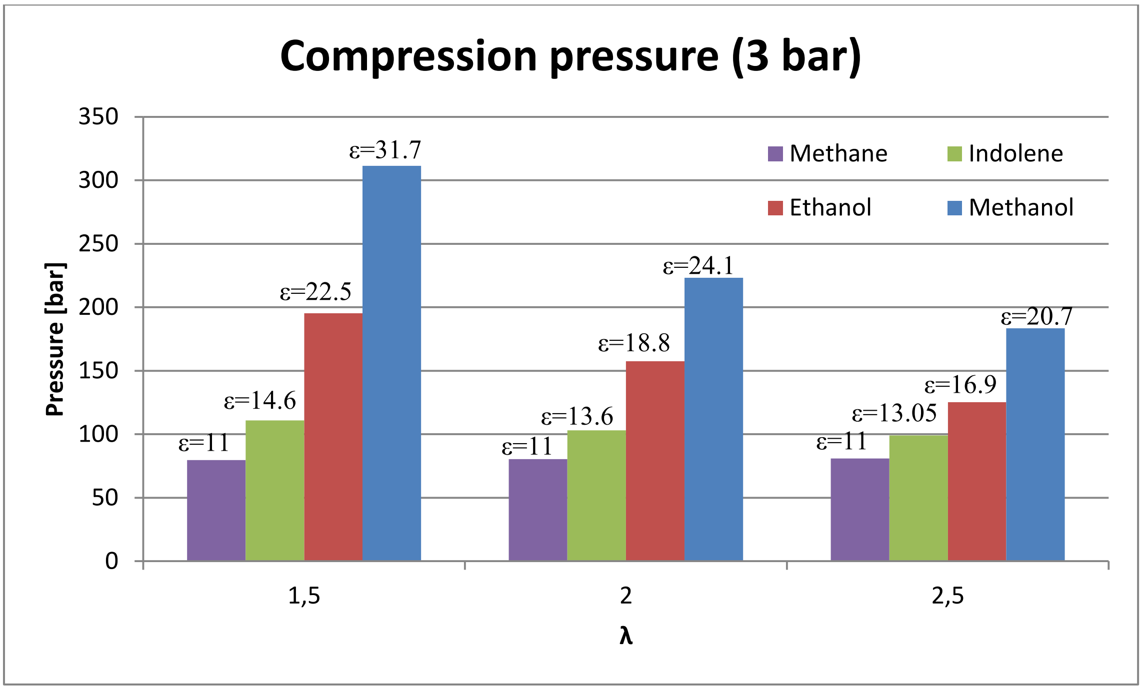

Figure 49. Compression pressures for dfferent lambdas at intake pressure of 3 bars.

Looking at the differences in compression pressures in the Figure 49, methanol naturally had the highest compression pressure since the compression ratio was the highest. When comparing these results to the results presented in the Figure 41, as expected, the differences between the fuels were more dramatic due to the significantly higher compression ratios used here. With ethanol and indolene, the compression pressures were below the typical maximum of an engine for all of the studied compression ratios. On the contrary, the compression ratio of 31.7 with methanol operation increased the compression pressure above 300 bars which is extremely high. For lambda value of 2.5, the compression pressure was clearly below 200 bars but for lambda value of 2 the pressure was 223 bars, which is therefore exceeding the typical maximum. However, since 200 bars is the typical maximum, in some applications engines can be run using even higher cylinder pressures. For example, the heavy duty research engine in Aalto University's engine laboratory has been running with maximum pressure of 250 bars. Although, as the compression pressure is already as high as 223 bars, the peak pressure during combustion could be too high. But then again, it is a matter of combustion phasing how much the peak pressure will increase during combustion.

The cylinder pressure in respect to crank angles followed the same kind of trend than it is illustrated in Figure 42. The maximum pressures are naturally higher since the compression ratios are higher in this chapter but as the trend is the same, there is no need to present the cylinder pressure curves here again. Maximum combustion pressures during the simulations are presented in Figure 50. Due to the simplified approach chosen in this thesis, the maximum pressures do not increase significantly compared to the compression pressures. This can be observed when comparing Figure 50 against Figure 49. Naturally, the maximum pressures follow the same order than the compression pressures since the highest combustion pressure is present with methanol combustion and the lowest with methane combustion.

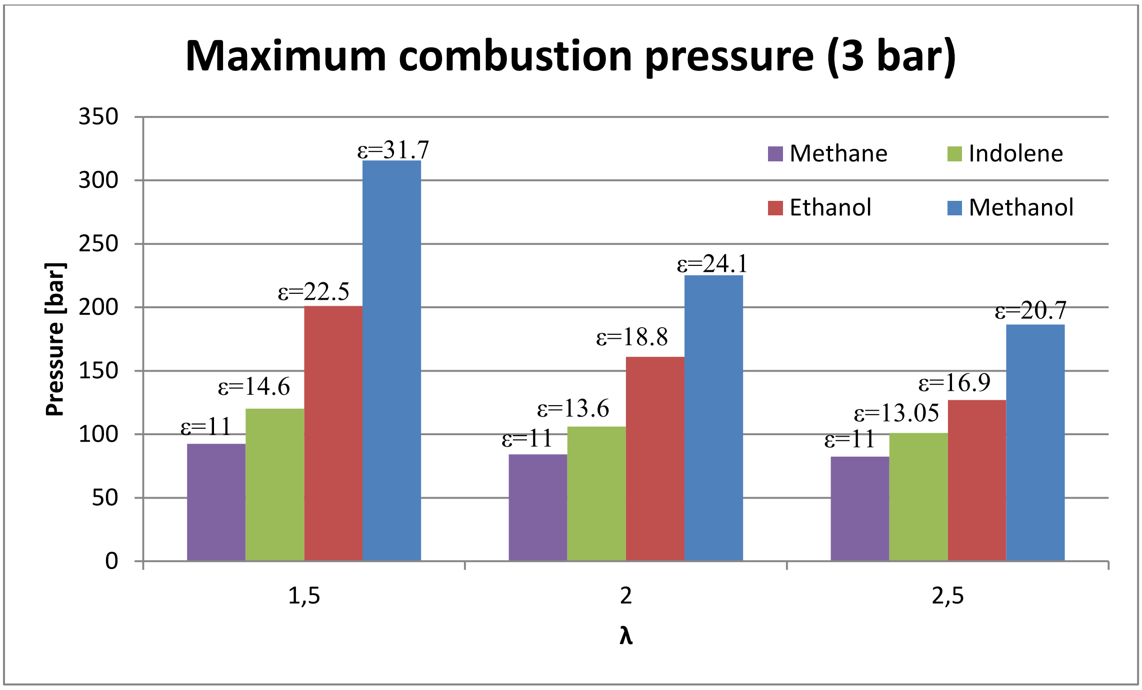

Figure 50. Compression pressures for operation at intake pressure of 2 bars with respect to lambda.

Based on the previous results concerning compression and maximum combustion pressure, the compression ratio could be increased quite safely to 20.7. Compression ratio of 24.1 could be too extreme for commercial engines but in research engines it could be possibly used with proper combustion phasing. However, when looking at the difference in the pressure levels between methanol operations with compression ratio of 24.1 and 20.7, safer option for compression ratio to suggest for experimental tests could be 22. Keeping in mind that with decreasing lambda the compression pressure decreases due to increased cooling effect, and with lambda value of 2.5 the compression pressure was well below 200 bars with 20.7 compression ratio, in that light the compression pressure should remain under 200 bars with compression ratio of 22. In addition, in the literature, compression ratio of 19.5 was used in stoichiometric, EGR diluted SI combustion. Since in SI combustion the point of ignition is defined with a single spark timing, in dual fuel combustion the combustion phasing can be adjusted more flexible with different injection strategy of the pilot fuel. Therefore, the peak pressure could be lower than in the SI engine with equal compression ratio. That said, the suggested compression ratio of 22 could be achievable in experimental tests.

In Figure 51, IMEP for different lambda values are presented. Methanol, again, provided the best performance over other fuels. Ethanol had the second highest IMEP with all lambda values except lambda value of 2.5. In the simulations something unexpected occurred and the author could not find a logical reason why the IMEP of ethanol at lambda 2.5 was lower than with indolene with the same lambda.

Nevertheless, since lambda value of 2 is the most interesting one for lean combustion, this unexpected behavior can be accepted. Comparing the IMEP of methanol to IMEP of methane, the improvement of methanol operation over methane operation is over 50 % at lambda value of 2. Looking at lambda value of 1.5, the improvement is even more significant as it is almost 66 %. However, since the compression pressure was extremely high with lambda value of 1.5, it should not be taken into consideration in the performance comparisons. In methanol operation, IMEP of 30 bars at lambda value of 2 is very high but it is still in the acceptable range. IMEP in this range would provide impressing performance in real engines.

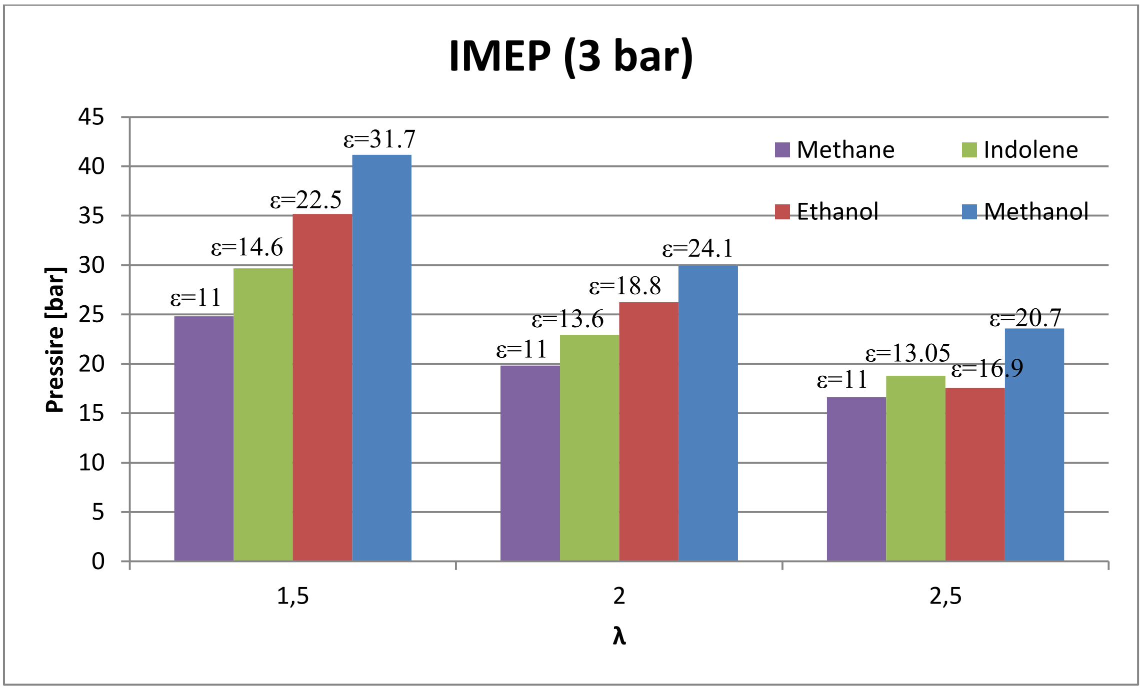

Figure 51. IMEP with respect to lambda.

Indicated efficiencies for different lambda values are presented in Figure 52. For methanol operation, the efficiency was above 50 % for every lambda value. It can be also noticed that the effect of increasing lambda on the efficiency was bypassed by the increasing compression ratio with decreasing lambda. When comparing the results in Figure 52 to the results in Figure 45, where constant compression ratio was used for every lambda value, the efficiency is not improving that dramatically anymore with increasing lambda. This is due to the relationship between compression ratio and indicated efficiency since higher compression ratio increases the efficiency. Although, here the maximum variation in lambda was in the range of one as in the Figure 45 it was in the range of two. Nevertheless, the differences are still very small due to the variations in compression ratios. Comparing methanol to methane, the methanol operation increases the indicated efficiency by 18 % at lambda value of 2. In chapter 6.4.1, the efficiency increase was around 14 % with compression ratio of 18 thus increasing the compression ratio further by 6.1 unit, the efficiency increases 4 % more. This kind of efficiency improvements mean radical improvements in engine fuel consumption.

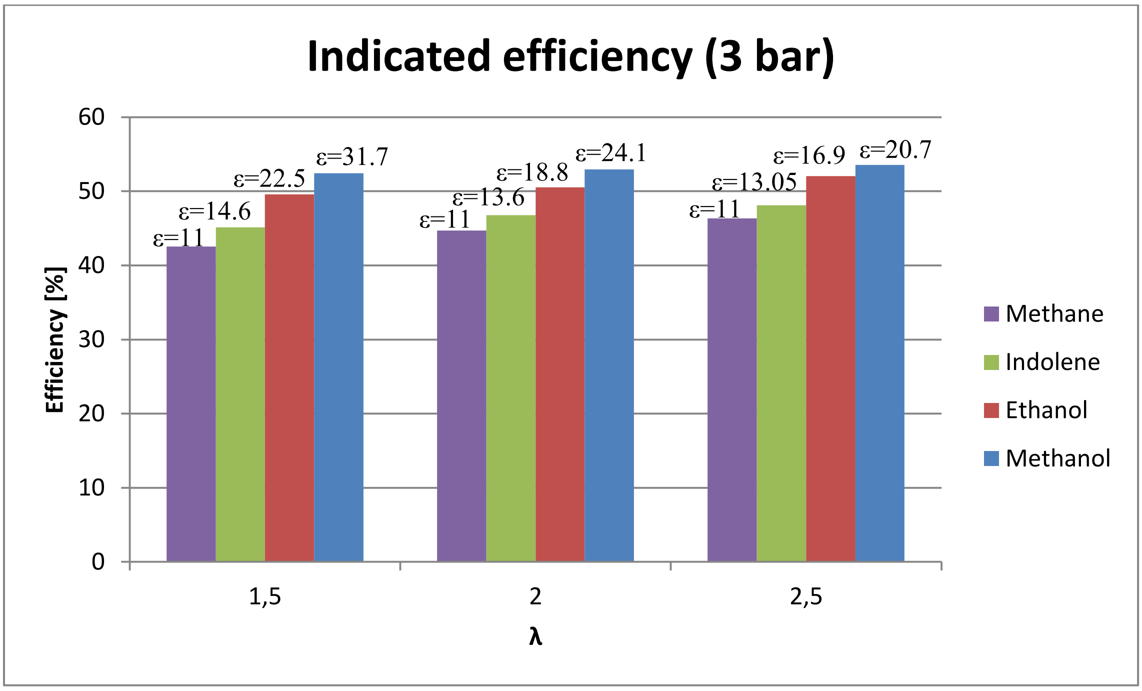

Figure 52. Indicated efficiency for different lambdas.

7 Conclusions

The objective of this study was to investigate the theoretical potential of methanol in dual fuel combustion by comparing it to other, commonly used fuels. Five different approaches were used in the simulations to illustrate the behavior of compression temperature, compression pressure and both trapped air mass and fuel energy. These approaches illustrated well the potential improvements of methanol compared to ethanol, indolene and methane. In addition, possible increments in compression ratio and fuel dependent performance improvements were are also shown in the results. Despite the fact that simulation results are not perfectly realistic, they give an illustration how the different fuels compare to each other.

According to the results in this thesis, when using equal compression ratio for each fuel, methanol lowered the compression temperature significantly. This behavior occurred regardless whether the fuel quantity was adjusted to correspond equivalent energy content or equivalent total lambda. The decrease in temperature was remarkable since at lambda value of two it decreased over 200K compared to methane. In percentage, the temperature reduction was over 22 % which is a really dramatic drop. Despite the significantly lower compression temperature, the difference between methanol and methane in compression pressure was not that significant. This is due to the significant cooling effect of methanol since more air and, correspondingly, more fuel is trapped in the cylinder increasing the total cylinder charge and compression pressure. Then again, more fuel in the cylinder equals higher power output for the engine. With equivalent lambda values, at lambda 2 the increase in trapped fuel energy was almost 40 percent between methane and methanol. This indicates huge improvement potential over methane, which is the main fuel component in natural gas fueled dual fuel engines. Since the emissions of NO_x are strongly dependent on the combustion temperature, the decreasing nature of temperature with methanol operation is also indicating a great potential in reducing the NO_x emissions.

Investigations of the potential for increasing the compression ratio with methanol indicated that compression ratio up to 24.1 could possibly be used in experimental tests. As it was discussed in this thesis, however, a compression ratio of 22 could be a safer option to begin with in the experimental tests. Nevertheless, since current natural gas dual fuel engines are operating with compression ratios in the range of 11 – 13, the increase in efficiency could be remarkable with such high compression ratio. This is indicated in the results, in which compression ratio of 24.1 combined with lean combustion resulted in really high indicated efficiency and IMEP values. At lambda value of 2, the indicated efficiency was almost 53 percent for methanol operation. Again, comparing methanol to methane, the potential increase in indicated efficiency was 18 percent which shows huge potential over methane. In addition, with the same conditions, the IMEP was nearly 30 bars for methanol as it was only around 20 bars for methane. This is a 50 percent improvement over methane which basically means that for the engine with same displacement, methanol operation provides 50 percent more torque.

In summary, methanol shows great potential for increasing power output while simultaneously decreasing the specific emissions of NO_x. Together with improved indicated efficiency and IMEP, methanol could simultaneously lower the fuel consumption and increase engine output torque. As an overall conclusion, methanol is a very noteworthy option as an alternative fuel in dual fuel combustion. The accuracy of the results presented in this thesis is mostly dependent on controlling the fuel evaporation in the actual experimental studies. If methanol is able to be evaporated mostly in the air, then the simulation results could correspond satisfyingly the improvements achieved in reality.

Bibliography

[1] Olah, G. A., Goeppert, A. & Prakash, G. K. S. 2009. Beyond Oil and Gas: The Methanol Economy. 2nd ed. Wiley-VCH. 334 pp. ISBN 978-3-527-31275-7.

[2] Dietsche, K.-H. 2011. Automotive Handbook. 8th ed. Robert Bosch GmbH. 1265 pp. ISBN 978-0-8376-1686-5.

[3] Tutak, W. 2014. Bioethanol E85 as a fuel for dual fuel diesel engine. Energy conversion and management, Vol 86, pp. 39–48. DOI: 10.1016/j.enconman.2014.05.016.

[4] Owen, K. & Coley, T. 1995. Automotive Fuels Reference Book. 2nd ed. SAE International. 963 pp. ISBN 1-56091-589-7.

[5] Matheson Tri-Gas. Lower and Upper Explosive Limits for Flammable Gases and Vapors (LEL/UEL) - Brochure. [Online]. [Sited: 15.6.2015]. Available: https://www.mathesongas.com/pdfs/products/Lower-(LEL)-&-Upper-(UEL)-Explosive-Limits-.pdf

[6] Song, J., Cheenkachorn, K., Wang, J., Perez, J., Boehman, A. L., Young, P. J. & Waller, F. J. 2002. Effect of oxygenated fuel on combustion and emissions in a light-duty turbo diesel engine. Energy and Fuels, Vol 16, No. 2, pp. 294–301. DOI: 10.1021/ef010167t.

[7] Mueller, C. J. & Musculus, M. P. 2001. Glow Plug Assisted Ignition and Combustion of Methanol in an Optical DI Diesel Engine. SAE Technical Paper, 2001-01-2004. DOI: 10.4271/2001-01-2004.

[8] Van Basshuysen, R. & Schäfer, F. 2004. Internal Combustion Engine Handbook. SAE International. 815 pp. ISBN 0-7680-1139-6.

[9] Karim, G. A. 2003. Combustion in Gas Fueled Compression: Ignition Engines of the Dual Fuel Type. Journal of Engineering for Gas Turbines and Power, Vol 125, No. 3, pp. 827-836. DOI:10.1115/1.1581894.

[10] ISO 5163. 2014. Determination of knock characteristics of motor and aviation fuels – Motor method. 39 pp. European committee of standardization.

[11] ISO 5164. 2014. Determination of knock characteristics of motor fuels – Research method. 39 pp. European committee of standardization.

[12] Korakianitis, T., Namasivayam, A. M. & Crookes, R. J. 2011. Natural-gas fueled spark-ignition (SI) and compression-ignition (CI) engine performance and emissions. Progress in Energy and Combustion Science, Vol 37, No. 1, pp. 89–112. DOI:10.1016/j.pecs.2010.04.002.

[13] Tian, G., Daniel, R., Li, H., Xu, H., Shuai, S. & Richards, P. 2010. Laminar burning velocities of 2,5-dimethylfuran compared with ethanol and gasoline. Energy and Fuels, Vol 24, no. 7, pp. 3898–3905. DOI: 10.1021/ef100452c.

[14] Veloo, P. S., Wang, Y. L., Egolfopoulos, F. N. & Westbrook, C. K. 2010. A comparative experimental and computational study of methanol, ethanol, and n-butanol flames. Combustion and Flame, Vol 157, No. 10, pp. 1989–2004. DOI: 10.1016/j.combustflame.2010.04.001.

[15] Metghalchi, M & Keck, J. C. 1982. Burning velocities of mixtures of air with methanol, isooctane, and indolene at high pressure and temperature. Combustion and Flame, Vol 48, pp. 191–210. DOI: 10.1016/0010-2180(82)90127-4.

[16] Warnatz, J., Maas, U. & Dibble, R. W. 1999. Combustion: Physical and Chemical Fundamentals, Modeling and Simulation, Experiments, Pollutant Formation. 2nd ed. Springer-Verlag Berlin Heidelberg. 378 pp. ISBN 978-3-540-45363-5.

[17] Königsson, F. 2014. On Combustion in the CNG-Diesel Dual Fuel Engine. Ph.D Thesis. Royal Institute of Technology. Stockholm, Sweden.

[18] Merker, G. P., Schwarz, C. & Teichmann, R. 2012. Combustion Engines Development. Springer-Verlag Berlin Heidelberg. 642 pp. ISBN 978-3-642-02951-6.

[19] Nowell, G. P. 1994. On the Road with Methanol: The present and future benefits of methanol fuel. Acurex Environmental Corporation. [Online]. [Sited: 20.5.205]. Available: http://www.afdc.energy.gov/pdfs/2474.pdf

[20] Weaver, C. & Turner, S. 1994. Dual Fuel Natural Gas/Diesel Engines:Techonology, Performance and Emissions. SAE Technical Paper, 940548. DOI: 10.4271/940548.

[21] Gunea, C., Razavi, M. R. M. & Karim, G. A. 1998. The Effects of Pilot Fuel Quality on Dual Fuel Engine Ignition Delay. SAE Technical Paper, 982453. DOI: 10.4271/982453.

[22] Lata, D. B. & Misra, A. 2011. Analysis of ignition delay period of a dual fuel diesel engine with hydrogen and LPG as secondary fuels. International Journal

of Hydrogen Energy, Vol 36, No. 5, pp. 3746–3756. DOI: 10.1016/j.ijhydene.2010.12.075.

[23] Christen, C. & Brand, D. 2013. Gas and Dual Fuel Engines as a Clean and Efficient Solution. Cimac Congress Paper. pp. 1–16, 2013. [Online]. [Sited: 25.11.2015]. Available: https://library.e.abb.com/public/55c1608fe200743385257c2f005ded5a/Full_Paper_No_187.pdf.

[24] Bauer, H. 2004. Gasoline-Engine Management. 2nd ed. Robert Bosch GmbH. 418 pp. ISBN 1-86058-434-9.

[25] Heywood, J.B. Internal Combustion Engine Fundamentals. McGraw-Hill series, 1988. 917 pp. ISBN 0-07-100499-8.

[26] Manivannan, A., Tamil, P. & Chandrasekaran, S. 2003. Lean Burn Natural Gas Spark Ignition Engine – An Overview Reprinted. SAE Technical Paper, 2003-01-0638. DOI: 10.4271/2003-01-0638.

[27] Wärtsilä Finland Corporation. 'Wärtsilä 50DF Engine Technology'- Brochure. [Online]. [Sited: 20.11.2015]. Available: http://www.wartsila.com/docs/default-source/Power-Plants-documents/w%C3%A4rtsil%C3%A4-50df.pdf?sfvrsn=2.

[28] Rong, M., He, X., Liu, H., Shang, Y., Zeng, W. , Li, X. & Liu, F. 2014. An Optical Investigation on the Combustion Characteristics of Gasoline-Diesel Dual-Fuel Applications. SAE Technical Paper, 2014-01-1310. DOI: 10.4271/2014-01-1310.

[29] Alla G. A. & Soliman, H. 2002. Effect of injection timing on the performance of a dual fuel engine," Energy Conversion and Management, Vol 43, No. 2, pp. 269–277. DOI: 10.1016/S0196-8904(00)00168-0.

[30] Serrano, D. & Bertrand, L. 2013. Exploring the Potential of Dual Fuel Diesel-CNG Combustion for Passenger Car Engine .Proceedings of the FISITA 2012 World Automotive Congress, Vol 201, pp. 365–376.2013. DOI: 10.1007/978-3-642-33777-2_11.

[31] Selim, M. Y. E. 2004. Sensitivity of dual fuel engine combustion and knocking limits to gaseous fuel composition. Energy Conversion and Management, Vol 45, No. 3, pp. 411–425. DOI: 10.1016/S0196-8904(03)00150-X.

[32] Duffour, F., Ternel, C. & Pagot, A. 2011. IFP Energies Nouvelles Approach for Dual Fuel Diesel-Gasoline Engines. SAE Technical Paper, 2011-24-0065. DOI: 10.4271/2011-24-0065.

[33] Kokjohn, S., Hanson, R., Splitter, D. & Reitz, R. 2010. Experiments and Modeling of Dual-Fuel HCCI and PCCI Combustion Using In-Cylinder Fuel Blending. SAE Int. J. Engines 2(2):24-39. DOI: 10.4271/2009-01-2647.

[34] Wei, L., Yao, C., Wang, Q., Pan, W. & Han, G. 2015. Combustion and emission characteristics of a turbocharged diesel engine using high premixed ratio of methanol and diesel fuel. Fuel, Vol 140, pp. 156–163. DOI: 10.1016/j.fuel.2014.09.070.

[35] Zou, H., Wang, L., Liu, S. & Li, Y. 2008. Ignition delay of dual fuel engine operating with methanol ignited by pilot diesel. Frontiers of Energy and Power Engineering in China, Vol 2, No. 3, pp. 285–290. DOI: 10.1007/s11708-008-0060-z.

[36] Badr, O., Karim, G. A. & Liu, B. 1999. An examination of the flame spread limits in a dual fuel engine," Applied Thermal Engineering, Vol 19, No. 10, pp. 1071–1080. DOI: 10.1016/S1359-4311(98)00108-2.

[37] Dronniou, N., Kashdan, J., Lecointe, B., Sauve, K. & Soler, D. 2014. Optical Investigation of Dual-fuel CNG/Diesel Combustion Strategies to Reduce CO2 Emissions. SAE Int. J. Engines 7(2), pp. 873-887. DOI: 10.4271/2014-01-1313.

[38] Wang, Q., Wei, L. , Pan, W. & Yao, C. 2015. Investigation of operating range in a methanol fumigated diesel engine. Fuel, Vol 140, No. October, pp. 164–170. DOI: 10.1016/j.fuel.2014.09.067.

[39] Sarjovaara, T., Alantie, J. & Larmi, M. 2013. Ethanol dual-fuel combustion concept on heavy duty engine. Energy, Vol 63, No. x, pp. 76–85. DOI: 10.1016/j.energy.2013.10.053

[40] Cheng, C. H. , Cheung, C. S., Chan, T. L., Lee, S. C. & Yao, C. D. 2008 . Experimental investigation on the performance, gaseous and particulate emissions of a methanol fumigated diesel engine. Science of the Total Environment, Vol 389, No. 1, pp. 115–124. DOI: 10.1016/j.scitotenv.2007.08.041

[41] Cheung, C. S. , Zhang, Z. H., Chan, T. L. & Yao, C. 2009. Investigation on the effect of port-injected methanol on the performance and emissions of a diesel engine at different engine speeds. Energy and Fuels, Vol 23, No. 11, pp. 5684–5694. DOI: 10.1021/ef9005516.

[42] Zhang, Z. H., Cheung, C. S., Chan, T. L. & Yao, C. D. 2009. Emission reduction from diesel engine using fumigation methanol and diesel oxidation catalyst.

Science of Total Environment, Vol 407, No. 15, pp. 4497–4505. DOI: 10.1016/j.scitotenv.2009.04.036.

[43] Yao, C., Cheung, C. S., Cheng, C. & Wang, Y. 2007. Reduction of smoke and NOx from diesel engines using a diesel/methanol compound combustion system. Energy and Fuels, Vol 21, No. 2, pp. 686–691. DOI: 10.1021/ef0602731.

[44] Zhang, Z. H., Cheung, C. S., Chan, T. L. & Yao, C. D. 2010. Experimental investigation on regulated and unregulated emissions of a diesel/methanol compound combustion engine with and without diesel oxidation catalyst. Science of the Total Environment, Vol 408, No. 4, pp. 865–872. DOI: 10.1016/j.scitotenv.2009.10.060.

[45] Königsson, F. 2012.Advancing the Limits of Dual Fuel Combustion. Licentiate thesis. Royal Institute of Technology. Stockholm, Sweden.

[46] Yao, C., Cheung, C. S., Cheng, C., Wang, Y., Chan, T. L. & Lee, S. C. 2008. Effect of Diesel/methanol compound combustion on Diesel engine combustion and emissions. Energy Conversion and Management, Vol 49, No. 6, pp. 1696–1704. DOI: 10.1016/j.enconman.2007.11.007.

[47] Brecq, G., Ramesh, A., Tazerout, M. & Le Corre, O. 2001. An Experimental Study of Knock in a Natural Gas Fuelled Spark Ignition Engine. SAE Technical Paper, 2001-01-3562. DOI: 10.4271/2001-01-3562.

[48] Xie, F. X., Li, X. P., Wang, X. C., Su, Y. & Hong, W. 2013. Research on using EGR and ignition timing to control load of a spark-ignition engine fueled with methanol. Applied Thermal Engineering, Vol 50, No. 1, pp. 1084–1091. DOI: 10.1016/j.applthermaleng.2012.08.003.

[49] Wyszynski, L., Stone, C. & Kalghatgi, G. 2002. The Volumetric Efficiency of Direct and Port Injection Gasoline Engines with Different Fuels. SAE Technical Paper, 2002-01-0839. DOI: 10.4271/2002-01-0839.

[50] Zhen, X., Wang, Y. & Zhu, Y. 2013. Study of knock in a high compression ratio SI methanol engine using LES with detailed chemical kinetics. Energy Conversion and Management, Vol 75, pp. 523–531. DOI: 10.1016/j.enconman.2013.07.001.

[51] Vancoillie, J., Demuynck, J., Sileghem, L. , Van De Ginste, M., Verhelst, S., Brabant, L. & Van Hoorebeke, L. 2013. The potential of methanol as a fuel for flex-fuel and dedicated spark-ignition engines. Applied Energy, Vol 102, pp. 140–149. DOI: 10.1016/j.apenergy.2012.05.065.

[52] Einewall, P., Tunestål, P. & Johansson, B. 2005. Lean Burn Natural Gas Operation vs. Stoichiometric Operation with EGR and a Three Way Catalyst. SAE Technical Paper, 2005-01-0250. DOI: 10.4271/2005-01-0250.

[53] Getzlaff, J., Pape, J., Gruenig, C., Kuhnert, D. & Latsch, R. 2007. Investigations on Pre-Chamber Spark Plug with Pilot Injection. SAE Technical Paper, 2007-01-0479. DOI: 10.4271/2007-01-0479.

[54] Davy, M., Evans, R. & Mezo, A.,2009. The Ultra Lean Burn Partially Stratified Charge Natural Gas Engine. SAE Technical Paper, 2009-24-0115. DOI: 10.4271/2009-24-0115.

[55] Brusstar, M., Stuhldreher, M., Swain, D. & Pidgeon, W. 2002. High Efficiency and Low Emissions from a Port-Injected Engine with Neat Alcohol Fuels. SAE Technical Paper, 2002-01-2743. DOI: 10.4271/2002-01-2743.